1981

Statistical Spectroscopy Study of Alpha Particle Transfer Strengths.

Calvin Ray Countee
Louisiana State University and Agricultural & Mechanical College

Countee, Calvin Ray

STATISTICAL SPECTROSCOPY STUDY OF ALPHA PARTICLE TRANSFER STRENGTHS

The Louisiana State University and Agricultural and Mechanical Col. PH.D. 1981

STATISTICAL SPECTROSCOPY STUDY

OF ALPHA PARTICLE TRANSFER STRENGTHS

A Dissertation

Submitted to the Graduate Faculty of the
Louisiana State University and
Agricultural and Mechanical College
in partial fulfillment of the
requirements for the degree of
Doctor of Philosophy

in

The Department of Physics and Astronomy

by
Calvin Ray Countee
B.A., Grambling State University, 1975
M.S., Louisiana State University, 1977
December 1981

ACKNOWLEDGEMENTS

I am deeply thankful to Dr. J. P. Draayer for suggesting this thesis problem and for his excellent guidance and support during the course of this work. Without his endless patience, constant encouragement and continuous help and support this work would not have been possible. I am also thankful to Dr. Ken Weeks for his assistance at various times and for his critical reading of this manuscript.

Part of the material in Chapter 4 is a result of a collaboration with Drs. J. P. Draayer, T. R. Halemane, and K. Kar. I am thankful to them for their collaboration.

I thank and appreciate the love and support of my wife and family. I also appreciate the good will of the entire faculty, staff and graduate students in the Department of Physics and Astronomy at LSU. In particular, I thank Drs. Duane G. Laurent, M. V. Ramana, Lou Adams, and graduate student Uday Gupta for their help and support.

Special thanks are due Ms. Martha Prather and Ms. Linda Gauthier for typing this manuscript, Ms. Nancy Harris for drawing the figures and Ms. Hortensia Delgado for help with the computer system.

Financial assistance for the publication of this dissertation was provided by the "Dr. Charles E. Coates

Memorial Fund of the LSU Foundation donated by George H. Coates."

Lastly, I acknowledge the System Network Computer Center (SNCC) staff and the Department of Physics and Astronomy for the computer facilities provided.

TABLE OF CONTENTS

LIST OF TABLES

LIST OF FIGURES

Page

ABSTRACT

Statistical nuclear spectroscopy or spectral distribution methods have been developed by French and coworkers as an alternative, applicable in huge model spaces, to the conventional shell model approach for studying nuclear structure. The theory is based on the operation of a central limit theorem in large model spaces which yields a shape close to Gaussian for the smoothed eigenstate density distribution.

The theory emphasizes the importance of traces of bilinear products of operators acting in a model space. Utilizing this and partitioning the model space according to group symmetries leads to an algorithm for expanding any interaction in terms of simpler operators. Detailed shell model comparison of excitation spectra, eigenstate overlaps and B(E2) transition strengths in ^{20}Ne and ^{22}Ne with a realistic interaction and its SU(3) trace-equivalent approximations are presented. SU(3) symmetry breaking by single-particle shell effects is also studied.

Spectral distribution methods are used to develop a statistical procedure for calculating alpha particle transfer strengths that is valid in large model spaces. The theory gives the strength function as a bilinear expansion in orthogonal polynomials defined by moments of the inter-

action in the initial and final state model spaces. Rapid convergence is assured by the operation of the central limit theorem. The method involves partitioning the fixed J,T initial (target nucleus) and final (residual nucleus) state model spaces according to the supermultiplet symmetry. Moments of a statistical approximation to the Brown-Kuo interaction are used to estimate the eigenenergies and configuration intensities for the initial and final state subspaces. Specific predictions for the reactions $^{18}O + \alpha \rightleftarrows {}^{22}Ne$ and $^{20}Ne + \alpha \rightleftarrows {}^{24}Mg$ are made. The results are compared with experimental values and with predictions of other nuclear models. A unique feature of the study, unlike what has been found for E2, M1, E4 strengths, is that the density weighted strength is not dominated by the density of states factor.

CHAPTER I

INTRODUCTION

Recent multi-nucleon transfer reaction studies of the type (^{6}Li,d) have led to a number of predictions for alpha particle spectroscopic strengths.[1-5] General formulations in the framework of the SU(3) model[1-3] and the j-j coupled shell model[4,5] have been brought to a state of development which makes specific predictions feasible. For nuclei in the lower half of the ds shell the SU(3) model provides good approximate wave functions for most low-lying positive parity levels. However, beyond mass 28 the SU(3) model is inadequate because spin-orbit forces are so strong they ruin the symmetry underlying the model. In higher mass regions detailed shell model calculations are not feasible because the dimensionalities of the matrices to be constructed and diagonalized become too large to handle even on modern computers. The purpose of this thesis is to develop a statistical procedure to calculate alpha particle spectroscopic strengths that is valid in large spaces. The theory[6-8] uses the lower order moments of an effective Hamiltonian H and a polynomial expansion of excitation strengths.[9] It is valid in large spaces that contain a number of active nucleons. The procedure will be used to calculate alpha particle spectroscopic strengths corresponding to alpha particle

stripping and pickup reactions for nuclei in the ds shell; however, the techniques used can be applied to nuclei in other mass regions.

In Chapter II, we will review a theoretical analysis of alpha particle spectroscopic amplitudes in the framework of the SU(3) model and review current knowledge in the experimental field about alpha transfer reactions in light nuclei. In Chapter III, we describe the spectral distribution method which we plan to use for alpha particle transfer strengths and briefly outline the concepts on which it is based. In Chapter IV, we show how by partitioning a model space according to group symmetries it is possible to construct simple approximations for all effective interactions and show how such approximations provide a measure for the goodness of symmetries. The lower moments of our effective interaction will be used to determine for a given nucleus the ground state energy as well as the intensities of the various configurations at a fixed energy. The lower order moments of our effective interaction will also be useful in our statistical spectroscopy study of alpha particle transfer strengths. In Chapter V we calculate the alpha particle transfer strengths for reactions of the type $^{18}O(^{6}Li,d)$ and $^{20}Ne(^{6}Li,d)$ using the spectral distribution method. This is done by partitioning the model space for the target and residual nucleus according to the SU(4)ST

symmetry and then using the lower moments of our effective interaction to determine the intensity function for each configuration. The simplest approximation to the strength will be a sum over the product of two configuration intensity functions weighted by the average strength with which the excitation operator couples the two configurations. In Chapter VI we conclude with a discussion of the approximations made, improvements in the technique and how the procedure can be used to calculate alpha particle transfer strengths in other mass regions.

CHAPTER II

REVIEW OF ALPHA PARTICLE SPECTROSCOPIC STRENGTHS

A. Reaction Picture

The ground state of an alpha particle consists of two protons and two neutrons in the most symmetrical spatial arrangement possible with J=0, parity π=+, and isospin T=0. The term alpha transfer is applied to any reaction in which two neutrons and two protons are transferred. One usually defines and calculates the spectroscopic amplitude for cases in which a cluster of four nucleons is in an internal Os state, like the ground state of the physical alpha particle. For the direct reaction of Fig. 1 one assumes that a cluster of x nucleons pre-existing in the projectile a=b+x is simply transferred intact to the nucleus A where the x nucleons as a whole are captured to form B, with minimal disturbance of A. The transfer occurs in a single step during the short time when the projectile is passing the target nucleus. In this stripping reaction the angular momentum transferred to the capturing nucleus A is J=L, where L is the orbital angular momentum of the captured nucleons. The change of parity is $\Delta\pi=(-1)^L$ and the change in isospin is $\Delta T=0$.

The differential cross section A(a,b)B of Fig. 1 is proportional to the superposition of structure

(spectroscopic) factors and kinematic (reaction) factors[2,4]

$$\frac{d\sigma}{d\Omega} = \frac{\mu_a \mu_b}{(2\pi\hbar^2)^2} \left(\frac{K_b}{K_a}\right) \frac{2J_B+1}{(2J_A+1)(2J_a+1)}$$

$$\sum_{J_x J'_x} \Big| \sum_{nLn'L'} A^{nLn'L'}_{J_x J'_x J} \; \beta^{nLn'L'}_{JM} \Big|^2 \qquad (2.1)$$

Here the μ and K are reduced masses and momentum transfer factors for a and b. The factor $\beta^{nLn'L'}_{JM}$ contains the kinetmatic dependence of the cross section and the factor $A^{nLn'L'}_{J_x J'_x J}$ the spectroscopic dependence. The J-sums are over the angular momentum J_x and J'_x of the x-transferred nucleons in B = A+x and a=b+x, respectively. The transferred x-nucleon cluster is described in the framework of the harmonic oscillator shell model and n gives the number of oscillator quanta for the relative motion of the x-nucleon cluster with respect to the nucleus A. Likewise n' gives the number of oscillator quanta for the relative motion of the x-nucleon with respect to b. The structure factors $A^{nL,n'L'}$ are given in terms of the two spectroscopic amplitudes, one for the B→A+x vertex and the other for the a→b+x vertex

$$A^{nL,n'L'} = \sum A_{nL}(B \to A+x) A_{n'L'}(a \to b+x) \qquad (2.2)$$

The sum is over the intrinsic states of the transferred nucleons. If the x-nucleon group is transferred in an unexcited internal state with zero intrinsic angular momentum, such as the (0s) internal state of an unexcited α-cluster, the sum reduces to one term and the structure factor, $A^{nL,n'L'}$, is equal to the product of the two spectroscopic amplitudes. In this case the differential cross section for the transfer reaction is also given by a product of a single spectroscopic factor and a reaction mechanism factor. In this study of alpha spectroscopic amplitudes we will be concerned only with the spectroscopic amplitudes A(B→A+x).

To define the spectroscopic amplitude for the nucleus B dissociating into A plus x-particles, we consider a function F defined as the overlap between the internal wave function of nucleus B and the internal wave function of nucleus A and the x-particle cluster [1,4]

$$F(A,B;\vec{r}_{xA}) = \binom{B}{x}^{\frac{1}{2}} \int [\Phi_A(\xi_A)\Phi_x(\xi_x)]^* \Phi_B(\xi_B) d\xi_B d\xi_x \qquad (2.3)$$

where ξ_A, ξ_B, and ξ_x are the internal coordinates of the nuclei A, B and x, respectively; and $\Phi_A(\xi_A)$, $\Phi_B(\xi_B)$, and $\Phi_x(\xi_x)$ their internal wave functions. Also $\vec{r}_{xA}$ is the relative coordinate between the c.m. of x and A. The combinational factor $\binom{B}{x}$ counts the number of

equivalent ways in which x particles can be transferred from the projectile a to the nucleus A without exciting the core of A. In general ϕ_x could be the ground state or an excited state of the x-particle cluster. However, we will assume that ϕ_x is the ground state of the x-particle cluster and thus has zero spin and zero isospin. We also assume that the c.m. motion of each nucleus A and B is in a Os state. Next we expand [for details see Ref. 4] the overlap function $F(A,B;\vec{r}_{xA})$ in terms of an orthonormal complete set of functions in the $\vec{r}_{xA}$ space $\{\phi_{NLm}(\vec{r}_{xA})\}$.

$$F(A,B;\vec{r}_{xA}) = \binom{B}{x}^{\frac{1}{2}} \int [\Phi_A(\xi_A)\Phi_x(\xi_x)]^* \Phi_B(\xi_B) d\xi_B d\xi_x$$

$$= \sum_n A_{n\ell}(A,B)\,\phi_{n\ell m}(\vec{r}_{xA}) \qquad (2.4)$$

The expansion coefficient $A_{n\ell}(A,B)$ is referred to as the spectroscopic amplitude for the nucleus B dissociating into A and x with relative motion $\phi_{n\ell}$. This spectroscopic amplitude is given by[1]

$$A_{n\ell}(A,B) = \binom{B}{x}^{\frac{1}{2}} \int [\Phi_A(\xi_A)\Phi_x(\xi_x)\phi_{n\ell m}(\vec{r}_{xA})]^* \Phi_B(\xi_B) d\xi_B \, d\vec{r}_{xA}$$

(2.5)

In order to evaluate the spectroscopic amplitude in Eq. (2.5) one needs the internal wave functions of the nuclei A, B, and x. However, the kind of wave function which can be handled easily is a shell model wave function $\psi_A(\zeta_A)$ which includes the effects of spurious center of mass motion. The shell model wave function is taken to be a finite linear combination of many-body harmonic oscillator wave functions. The set of coordinates ζ_A has three more degrees of freedom than the internal coordinates ξ_A. The relation between the shell model wave functions and the internal wave functions is given by[1,3]

$$\psi_A(\zeta_A) = \phi_{n\ell m}(\vec{r};\nu)\,\Phi_A(\xi_A) \tag{2.6}$$

where $\phi_{n\ell m}(\vec{r};\nu)$ is the harmonic oscillator wave function

$$\phi_{n\ell m}(\vec{r};\nu) = \phi_{n\ell}(r,\nu)Y_{\ell m}(\hat{r}) \tag{2.7}$$

and $\nu = m_o\omega/\hbar$ is the oscillator size parameter. Using shell model wave functions, Ichimura et al.[1] and also Kurath et al.[4] has shown that the spectroscopic amplitude can be rewritten in the form

$$A_{n\ell}(B\to A+x) = \left(\frac{B}{x}\right)^{\frac{1}{2}}\left(\frac{B}{A}\right)^{\frac{1}{2}n}\ \Sigma\langle\psi_A;\psi_x|\}\psi_B\rangle\langle\Phi_x(\xi_x);\phi_{n\ell m}(\vec{r})\,|\psi_x\rangle \tag{2.8}$$

where $\langle \psi_A ; \psi_x | \} \psi_B \rangle$ is a four body shell model coefficient of fractional parentage. The factor $\langle \Phi_x(\xi_x) ; \phi_{n\ell m}(\vec{r}) \, \psi_x \rangle$, the G factor of Refs. 1, 2, 4, is the overlap of the x-nucleons in a state $|\psi_x\rangle$ with the x-nucleon internal wave function $\Phi_x(\xi_x)$. The sum is over all possible x nucleon states $|\psi_x\rangle$. If the x-particle cluster is transferred in an unexcited $(Os)^x$ internal state, the above summation collapses to a single term.

In the next section we will discuss how to calculate the spectroscopic amplitude in the framework of the SU(3) representation of the harmonic oscillator shell model.

B. Calculation of Spectroscopic Amplitudes

Since SU(3) is known from independent shell model calculations to be an approximately good symmetry for nuclei in the lower half of the ds shell it is advantageous to calculate α-spectroscopic amplitudes in the framework of the SU(3) model. This has been done by Ichimura et al.,[1] Hecht et al.,[2] and Draayer.[3] They concluded that most of the α-strength is concentrated in the ground state rotational band in a good SU(3) nucleus. In this model the spectroscopic amplitude is reduced to the calculation of a full four nucleon coefficient of fractional parentage. The required coefficient of fractional parentage can be factorized into two parts. The first,

SU(6)/SU(3) factor,[2] contains all the spatial symmetry and spin-isospin dependence. The second, SU(3)/R(3) factor,[3] contains the full angular momentum dependence.

In the SU(3) model the states of a nucleus are specified by $[f]\alpha(\lambda\mu)\beta ST\kappa_L LJ$ or alternately by $[f]\alpha(\lambda\mu)\beta ST\kappa_S\kappa_J J$, where [f] and $(\lambda\mu)$ label the space and SU(3) symmetries, respectively; α is used to distinguish multiple occurrences of a given $(\lambda\mu)$ in a specific [f]; β is used to distinguish multiple occurrence of a given ST in a specific spin-isospin symmetry $[\tilde{f}]$ contragredient to [f]. The labels κ_L, κ_S, and κ_J refer to projections of the angular momenta L, S, J. The labels κ are generalizations of the K used by Elliott; κ refers to orthogonalized states.[3] The ground state of our x-particle cluster is specified by $[f](\lambda\mu)STLJ \equiv [x](no)S_oT_oL_oJ_o$. Under the assumption that the states of nuclei A and B have pure $[f]\alpha(\lambda\mu)\beta ST$ symmetry labels and the four nucleon cluster is in its ground state the spectroscopic amplitude (2.8) can be written as[1-3]

$$A_{n\ell sj}(B\to A+x) = G\binom{B}{x}\left(\frac{B}{A}\right)^{\frac{1}{2}n} A^R_{n\ell sj}$$

$$\langle [f]\alpha(\lambda\mu)\beta S_A T_A ; [x](no)L_o S_o T_o \,|\}\, [f']\alpha'(\lambda'\mu')\beta' S'_B T'_B\rangle$$

$$\langle TM_T ; T_o M_{T_o} \,|\, T'_B M'_{T_B}\rangle \qquad (2.8)$$

$A^{R}_{n\ell sj}$ is the SU(3)/R(3) part of the x particle cfp and contains the full angular momentum dependence. It has been evaluated and tabulated by Draayer[3,10]

$$A^{R}_{n\ell sj} = \sum_{\substack{\kappa_L L_A \\ \kappa'_L L'_B}} C_{\kappa_L L_A} C_{\kappa'_L L'_B} \; X \begin{Bmatrix} L_A & S_A & J_A \\ L_o & S_o & J_o \\ L_B & S_B & J_B \end{Bmatrix} \langle (\lambda\mu)\kappa_L L_A; (no) L_o \, || \, (\lambda'\mu')\kappa'_L L'_B \rangle \tag{2.9}$$

X{ } is a unitary 9-j symbol which accounts for the conversion from jj to LS coupling; $\langle (\lambda\mu)\kappa_L L_A; (no) L_o \, || \, (\lambda'\mu')\kappa'_L L'_B \rangle$ is a reduced SU(3)$\rightarrow$R(3) Wigner coefficient; and $C_{\kappa_L L_A}$ $C_{\kappa'_L L'_B}$ are the transformation coefficients from states of good κ_LLSJ to states of good $\kappa_S \kappa_J$SJ. In Eq. (2.8) the factor $\langle [f]\alpha(\lambda\mu)\beta ST; [x](no) L_o S_o T_o \, | \} [f']\alpha' (\lambda'\mu')\beta' S'_B T'_B \rangle$ is the SU(6)/SU(3) and SU(4)ST factors of the x-particle cfp. It contains the spatial symmetry and spin-isospin dependence of the full cfp. It has been evaluated and tabulated by Hecht and Braunschweig[2,11]

$$\langle [f]\alpha(\lambda\mu)\beta ST; [x](no) L_o S_o T_o \, | \} [f']\alpha'(\lambda'\mu')\beta' S'_B T'_B \rangle = CD \tag{2.10}$$

with C the SU(6)/SU(3) factor

$$C = \left[\binom{n}{x}\frac{\dim[f]}{\dim[f']}\right]^{\frac{1}{2}} \langle [f]\,\alpha(\lambda\mu);[x](no)\,|\}\,[f']\alpha'(\lambda'\mu')\rangle \tag{2.10a}$$

and D the SU(4)ST factor

$$D = \langle \tilde{[f]}\beta\, S_A T_A; [1^x] S_o T_o |\}\, \tilde{[f']}\beta'\, S_B T_B' \rangle \ . \tag{2.10b}$$

For α-particle transfers the representation $[1^4]$ corresponds to an SU(4) scalar with $S_o=T_o=0$; and the SU(4) factor is trivial, $\langle \tilde{[f]}\beta\, S_A T_A; [1^4] S_o=T_o=0|\}\, \tilde{[f']}\beta'\, S_B' T_B' \rangle = \delta_{\tilde{[f]}\tilde{[f']}}\delta_{\beta\beta'}\delta_{S_A S_B'}\delta_{T_A T_B'}$. The corresponding SU(6) restriction is [f'] = [4f] with couplings to other spatial symmetries forbidden. The G in Eq. (2.8) is used to represent the overlap, $\langle \phi_x(\xi_x); \phi_{n\ell m}(\vec{r})\,|\psi_x\rangle$, of the x-nucleon cluster wave function and the x-nucleon shell model wave function. For x=4, this overlap or G factor has been given by Ichimura et al.[1] and has the simple form

$$G = \left[\frac{n!}{4^n n_1! n_2! n_3! n_4!}\right]^{\frac{1}{2}} \left[\frac{4!}{a!b!c!d!}\right]^{\frac{1}{2}} \times \delta_{[f][4]}\delta_{S_o O}\delta_{T_o O}\delta_{\lambda n} \tag{2.11}$$

for four nucleon transfers in the configuration $n_1n_2n_3n_4 \pm n_u^a n_v^b n_w^c n_z^d$ where a+b+c+d = 4, n_i is the number of oscillator quanta of the i^{th} transferred particle, and $n = n_1+n_2+n_3+n_4$ is the total number of oscillator quanta in the transferred cluster. For example, the transfer of a $(ds)^4$ cluster a=4, b=c=d=0, with $n_1=n_2=n_3=n_4=2$ and n=8 has an overlap value of G=1.

By combining the SU(3)/R(3) spectroscopic factors tabulated by Draayer with the SU(6)/SU(3) coefficient of fractional parentage calculated by Hecht and Braunschweig, it is possible to predict absolute values of α-spectroscopic amplitudes, to assess quantitatively the effects of representation mixing, and to compare the α-transfer strengths to excited rotational bands with those for the ground state band. The predicted amplitudes in Table 1 are for stripping and pickup strengths for even A targets. These values correspond to the square of the spectroscopic amplitude as defined in Eq. (2.8). The tabulated results are all relative to the absolute value of the predicted ground-state to ground-state strength between dominant representations of the target and residual nuclei. The numbers in parenthesis are the absolute value of the ground-state to ground-state strength. All other numbers are relative to the predicted ground state strength and are therefore to be compared to unity. In the $^{24}Mg \rightarrow ^{20}Ne+\alpha$ pickup

reaction the 2^+ member of the ground state band is predicted to be more weakly populated than other members of the ground state band. Spectroscopic strengths extracted from the experimental data give a similar result. In $^{20}Ne+\alpha\rightarrow^{24}Mg$ the $J^\pi=4^+$ of the $\kappa_J=2$ band is predicted to be more strongly favored over the 4^+ of the ground state $\kappa_J=0$ band. Transfer strengths that are predicted to be strong/weak remain so when SU(3) representation mixing is taken into account.[3]

The quantity $\Sigma(\kappa_J)$ represents that fraction of the total strength which goes into the κ_J band.[3] $\Sigma(\kappa_J)$ shows that transitions to members of the ground state band are not necessarily favored but that a sizeable fraction is transferred to members of the excited bands. For example, in the stripping reaction $^{20}Ne+\alpha\rightarrow^{24}Mg$ transitions to the ground state band are only 15% of the total stripping strength.

C. Experimental Results

Multi-nucleon transfer reaction experiments with ^6Li projectiles furnish a selective probe with which to study the structure of light ds shell nuclei. Studying α-particle transfers induced by reactions of the type (^6Li,d) or (d,^6Li) are the most useful because ^6Li is the lightest projectile available for alpha particle

stripping and the transferred nucleons are a tightly bound $(0s)^4$, S=T=0 cluster with a simple well defined structure. This reduces to a minimum the structural complications associated with the multi-particle character of the transferred group of nucleons. When all factors, including experimental convenience, spectroscopic strength, and ease of analysis of results are considered, the $(^6Li,d)$ reaction should be the most useful for extracting reliable structure information.

Many efficient distorted wave Born approximations (DWBA) codes, e.g., the zero range code DWUCK[12] and the finite range code LOLA,[13,14] are available for analyzing heavy ion alpha particle transfer data. These codes make it possible to compare experimental results with theoretical predictions based on nuclear models. One usually assumes that if the experimental angular distribution is well fitted via DWBA calculations the reaction proceeds entirely by direct alpha transfer. The alpha particle transfer strength is expressed in the form of an experimental spectroscopic factor defined as the ratio of the experimental cross section to a DWBA cross section.

$$S_{exp} = \frac{(d\sigma/d\Omega)_{exp}}{(d\sigma/d\Omega)_{DWBA}} \qquad (2.12)$$

In principle S_{exp} can be compared directly with a theoretical spectroscopic factor S produced by calculations

based on a nuclear model. The accuracy of the result is limited by uncertainties in $(d\sigma/d\Omega)_{DWBA}$ due to the approximate nature of the theory and by ambiguities in the input parameters. Exact finite range DWBA calculations produce absolute cross sections that are very sensitive to the values of several input parameters. For example, an increase of 10% in the radius parameter of the bound state wave function may double the cross section with little change in the angular distribution.[15,16] Absolute strengths calculated via DWBA are very unreliable because of this strong dependence of the calculated cross sections on the bound state parameters.[15,16] Many discussions of DWBA theory and the required input parameters can be found in the literature.[17-19]

Anantaraman and others have studied $^{18}O(^{6}Li,d)$ and $^{20,22}Ne(^{6}Li,d)$ reactions with a 32.0 MeV ^{6}Li beam from the Rochester MP tandem accelerator.[16,20] Their angular distributions were limited to angles below $\theta = 60°$. The shapes of their measured angular distributions were characteristic of a direct transfer of an α-cluster. They performed an exact finite range DWBA analysis with the code LOLA using a set of optical model parameters[21] determined from elastic scattering on ^{40}Ca.

The relative spectroscopic strengths, S_{exp}, were calculated and normalized to unity for the ground state to ground state transitions. A comparison of these

strengths with theoretical predictions based on the SU(3) pure symmetry model[3] and the j-j coupled shell model[21-23] are shown in Tables 2 and 3. The theoretical predictions are in good agreement with each other and with the experimental results. As predicted, for $^{20}Ne(^{6}Li,d)$ the 2^+ level of the ground state band in ^{24}Mg is much more strongly populated than the 4^+ level whereas the opposite is true for the excited K=2 band. For $^{18}O(^{6}Li,d)$ the 2^+ and 4^+ levels of the ground state band of ^{22}Ne are not as strongly populated relative to the 0^+ level as model calculations predict. The discrepancy between experiment and theory in the strengths for the 2^+(1.27 MeV) and 4^+(3.36 MeV) levels has been explored further by Anantaraman. This discrepancy disappeared when he analyzed 38 MeV data with known particle-hole components in the ^{16}O ground state wave function. He suggested that core polarization may be significant and with the 32 MeV data other reaction modes may be significant.[24]

Oelert and others[25] have studied the four nucleon transfer reaction $(d,^{6}Li)$ on ^{24}Mg with an 80 MeV deuteron beam from the Jülich Isochronous Cyclotron (JULIC). The angular range for detecting reaction products was typically 8°-35° lab. The analysis of their data was done with the exact finite range code LOLA. A description of the input parameters used with the code is in Ref. 26. A comparison of their experimental spectroscopic strengths

with detailed shell model calculation of Bennett[26] and the SU(3) pure symmetry calculations of Draayer[3] are shown in Table 4. The spectroscopic strengths are normalized to the ground state transition spectroscopic strength which itself is given relative to the $^{20}Ne \rightarrow ^{16}O+\alpha$ ground state transition. For members of the ground state band (0^+, 2^+, 4^+, 6^+ and 8^+ at 0.0, 1.634, 4.248, 8.777, and 11.949 MeV, respectively) there is satisfactory agreement between the experimental results and theoretical predictions. In general the experimental relative spectroscopic strengths are about a factor of 2 larger than the theoretical ones.

Figure Captions

1. For a direct reaction, X nucleons are transferred from the projectile a = b + X onto the target A, leaving the rediual nucleus B = A + X in either its ground state or an excited state.

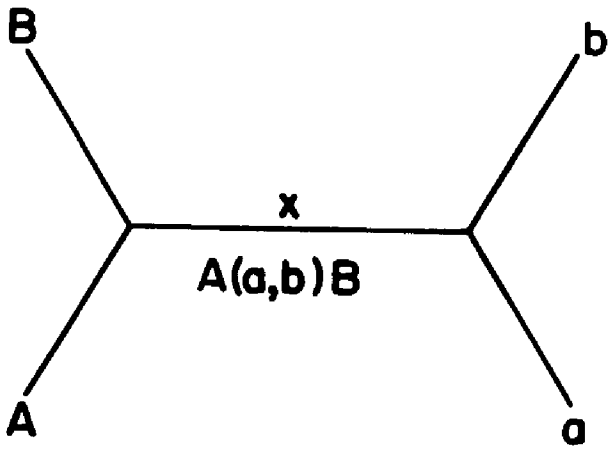

Figure 1

Table Captions

1. $[A_{n\ell sj}(B\ A+x)]^2$ as defined by equation 2.8 for α-transfers among stable ds-shell nuclei. The $A^R_{n\ell sj}$ factors are from ref. 3 and the SU(6)/SU(3) and SU(4)ST factors of the four particle CFP are from ref. 2.

2. Relative spectroscopic strengths for $^{20}Ne(^6Li,d)\ ^{24}Mg$.

3. Relative spectroscopic strengths for $^{18}O(^6Li,d)\ ^{22}Ne$.

4. Relative spectroscopic strengths for $^{24}Mg(d,^6Li)\ ^{20}Ne$.

Table 1

Stripping	J' for $K_J' = 0$						J' for $K_J' = 2$					J' for $K_J' = 4$			
$A(\lambda\mu)O^+ \rightarrow B(\lambda'\mu')$	0	2	4	6	8	$\Sigma(K_J')$	2	4	6	8	$\Sigma(K_J)$	4	6	8	$\Sigma(K_J)$
$^{18}O(00) \rightarrow {}^{22}Ne(82)$	(0.41)	0.77	0.36	0.04	0.07	27	0.00	0.06	0.33	1.23	73				
$^{20}Ne(80) \rightarrow {}^{24}Mg(84)$	(0.49)	0.38	0.00	0.15	0.00	15	0.05	0.46	0.71	0.05	43	0.00	0.04	0.80	43
$^{22}Ne(82) \rightarrow {}^{26}Mg(48)$	(0.28)	0.24	0.12	0.06	0.03	27	0.05	0.01	0.00	0.00	2	0.75	0.26	0.10	71

Pickup	J for $K_J = 0$						J for $K_J = 2$				
$B(\lambda'\mu')O^+ \rightarrow A(\lambda\mu)$	0	2	4	6	8	$\Sigma(K_J)$	2	4	6	8	$\Sigma(K_J)$
$^{22}Ne(80) \rightarrow {}^{18}O(40)$	(0.41)	0.00	2.28								
$^{24}Mg(84) \rightarrow {}^{20}Ne(80)$	(0.49)	0.13	0.80	1.84	1.02	100					
$^{26}Mg(48) \rightarrow {}^{22}Ne(82)$	(0.28)	0.77	0.11	0.21	1.53	42	1.32	0.23	0.17	3.29	58

TABLE 2

E_x(MeV)	J^π	K(λμ)	$S_{exp}(^6Li,d)$ [a]	S[SU(3)] [b]	S(KUO)
0.0	0^+	0(84)	1.00	1.00	1.00
1.37	2^+	0(84)	0.42	0.37	0.44
4.12	4^+	0(84)	0.03	0.00	0.04
4.24	2^+	2(84)	0.13	0.05	0.02
6.01	4^+	2(84)	0.28	0.46	0.29
6.43	0^+	0(46)	3.87	0.86	0.84
7.35	2^+	0(46)	0.37	0.22	0.05
8.12	6^+	0(84)	0.09 ± 0.04	0.15	0.00
8.65	2^+	-	0.22	-	-

a) From Ref. 16.

b) Pure SU(3) symmetry limit using K(λμ) quantum numbers. Ref. 3.

c) Shell model calculations using KUO interaction. Ref. 23.

TABLE 3

E_x(MeV)	J^π	K(λμ)	$S_{exp}(^6Li,d)$[a]	S[SU(3)][b]	S(KUO)[c]
0.00	0^+	0(82)	1.00	1.00	1.00
1.27	2^+	0(82)	0.32	0.77	0.76
3.36	4^+	0(82)	0.10	0.36	0.40
4.46	2^+	1(63)	0.08	0.24	0.00
5.36	2^+	2(82)	0.04	0.00	-
5.52	4^+	1(63)	0.04	0.65	0.06
5.91	3^-	-	0.03	-	-
6.12	2^+	-	very small	-	-
6.24	0^+	0(44)	0.86	<0.95	-
6.31	6^+	0(82)	unresolved	0.04	0.04
6.34	4^+	2(82)	unresolved	0.06	-
7.34	0^+	-	0.75	-	-
7.63	2^+	-	0.30	-	-
7.72	3^-	-	0.12	-	-
8.14	2^+	-	0.16	-	-

a) From Ref. 20.

b) Pure SU(3) symmetry limit using (λμ) quantum numbers. Ref. 3.

c) Shell model calculations using KUO interaction. Ref. 23.

TABLE 4

E_x(MeV)	J^π	K(λμ)	$S_{exp}(d,Li^6)$ [a]	S[SU(3)] [b]	S(CW) [c]
0.00	0^+	0(80)	0.45	0.49	0.59
1.63	2^+	0(80)	0.35	0.13	0.20
4.25	4^+	0(80)	0.96	0.80	0.41
8.78	6^+	0(80)	0.82	1.84	0.71
11.95	8^+	0(80)	0.64	1.02	0.32
6.72	0^+	0(42)	<0.1	0.90	0.09
7.42	2^+	0(42)	<0.02	0.00	0.01
9.99	4^+	0(42)	0.43	1.62	0.20

a) From Ref. 25.

b) Pure SU(3) symmetry limit using K(λμ) quantum number. Ref. 2 and 3.

c) Shell model calculations using Chung Wildenthal interaction. Ref. 26.

CHAPTER III

FUNDAMENTALS OF SPECTRAL DISTRIBUTION METHODS

A. Moments and Distributions

There has been steady progress in attempts to give a microscopic description of nuclear structure in the framework of the conventional shell model. For most microscopic models there are severe limitations on the dimensionalities of the vector spaces in which one can work. The dimensionalities of the matrices to be constructed and diagonalized are often too large even for the best of modern computers. Spectral distribution methods offer an alternative to the conventional approach for studying nuclear structure.[6-9] These methods do not consider the detailed spectrum of the Hamiltonian operator nor detailed strengths for various processes. They deal instead with distributions associated with these quantities, examining these distributions in terms of their moments.

We assume, as in almost all spectroscopy, that our model space is a space generated by distributing m particles over N single particle states and that we have available effective interactions and effective operators which act in the model space. The dimensionality of our model space is $d(m) = \binom{N}{m}$. It has been shown[27-29] that a central limit theorem (CLT) is operable in a many

particle model space. As a consequence of this CLT, in the limit of large particle number, the smooth eigenvalue distribution of most conventional nuclear Hamiltonians in the model space is very close to Gaussian. This distribution is essentially determined by the two lowest moments of the Hamiltonian.

$$M_1(m) = \langle H \rangle^m = \frac{\langle\langle H \rangle\rangle^m}{d(m)} = \epsilon(m) \tag{3.1}$$

$$M_2(m) = \langle H^2 \rangle^m = \frac{\langle\langle H^2 \rangle\rangle^m}{d(m)} = \epsilon^2(m) + \sigma^2(m) \tag{3.2}$$

where $d(m)$ is the dimensionality of the model space and the superscript m denotes that the space is an m-particle space. In (3.1), (3.2) and throughout the rest of this thesis, we use the convention that a single bracket $\langle\ \rangle$ denotes the average of the expectation values of the operator over a complete set of states in the space, whereas a double bracket $\langle\langle\rangle\rangle$ denotes the trace. $\epsilon(m)$ and $\sigma(m)$ are the centroid and width of the energy spectrum.

We can partition our model space into subspaces. As a result of the CLT the eigenvalue density of any operator acting in our subspaces will be close to Gaussian, thus the density for the whole space becomes a superposition of Gaussians. One of the simplest decompositions comes from dividing the N single particle states into

orbits, $N \rightarrow N_1, N_2, N_3 \ldots N_\ell$. Here $N = \sum_{i=1}^{\ell} N_i$ where N_i is the number of states in the i^{th} orbit. Next we assign the m particles to the various orbits, $m \rightarrow m_1, m_2, \ldots m_\ell$ where m_i is the number of particles in the i^{th} orbit and $m = \sum_{i=1}^{\ell} m_i$. Each configuration is then defined by a partition $\vec{m} \equiv [m_1, m_2, \ldots m_\ell]$. As an example consider $(ds)^{12}$ for which N=24, m=12 and d(m)= 2,704,156. Now the ds shell can be divided into three orbits $d_{5/2}$, $d_{3/2}$ and $s_{1/2}$ for which N_1=12, N_2=8, and N_3=4. The m=12 particles can be distributed among the three orbits 45 different ways, that is, the $(ds)^{12}$ space can be decomposed into 45 configurations.

If the model space is partitioned according to a particular group symmetry then the subspaces or configurations will be labelled by the irreducible representations of the group. The moments of the distributions will be a function of operators that are group invariants. The configuration moments can be used to study the goodness of the group symmetry and the admixing of different representations.[30-32] Using a procedure due to Ratcliff[8] the moments can also be used to determine for a given nucleus, the ground state and low energy spectrum.

B. The Central Limit Theorem

The Gaussian behavior of the model space eigenvalue density has been known for some years and is by now well understood.[27-29] The CLT requirements are that the variables be additive and statistically independent.[33] For a "dilute" system of non-interacting particles, one with $m \ll N$ where N is the number of single particle states, the energies for different particles are additive and independent since there is no effective Pauli principle as $N \to \infty$. The m-particle density $\rho_m(E)$ is simply the m-fold convolution of the single particle density ρ_1 with itself

$$\begin{aligned} \rho_m(E) &= \int \rho_{m-1}(E-E')\rho_1(E')dE' \\ &= \rho_{m-1} \circledcirc \rho_1[E] \\ &= \rho_1 \circledcirc \rho_1 \circledcirc \rho_1 \circledcirc \ldots \circledcirc \rho_1[E] \end{aligned} \tag{3.3}$$

Then by the most elementary version of the central limit theorem, $\rho_m \to$ Gaussian for large m.

For interacting particles the energies are not additive because of the effect of the interactions, and thus the straightforward convolution argument fails and the density may or may not be Gaussian. In this case one

considers the shape of the density for an ensemble of Hamiltonians instead of a single Hamiltonian and then shows that the ensemble density is the characteristic form for all but a negligible fraction of the Hamiltonians in the ensemble. The ensemble is a Gaussian Orthogonal Ensemble of two-body interactions, that is, the two-body matrix elements are statistically independent and distributed by a zero-centroid Gaussian law. It is found[29] that the ensembled averaged density becomes Gaussian for large particle numbers (about m=4 particles) and that only a negligible fraction of the members give deviant densities. For most Hamiltonians then we have effectively a CLT for interacting as well as noninteracting particles. We can conclude that most of the nuclear Hamiltonians which give reasonable agreement with experimental data are characteristic members of the ensemble and therefore, for large particle number, their eigenvalue density is close to Gaussian.

C. Polynomial Expansions for Expectation Values and Strength Functions

In this section we will briefly discuss the general theory of strength distributions and sum rule quantities for various excitation operators.

Let H be the Hamiltonian for the nuclear system and O be an excitation operator which induces transitions

$|W\rangle \xrightarrow{O} |W'\rangle$ between starting states $|W\rangle$ and final states $|W'\rangle$. Then the microscopic transition strength is defined as[9]

$$R(W,W') = |\langle W'|O|W\rangle|^2 \tag{3.4}$$

where we label the states by their energies and where the $|W\rangle$ states span the initial model subspace (an eigenspace of H) and the $|W'\rangle$ the final model subspace. Depending on the nature of the excitation, the initial and final states may be taken as belonging to the same model subspace or different model subspaces. The p^{th} order energy weighted sum rule[9] associated with O is defined as the expectation value of the moment operator, $M_p = O^+H^pO$

$$\begin{aligned} M_p(W) &= \sum_{W'} R(W',W)(W')^p \\ &= \int I'(W')(W')^p R(W',W)dW' \\ &= \langle W|O^+H^pO|W\rangle \end{aligned} \tag{3.5}$$

where $I'(W')$ is the eigenstate density in the final state space. If d and d' are the dimensionalities of the initial and final state spaces then the eigenstate densities of the initial and final state spaces are given by

$$I(W) = d\rho(W) = \sum_i \delta(W_i - W)$$

$$I'(W') = d'\rho(W') = \sum_i \delta(W_i' - W') \tag{3.6}$$

where $\rho(W)$ and $\rho(W')$ are the initial and final probability densities. Using (3.6) the transition strength can be written as

$$R(W,W') = \frac{1}{I'(W')} \langle W|O^+\delta(H-W')O|W\rangle$$

$$= \frac{d}{I'(W')I(W)} \langle O^+\delta(H-W')O\delta(H-W)\rangle^m \tag{3.7}$$

Likewise the p^{th} order energy weighted sum rule can be written as

$$M_p(W) = \frac{1}{I(W)} \langle O^+ H^p O\delta(H-W)\rangle^m \tag{3.8}$$

Associated with each non-negative-definite density $\rho(W)$ is a unique set of orthonormal polynomials $P_\mu(W)$ and $P_\mu'(W')$ such that[33]

$$\int P_\mu(W)P_\nu(W)\rho(W)dW = \delta_{\mu\nu} \tag{3.9}$$

$$\rho(W) \sum_\mu P_\mu(H)P_\mu(W) = \delta(H-W) \tag{3.10}$$

with similar relations between $\rho(W')$ and $P'_\mu(W')$. These polynomials can be constructed explicitly in terms of the density moments

$$M_p = \int \rho(W) W^p dW = \langle H^p \rangle^m \quad . \tag{3.11}$$

The polynomial of order μ requires density moments of orders up to 2μ and is given by

$$[D_\mu D_{\mu-1}]^{1/2} P_\mu(W) = \begin{vmatrix} 1 & M_1 \cdots\cdots M_\mu \\ M_1 & M_2 \cdots\cdots M_{\mu+1} \\ \vdots & \\ M_{\mu-1} & M_\mu \cdots\cdots M_{2\mu-1} \\ 1 & W \cdots\cdots W^\mu \end{vmatrix} \tag{3.12}$$

where D_μ is the determinant with the last row replaced by $[M_\mu, M_{\mu+1}, \ldots M_{2\mu}]$. The first two polynomials are

$$P_o(W) = 1, \; P_1(W) = (W-\varepsilon)/\sigma \tag{3.13}$$

where $\varepsilon = M_1$ is the centroid and $\sigma^2 = M_2 - M_1$ is the variance. When the density is Gaussian, i.e.,

$$\rho(W) = \frac{1}{\sqrt{2\pi\sigma^2}} \exp -\left\{ \frac{(W-\varepsilon)^2}{2\sigma^2} \right\} \tag{3.14}$$

the polynomial $P_\mu(W)$ are related to the Hermite polynomials H_μ by

$$P_\mu(W) = \mu!\ He_\mu[(W-\varepsilon)/\sigma] \tag{3.15}$$

where

$$He_\mu(x) = 2^{-\mu/2}\ H_\mu(x/\sqrt{2})$$

When the density is of the chi-squared type, the P_μ are related to the Laguerre polynomials. For a discrete density distribution the number of polynomials is finite and equal to the number of distinct eigenvalues.

Substituting (3.10) in (3.7) and (3.8) yields polynomial expansions for the strength function and for the expectation value of an arbitrary operator K, not necessarily the moment operator M_p,[9]

$$R(W',W) = (dd')^{-1} \sum_{\mu\nu} \langle\langle 0^+ P'_\mu(H) 0 P_\nu(H)\rangle\rangle^m\ P'_\mu,(W')P_\nu(W) \tag{3.16}$$

$$\langle W|K|W\rangle \equiv K(W) = \sum_\nu \langle KP_\nu(H)\rangle^m\ P_\nu(W)\ . \tag{3.17}$$

With $K = 0^+H^p0$ (3.17) becomes a polynomial expansion for the p^{th} order energy weighted sum rule $M_p(W)$. Multiplying the LHS of (3.16) by I'(W') and then integrating we get

$$\int I'(W')R(W',W) = \sum_{\nu} \langle 0^{+}0 P_{\nu}(H)\rangle^{m} P_{\nu}(W) \qquad (3.18)$$

the non-energy weighted (NEW) sum rule quantity. Thus the replacement of K with $0^{+}0$ in (3.17) gives us the NEW sum rule. Equations (3.16)-(3.18) are formally exact. It can be shown that[9] when the density is Gaussian and remains so under $H \to H+\alpha K$ for infinitesimal α, then only the zero'th and first order polynomial in these expansions contribute. Thus in the CLT limit (3.16) and (3.17) can be approximated by

$$K(W) \overset{CLT}{} \langle K\rangle^{m} + \langle K(H-\varepsilon)\rangle^{m} \frac{(W-\varepsilon)}{\sigma} \qquad (3.19)$$

$$R(W,W') \overset{CLT}{} (d')^{-1} \left[\langle 0^{+}0\rangle^{m} + \langle 0^{+}(H-\varepsilon')0\rangle^{m} \frac{(W'-\varepsilon')}{\sigma'} + \langle 0^{+}0(H-\varepsilon)\rangle^{m} \frac{(W-\varepsilon)}{\sigma} + \langle 0^{+}(H-\varepsilon')0(H-\varepsilon)\rangle^{m} \frac{(W'-\varepsilon')(W-\varepsilon)}{\sigma'\sigma} \right] \qquad (3.20)$$

Equations (3.19) and (3.20) can also be derived by a linear response theory.[34]

For very large spaces the CLT approximations will not be sufficiently accurate in the ground state domain and consequently correction terms are required. Of

course we could achieve better accuracy by adding higher order terms to the general expansions (3.16), (3.17). The traces required for these corrections, however, become rapidly harder and harder to evaluate as the order increases. A straightforward solution is provided by configuration partitioning, i.e., partitioning the model space into subspaces. The configuration densities (the density of each subspace) are to some extent localized in the spectrum and it is natural to introduce orthonormal polynomials for each configuration and produce the overall result by combining the contributions of all the configurations. Each configuration term looks after a part of the total spectrum and when many such configurations are present, one gets high accuracy even with low order polynomials. With configuration partitioning (3.16) and (3.17) can be written as[9]

$$K(W) = \sum_{\vec{m}} \frac{I_{\vec{m}}(W)}{I_m(W)} K(W:\vec{m}) \tag{3.21}$$

where

$$K(W:\vec{m}) = \sum_{\nu} \langle KP_{\nu}^{(\vec{m})}(H) \rangle^{\vec{m}} P_{\nu}^{(\vec{m})}(W) \tag{3.22}$$

and

$$R(W'm';Wm) = \sum_{\vec{m}\vec{m}'} \frac{I^{\vec{m}'}(W') I^{\vec{m}}(W)}{I_{m'}(W') I_{m}(W)} R(W'\vec{m}';W\vec{m}) \qquad (3.23)$$

where

$$R(W'\vec{m}';W\vec{m}) = (d_{\vec{m}}^{\pm})^{-1} \Sigma \langle O^{+}(\vec{m}'-\vec{m}) P_{\mu}^{(\vec{m}')}(H) O P_{\nu}^{(\vec{m})}(H) \rangle^{\vec{m}}$$

$$P_{\mu}^{(\vec{m}')}(W') P_{\nu}^{(\vec{m})}(W) \qquad (3.24)$$

The superscripts and subscripts $\vec{m}$ and $\vec{m}'$ label the subspaces and indicate that the corresponding quantities should be evaluated in that subspace. The polynomials used above are determined by their configuration densities. In the configuration traces there is no restriction on the intermediate states. All the correlation and interference effects are thus properly included and the result is formally exact. The CLT result is obtained by including all polynomials of order ≤ 1; thus $(\mu,\nu) = (0,0), (0,1), (1,0), (1,1)$.

In this thesis, the alpha particle spectroscopic amplitudes will be evaluated in the CLT limit of the polynomial expansion scheme. Our initial and final state model space will be partitioned according to the supermultiplet symmetry group. Recently, for electromagnetic excitation operators[9] and allowed beta decay,[35] detailed comparison with shell model results have shown the success of the CLT limit expansion.

CHAPTER IV

STATISTICAL APPROXIMATIONS TO MODEL INTERACTIONS

A. Theory

In this chapter we show how by partitioning a model space according to group symmetries it is possible to construct simple approximations for all effective interactions.[31,36] The approximations are in terms of simple operators which have physical significance, for example, an expansion of H in terms of the quadrupole-quadrupole and pairing operators. Such expansions can yield physical insight into the types of forces that dominate an interaction, provide a measure for the "goodness" of symmetries, and offer an opportunity to simplify and extend model calculations. These approximations will be useful in our statistical spectroscopy study of alpha particle spectroscopic strengths.

The formal operations of statistical spectroscopy are concerned with the $\binom{N}{m}$ dimensional vector space formed by distributing m fermions over N single particle states.[6,8] If $|\alpha(k)>$ labels a k-particle state vector and $<\alpha(k)|$ its adjoint, then the set of all $|\alpha(k)><\beta(k)|$ form a basis in terms of which any k-body operator defined in the model space can be expanded

$$O(k) = \sum_{\alpha\beta} <\alpha(k)|O(k)|\beta(k)>|\alpha(k)><\beta(k)| \qquad (4.1)$$

To compare operators acting in the space we assign to each a norm. The norm must be compatible with the unitary norm used for the state vectors of the system. Thus it must be defined in such a way that the norm of the sum of two operators is not greater than the sums of their norms and that the norm of the product of two operators will not be greater than the product of the norms. These requirements are met by the Euclidean norm[7] defined by

$$||O||^2 = \mathrm{Tr}(O^+O) = <<O^+O>>^m = d(m)<O^+O>^m \qquad (4.2)$$

where $<< >>^m$ denotes a trace over all m-particle states, d(m) in number, and $<>^m$ the corresponding average. The Euclidean norm is the inner product of an operator with itself, a notion that can be extended to define operator orthogonality. Two operators O_i, O_j are orthogonal if $<O_iO_j> = 0$. The inner product of two operators O_i, O_j can be used to measure the similarity of the operators. This measure is provided by the correlation coefficient

$$\zeta(O_i, O_j) = \frac{<<O_iO_j>>}{||O_i||\,||O_j||} = \cos\theta_{ij} \qquad (4.3)$$

The numerical value of the correlation coefficient lies between -1 and +1. Typically a correlation with $|\zeta| \geq 0.6$ indicates a close similarity between the operators. In general norms and correlation coefficients are particle number dependent. When each operator transforms irreducibly under the group of unitary transformations among single particle basis states, the dependence on particle number divides out. The correlation coefficient may also be regarded geometrically as the cosine of the angle between O_i and O_j.

The set of all independent k-body hermitian operators (all operators considered will be hermitian) acting on the model space forms a finite-dimensional linear vector space.[37] Thus we can set up a basis of operators in the model space, construct an orthogonal basis by a Gram-Schmidt orthogonalization process and obtain an expansion of any given operator acting within the model space in terms of a complete, linearly independent set of basis operators. Thus if $O = \{O_1, O_2, O_3, \ldots O_\ell\}$ is such a set, any operator H can be expanded as

$$H = a_1 O_1 + a_2 O_2 + \ldots a_\ell O_\ell + X \qquad (4.4)$$

The coefficients a_i can be determined in terms of the traces $\langle\langle HO_i \rangle\rangle$ and $\langle\langle O_i O_j \rangle\rangle$ by solving the system of

equations

$$\langle\langle H O_i \rangle\rangle = \sum_{j=1}^{\ell} \langle\langle O_i O_j \rangle\rangle \quad ; \quad i = 1,2,\ldots\ell \tag{4.5}$$

If the set $O = \{O_i\}$ spans the space then X vanishes and Eq. (4.4) represents an exact expansion of H. If the set is incomplete then the norm of H-X compared to the norm of H provides a measure for the completeness of the expansion. Eq. (4.4) can also be interpreted as the projection of H onto the subspace spanned by the set $\{O_i\}$.

As a consequence of the central limit theorem, the smooth eigenvalue density for most Hamiltonians acting in the model space will be close to Gaussian. This eigenvalue distribution can be determined once the lower order moments of the Hamiltonian are known. The first order moment is the centroid ε, which fixes the location of the spectrum

$$\varepsilon(m) = d^{-1}(m)\langle\langle H \rangle\rangle^m = \langle H \rangle^m \tag{4.6}$$

The second order central moment, σ^2, is the variance,

$$\sigma^2(m) = d^{-1}(m)\langle\langle (H-\varepsilon(m))^2 \rangle\rangle^m = \langle (H-\varepsilon(m))^2 \rangle^m \tag{4.7}$$

The width, $\sigma(m)$, is a Euclidean norm and thus a natural

measure of the size of an operator.

The states of the model space belong to the anti-symmetric irreducible representation irrep $[1^m]$ of the group U(N) of unitary transformation among the N single particle states, and can be classified according to the irreps of subgroups of U(N). For each subgroup $G \supset U(N)$ it is possible to construct an operator that reproduces the traces of the Hamiltonian H in all irreps of the group G contained in the irreps $[1^m]$ of U(N). Such an operator is called a trace-equivalent operator, $H^{TE}(G)$. The operator $H^{TE}(G)$ will be obtained as a linear combination of one-body and two-body operators (constructed from the group generators) that are group scalars in G.

The scalar trace of H is given by

$$\langle\langle H\rangle\rangle^m = \sum_x \langle mx|H|mx\rangle = d(m)\langle H\rangle^m \qquad (4.8)$$

where the sum is over all states, $d(m) = \binom{N}{m}$ in number, belonging to the irrep $[1^m]$ of U(N). The sum is a U(N) contraction so only those parts of H that are proportional to U(N) scalars contribute. The only scalar under U(N) is n, the number operator, so H^{TE} will be a polynomial function of degree two in n and will reproduce the average of H in the (0+1+2) particle space as well as the m>2 particle space. Thus we have

$$H^{TE}(U(N)) = a_1 + a_2 n + a_3 n^2 \tag{4.9}$$

where the a_α can be determined from matrix inversion (Eq. (4.5)) or from input averages in the (0+1+2) particle spaces. Hence

$$\begin{aligned} H^{TE}(U(N)) &= [(1-n)(2-n)/2]\langle H\rangle^0 \\ &\quad + [n(2-n)]\langle H\rangle^1 \\ &\quad + [n(n-1)/2]\langle H\rangle^2 \end{aligned} \tag{4.10}$$

where $\langle H\rangle^0$, $\langle H\rangle^1$ and $\langle H\rangle^2$ are input averages.

When we partition the model space according to the direct product decomposition $U(N) \supset U(p) \otimes U(q)$ where $pq=N$ (for the isospin group $p = N/2$, $q = 2$) the subspaces are labelled according to the irreps of $U(q)$ [$U(p)$] contained in the irreps $[1^m]$ of $U(N)$. For a fermion system the irreps of $U(q)$ and $U(p)$ are conjugate to one another, thus any state belonging to an irrep of $U(q)$ also belongs to the conjugate irrep of $U(p)$. The traces of interest are of the type

$$\begin{aligned} \langle\langle H\rangle\rangle^{m\Gamma} &= \sum_x \langle m\Gamma x||H||m\Gamma x\rangle \\ &= d(m\Gamma)\langle H\rangle^{m\Gamma} \end{aligned} \tag{4.11}$$

The sum is over all equivalent irreps, d($m\Gamma$) in number, that carry the label [$m\Gamma$], of U(p) which because of the antisymmetry requirements for fermions implies a sum over basis states of the conjugate irrep[$\tilde{m\Gamma}$] of U(q). If the sum is a U(q)[U(p)] contraction then the trace equivalent operator $H^{TE}(U(P))$ will be a polynomial function of one and two body operators constructed from generators of the complementary group U(p)[U(q)]. For scalars in U(p), the operator $H^{TE}(U(P))$ will be a polynomial function of the invariants of the group U(p). For non-scalars of tensorial rank Δ in U(p), the trace quivalent operator H^{TE} will be a polynomial function of the invariants of U(p) plus any tensors of rank Δ constructed from generators of U(p). A consequence of the requirement that the U(p) and U(q) irreps be conjugate to one another is that any scalar operator that reproduces traces of H in U(q) also reproduces traces of H in U(p).

For the decomposition $U(N)\supset U(p)\otimes U(q)$ with U(p) further reduced with respect to the group K and U(q) reduced with respect to the group L (for the SU(3)/SU(4)ST symmetry in the (ds) shell N=24, p=6, q=4, K=SU(3), L= $SU(4)\supset SU_S(2)\otimes SU_T(2)$) the subspaces are labelled according to the irreps of U(p) and K and U(q) and L contained in the antisymmetric irrep[1^m] of U(N). For K scalars and sums over basis states of an irrep of U(q), i.e., over equivalent U(p) irreps, the trace equivalent operator

$H^{TE}_{(K/L)}$ will be a function of the invariants of U(p), the invariants of K and other K scalars one can form from the generators of U(p). Scalars in U(p) are necessarily scalars in K but not vice versa, hence in propagating K scalars in U(p) one would in general need non-invariant U(p) operators.

If $\{O_\alpha\}$ are the operators necessary to reproduce the trace of H in every subspace, labelled g, of the model space then

$$H^{TE}(G) = a_1 O_1 + a_2 O_2 + \ldots a_\ell O_\ell \tag{4.12}$$

with

$$\langle H \rangle^g = \varepsilon(g) = \langle H^{TE}(G) \rangle^g \tag{4.13}$$

The coefficients a_α can be determined from matrix inversion (see Eq. (4.5)) or from input averages in the defining space irreps. Eq. (4.12) represents a partial expansion of H in terms of operators that reproduce subspace centroids. The norm of $H^{TE}(G)$ compared to the norm of H is a measure for completeness of the expansion. The set of operators $\{O_\alpha\}$ preserves the group symmetry thus the ratio $||H^{TE}(G)||/||H||$ is a measure of the goodness of the symmetry.

The centroid $\varepsilon(m)$ and the variance $\sigma^2(m)$ of the m-particle model space are related to the subspace centroids $\varepsilon(g)$ and variance $\sigma^2(g)$ by

$$\varepsilon(m) = \sum_g \frac{d(g)}{d(m)} \varepsilon(g) \tag{4.14}$$

$$\sigma^2(m) = \sum_g \frac{d(g)}{d(m)} \{\sigma^2(g) + (\varepsilon(m)-\varepsilon(g))^2\} \tag{4.15}$$

where $d(g)$ is the dimensionality of the subspace labelled g and $d(m)$ is the dimensionality of the m-particle model space. The first term in Eq. (4.15) is the average variance of the subspaces and is associated with the spreading H generates within the subspaces whereas the second term is associated with a displacement of the subspace centroids, $\varepsilon(g)$, from the model space centroid, $\varepsilon(m)$. The trace equivalent operator, $H^{TE}(G)$, reproduces only that part of $\sigma^2(m)$ associated with the displacement of the subspace centroids. One can extend $H^{TE}(G)$ such that its width contains some spreading. This is done by expanding the total Hamiltonian minus its trace equivalent part in terms of some additional traceless operators. The operators are made traceless in every irrep of the subgroup G in order to preserve the group structure built into $H^{TE}(G)$. If Q_i, $i = 1,2,...p$ are our additional operators then the extended trace-equivalent approximation becomes

$$H'(G) = H^{TE}(G) + \sum_{i=1}^{P} b_i (Q_i - Q_i^{TE}(G) \qquad (4.16)$$

where as before the coefficients b_i can be determined by matrix inversion. If these additional operators preserve the symmetry they generate internal spreading, for example, L^2 when G = SU(3). If they do not, for example, the orbital number operator $\sum_r n_r$ when G = SU(3), they are symmetry breaking and generate external spreading, external because of coupling among subspaces $g' \neq g$.

B. Shell Model Examples

The SU(3) symmetry was suggested by Elliott[43] to describe the collective rotational effects in light nuclei. These collective features manifest themselves not only in the energy level spacings but also in the transition probabilities between levels. States constructed according to the SU(3) scheme possess many of the gross properties of states of light ($A \leq 24$) nuclei.

In the ds shell, the SU(3) group is obtained by first partitioning the model space into its space and spin-isospin parts, $U(24) \supset U(6) \otimes U(4)$, and then by further reducing U(6) with respect to SU(3). The subspaces are labelled by $\{m[f], \alpha(\lambda\mu)\}$ where [f] is the label for U(6) irreps and $(\lambda\mu)$ labels the SU(3) irreps. The α is used

to distinguish multiple occurrences of a given $(\lambda\mu)$ in a specific [f]. The trace equivalent operator with respect to the SU(3) group in the ds shell of a (0+1+2)-body Hamiltonian will be a polynomial function of the zero, one and two body invariants of U(4) and SU(3). Thus we have

$$H^{TE}(SU(3)) = a_1 + a_2 n + a_3 n^2 + a_4 G_2 + a_5 C_2 \qquad (4.17)$$

where G_2 is the casmir invariant of U(4) and C_2 is the casmir invariant of SU(3). The coefficients a_α are determined from the five input centroids of the (0+1+2)-particle defining space. Thus for the BK interaction we have[38,44]

$$\begin{aligned} H^{TE}(SU(3)) = {} & \tfrac{1}{2}(n-1)(n-2)\varepsilon(0[0],(00)) \\ & - n(n-2)\varepsilon(1[\tilde{1}],(20)) \\ & + \tfrac{1}{72}[2n(7n-15)-6G_2+C_2]\varepsilon(2[\tilde{1^2}],(40)) \\ & + \tfrac{1}{72}[4n(n+21)-12G_2-C_2]\varepsilon(2[\tilde{1^2}],(02) \\ & + \tfrac{1}{4}[n(n-5)+G_2]\varepsilon(2[\tilde{2}],(21)) \end{aligned} \qquad (4.18)$$

where the input centroids $\varepsilon(m[\tilde{f}],(\lambda\mu))$ are 0.0, -2.302, -8.333, -6.130, -4.056 MeV for the 0, 1, 2 particle defining space irreps, respectively. G_2 has eigenvalue

$\tilde{f}_1^2+\tilde{f}_2^2+\tilde{f}_3^2+\tilde{f}_4^2+3\tilde{f}_1+\tilde{f}_2-\tilde{f}_3-3\tilde{f}_4$ where $[\tilde{f}]$ is the conjugate of $[f]$ and C_2 has eigenvalue $4(\lambda+\mu+3)(\lambda+\mu)-4\lambda\mu$. For $(ds)^6$ the $\binom{24}{6} = 134596$ dimensional model space breaks into 90 subspaces under SU(3) partitioning and the width of $H^{TE}(SU(3))$ is about 69% of the width of the full BK interaction. In Fig. 2 the width of $H^{TE}(SU(3))$ is plotted as continuous function of particle number and is compared with the widths of the BK interaction.

$H^{TE}(SU(3))$ does not take account of spin and isospin splittings and moreover, within a given $(\lambda\mu)$, all L-values are degenerate. This can be corrected and the approximation extended with symmetry preserving operators L^2, S^2, and T^2. For the BK interaction and $(ds)^6$ we find

$$H'(SU(3)) = H^{TE}(SU(3)) + 0.132[L^2-L^{2TE}(SU(3))]$$

$$+ 0.028[T^2-T^{2TE}(SU(3))]$$

$$- 0.628[S^2-S^{2TE}(SU(3))] \qquad (4.19)$$

where the operators L^2, S^2, and T^2 were made traceless with respect to the SU(3) group. This approximation, which generates about 74% of the total width of H, is also plotted in Fig. 2. A large part of the remaining width is due to the splitting of the single particle

orbitals. When we extend H'(SU(3)) to include the orbital number operators, $\sum_r n_r$, the width increases to about 96% thus showing the importance of single particle shell structure.

In Figs. 3 and 4 excitation spectra[36] for ^{20}Ne and ^{22}Ne generated by the H'(SU(3)) of Eq. (4.19), labelled SU3, and the extension including the $\sum_r n_r$, labelled SU3+SPE, are given alongside the corresponding experimental and BK results. For ^{20}Ne the SU3 approximation produced a ground state about 4 MeV higher than that produced by the BK interaction and about 2 MeV higher than the SU3+SPE approximation. The SU3+SPE approximation reproduced almost exactly the 6_1^+, 2_3^+, and 8_1^+ states while the 4_2^+ and 0_2^+ states of H'(SU(3)) lie about 1 and 2 MeV higher, respectively, than for H itself. In the SU3 approximation the 0_1^+, 2_1^+, 4_1^+, 6_1^+, and 8_1^+ are from $[f](\lambda\mu) \equiv [4](80)$, the 0_2^+, $2_{2,3}^+$, $4_{2,3}^+$ from [4](42), and the 0_3^+, 2_4^+ doublet from [31](61). The degeneracies are of two types, one for multiple occurrences of the same L in a given $(\lambda\mu)$, for example the 13 MeV $2_{2,3}^+$ doublet. The second is for different J values but all from the same L,S coupled states, for example the 14.5 MeV 0^+, 2^+ doublet from $(\lambda\mu) = (61)$ with L=1, S=1. The qualitative features for ^{22}Ne, Fig. 4, are very similar to those for ^{20}Ne. The SU3 approximation produced the ground state of ^{22}Ne about 5.8 MeV higher than the BK interaction and about 4.5 MeV higher than the SU3+SPE approximation. The SU3+SPE

states lie on the average about 1.5 MeV higher than the BK interaction. In the SU3 limit the 0^+_1, $2^+_{1,2}$, $4^+_{1,2}$ and $6^+_{1,2}$ states of ^{22}Ne are from [42](82). The 0^+_2, 2^+_3 and 2^+_4, 4^+_3 degeneracies are from [411](90).

In Tables 5 and 6 we compare eigenstate overlaps and BE2 transition strengths for ^{20}Ne generated using the BK interaction and the SU3+SPE and SU3 approximations. In Tables 7 and 8 we make similar comparison for ^{22}Ne. For ^{20}Ne the yrast eigenstates of BK have a large overlap with eigenstates belonging to the $(\lambda\mu)=(80)$ configuration, 77%, 82%, 76% for 0^+_1, 2^+_1, 4^+_1 respectively. For the $0^+_{2,3}$ states the SU(3) overlaps drop to 45% and 7%. Though the 2^+ overlap matrix is close to diagonal, it is clear that the BK $4^+_{2,3}$ states are not doublets of $(\lambda\mu)=(42)$. The sum of the projections to the first five levels is greater than 85% except for the 2^+_2 and 4^+_3 states of SU3 for which the sums are 58% and 67% respectively. For ^{20}Ne the SU3 limit produced zero E2 strength among states belonging to different $(\lambda\mu)$ representations. This is because the E2 operator is a generator of the SU(3) symmetry group. The E2 strengths among states belonging to the same $(\lambda\mu)$ representation agree reasonably well with the BK results. In general the approximations predicted strong transitions that are strong and weak transitions that are weak.

The qualitative features of ^{22}Ne are very similar to those of ^{20}Ne. The overlaps and BE2 strengths for states belonging to $(\lambda\mu)=(82)$ agree reasonably well with the BK results. The overlaps for $0^+_{2,3}$ and 2^+_3, 4^+_3 states are very small. Though the summed values are again large, showing the similarity in the gross if not the detailed structure.

The comparisons show that the microscopic details for the lowest members of each spin as generated using a realistic effective interaction can be reasonably well reproduced with the SU3 and SU3+SPE trace equivalent approximations. The width ratio is a good indication of the reliability. For other states level-by-level comparisons of eigenenergies, overlaps and BE2 strengths show some significant differences. Nonetheless, over a range of energy that includes several states, averaged results are in good agreement.

C. SU(3)/SU(4)ST Effective Operator

In our statistical spectroscopy study of alpha particle transfer strengths we will partition our model space according to the supermultiplet (SU(4)ST) and SU(3) symmetry groups. Recall that statistical spectroscopy relies on low order moments of the nuclear Hamiltonian H which under partitioning the space by a group symmetry are related to averages of powers of H over states

belonging to irreps of the symmetry group. If H is a (0+1+2)-body operator then we can propagate averages of H simultaneously in the irreps of the SU(4)ST and SU(3) symmetry groups.[37] In the ds shell, the propagation is simple because the number of polynomial invariants equals the number of independent input irrep averages. This can be demonstrated from Table 9 where we count the number of polynomial invariants and irreps in the defining space. There are seven (0+1+2) body group invariants, namely, 1, n, n^2, C_2, G_2, S^2, T^2. Here G_2 is the casimir invariant of U(4). For zero particles in the ds shell there is one irrep, [0]. For one particle (m=1) in the ds shell there is one U(6) irrep, [1], with a $(\lambda\mu)$ of (2,0) and one U(4) irrep, $[\tilde{1}]$, with a $S=T=\frac{1}{2}$. The centroid of H in these two subspaces are equal because of the conjugate relationship between the U(6) and U(4) irrep. Thus for the m=1 particle space there is only one independent input irrep average. For two particles (m=2) in the ds shell, there are three two particle irreps of the SU(3) group denoted by $2[1^2](2,1)$, 2[2](4,0) and 2[2](0,2). In the case of the SU(4)ST group, there are four two particle irreps denoted by $2[\tilde{2}]11$, $2[\tilde{2}]00$, $2[\tilde{1}^2]10$, and $2[\tilde{1}^2]01$. The conjugate relationship between the U(6) and U(4) irreps demand that the centroid of H in the U(6) irrep $[1^2]$ be equal to the centroid of H in the U(4) irrep $[\tilde{2}]$ and the centroid of H in the U(6) irrep [2] be equal to the centroid of H in the U(4)

irrep $[\tilde{1}^2]$. Thus there are seven irrep averages in the m=2 particle space but only five of them are independent. Therefore in the (0+1+2) particle space there are seven independent input averages and seven polynomial invariants. We cannot propagate averages of H^2 (0+1+2+3+4-body operator) because the number of polynomial invariants is less than the number of independent irrep averages in the (0+1+2+3+4)-particle defining space. Again this can be demonstrated from Table 9. For three particles (m=3) in the ds shell, there are eight three particle irreps of the SU(3) group. There are three SU(3) irreps contained in the U(6) irrep [3], three SU(3) irreps in the U(6) irrep [21] and two SU(3) irreps in the U(6) irrep $[1^3]$. In the case of the SU(4)ST group, there are six three particle irreps. There is one SU(4)ST irrep contained in the U(4) irrep $[\tilde{1}^3]$, three SU(4)ST irreps in the U(4) irrep $[\tilde{\tilde{2}}\tilde{1}]$ and two SU(4)ST irreps in the U(4) irrep $[\tilde{3}]$. The conjugate relationship between the U(6) and U(4) irreps demands that the centroid of H in the U(6) irreps [3], [21] and $[1^3]$ are equal, respectively to the centroids of H in the U(4) irreps $[\tilde{1}^3]$, $[\tilde{\tilde{2}}\tilde{1}]$, and $[\tilde{3}]$. Thus there are fourteen irrep averages in the m=3 particle space but only eleven independent irrep averages. Following the same counting procedure we find that there are thirty-six SU(3) and SU(4)ST irrep averages in the m=4 particle space but only thirty-one of them are independent.

Therefore in the (0+1+2+3+4) particle space there are fifty independent input averages but only thirty-two polynomial invariants.

In cases where the propagation is not simple Draayer[41] suggests one find the "optimum representation" for a restricted set of operators by requiring the norm of the approximation to be as large as possible, see Eqs. (4.4-4.5). Parikh[38-40] and others have defined and evaluated an "equivalent width". Here one would assume that for a given particle number m and SU(4) irrep $[\tilde{f}]$ all widths for the various $(\lambda\mu)$ST multiplets are equal. In the present study we will approximate H using the theory outlined earlier by an effective H whose scalar width acounts for about 96% of the total width of H and whose SU(3)/SU(4)ST centroids and widths can be evaluated exactly.

C.1 The SU(3)/SU(4)ST Symmetry

In the sd shell, the SU(3)/SU(4)ST symmetry group is obtained by the decompositions U(24)⊃U(6)⊗U(4) with the further decompositions U(6)⊃SU(3) and U(4)⊃SU(4)⊃ $SU_S(2)\otimes SU_T(2)$. The U(4) decomposition involves the direct product of spin and isospin SU(2) groups. The irreps are labelled by the quantum numbers $\{m[f]\alpha(\lambda\mu);[\tilde{f}]\beta ST\}$ where [f] labels the U(6) irreps and $(\lambda\mu)$ labels the SU(3) irreps contained in [f]. The α is used to

distinguish multiple occurrences of a given $(\lambda\mu)$ in a specific [f]. The $[\tilde{f}]$ labels the U(4) irreps and ST labels the SU(2) irreps contained in $[\tilde{f}]$. The β is used to distinguish multiple occurrences of a given ST in a specific $[\tilde{f}]$. We will omit the [f] label since it is the conjugate of $[\tilde{f}]$ and is obtained by interchanging rows and columns of Young Tableau. For a (0+1+2)-body H the invariants n, G_2 of U(4), C_2 of SU(3) and S^2, T^2 of SU(2) form a basis for expanding the trace equivalent operator. Thus[37]

$$H^{TE}(SU(3)/SU(4)ST) = a_1 + a_2 n + a_3 \binom{n}{2} + a_4 G_2 + a_5 C_2 + a_6 S^2 + a_7 T^2 \qquad (4.20)$$

Solving for the coefficients a_α by matrix inversion we get for the BK interaction

$$H^{TE}(SU(3)/SU(4)ST) = -3.92n - 1.406\binom{n}{2} + 0.822G_2 - 0.122C_2 - 0.628S^2 + 0.028T^2 \qquad (4.21)$$

The trace equivalent operator can also be expressed in terms of the independent SU(3) and SU(4)ST defining

space averages[37]

$$H^{TE}(SU(3)/SU(4)ST) = \frac{1}{2}(n-1)(n-2)\,\varepsilon(0[0]00)$$

$$- n(n-2)\,\varepsilon(1[\tilde{1}]\tfrac{1}{2}\,\tfrac{1}{2})$$

$$+ \frac{1}{72}\left[2n(7n-15) - 6G_2 + C_2 + \frac{180}{7}(S^2-T^2)\right]$$

$$\varepsilon(2[\tilde{1}^2](4,0))$$

$$+ \frac{1}{72}\left[4n(n+21) - 12G_2 - C_2 + \frac{72}{7}(S^2-T^2)\right]$$

$$\varepsilon(2[\tilde{1}^2](0,2))$$

$$+ \frac{1}{2}(T^2-S^2)\,\varepsilon(2[\tilde{1}^2]01)$$

$$+ \frac{1}{36}\left[-n^2 - 10(S^2+T^2) + 4G_2\right]\varepsilon(2[\tilde{2}]00)$$

$$+ \frac{1}{36}\left[-4n + 10n^2 + 10(S^2+T^2) + 5G_2\right]\varepsilon(2[\tilde{2}](2,1)) \qquad (4.22)$$

where $\varepsilon(m[\tilde{f}](\lambda\mu))$ and $\varepsilon(m[\tilde{f}]ST)$ are SU(3) and SU(4)ST input averages respectively. For six particles in the sd shell, the SU(4) group partitions the model space into 48 subspaces, the SU(3) group 90 subspaces, the SU(3)/SU(4)ST group partitions the model space into

430 subspaces. The width of $H^{TE}(SU(3)/SU(4)ST)$ is about 74% of the width of H and is plotted in Fig. 5 as a continuous function of particle number. As expected, the width of $H^{TE}(SU(3)/SU(4)ST)$ is greater than that of $H^{TE}(SU(3))$ and $H^{TE}(SU(4))$ which are about 69% of H. When $H^{TE}(SU(3)/SU(4)ST)$ is extended to include projections along the symmetry breaking operators $\sum_r n_r$ we get for the BK interaction

$$H'(SU(3)/SU(4)ST) = H^{TE}(SU(3)/SU(4)ST)$$
$$- 1.001(n_1 - n_1^{TE}(SU(3)/SU(4)ST) + 4.194(n_2 - n_2^{TE}(SU(3)/SU(4)ST) \quad (4.23)$$

where n_1 is the number operator for the $d_{5/2}$ orbital and n_2 is the number operator for the $d_{3/2}$ orbital. This effective interaction accounts for about 96% of the total width of H. This represents a 25% increase in the width thus showing the importance of single particle shell structure. When $H^{TE}(SU(3)/SU(4)ST)$ is extended further to include projections along the symmetry preserving operator L^2 we get for the BK interaction

$$H''(SU(3)/SU(4)ST) = H^{TE}(SU(3)/SU(4)ST)$$
$$- 1.7051(n_1 - n_1^{TE}(SU(3)/SU(4)ST)$$
$$+ 3.4933(n_2 - n_2^{TE}(SU(3)/SU(4)ST) + 0.1285(L^2 - L^{2TE}(SU(3)/SU(4)ST) \quad (4.24)$$

Comparing with H'(SU(3)/SU(4)ST) we find that the L^2 term accounts for an additional 2% increase in the width. The width of H'(SU(3)/SU(4)ST) and H"(SU(3)/SU(4)ST) are compared with those of H^{TE}(SU(3)/SU(4)ST) and the BK interaction[44] in Fig. 5.

C.2 Evaluation of Spectral Moments

With the assumption of normality of the distribution of states belonging to a definite (m[f](λμ)ST) the following two moments characterize the spectral distribution

$$\langle H \rangle^g = d^{-1}(g) \sum_{i \varepsilon g} \langle i|H|i \rangle$$

$$= \langle H^{TE} \rangle^g$$

$$= \varepsilon(g) \qquad (4.25)$$

$$\langle H^2 \rangle^g = d^{-1}(g) \sum_{i \varepsilon g} \langle i|H^2|i \rangle \qquad (4.26)$$

where $g \equiv \tilde{m[f]}(\lambda\mu)ST$ and d(g) is the total number of states over which the sum is taken,

$$d(g) = d(SU_S(2) \times SU_T(2)) \times d(SU(3)) \qquad (4.27)$$

where $d(SU_S(2) \times SU_T(2))$ is the dimensionality of the $SU_S(2) \times SU_S(T)$ irrep subspace and d(SU(3)) is the

dimensionality of the SU(3) irrep,

$$d(SU_S(2) \times SU_T(2)) = (2S+1)(2T+1) \tag{4.28a}$$

$$d(\lambda\mu) = \frac{1}{2}(\lambda+1)(\mu+1)(\lambda+\mu+2) \tag{4.28b}$$

The first moment is the centroid energy and the second moment determines the variance defined as

$$\sigma^2(g) = \langle H^2 \rangle^g - \{\langle H \rangle^g\}^2 \tag{4.29}$$

Equations (4.25-4.29), together with Eq. (4.23), tells one how to calculate exactly the centroids and widths of a definite $(m\tilde{[f]}(\lambda\mu)ST)$ throughout the sd shell. Results of such calculations for the SU(3)/SU(4)ST approximation (4.23) are shown in Tables 10-12.

The SU(3) centroids and widths are related to the SU(3)/SU(4)ST centroids and widths by the relations

$$\varepsilon(m\tilde{[f]}(\lambda\mu)) = \sum_{S,T\varepsilon\tilde{[f]}} \frac{d(m\tilde{[f]}(\lambda\mu)ST)}{d(m\tilde{[f]}(\lambda\mu))} \varepsilon(m\tilde{[f]}(\lambda\mu)ST) \tag{4.30}$$

$$\sigma^2(m\tilde{[f]}(\lambda\mu)) = \sum_{S,T\varepsilon\tilde{[f]}} \frac{d(m\tilde{[f]}(\lambda\mu)ST)}{d(m\tilde{[f]}(\lambda\mu))} \{\sigma^2(m\tilde{[f]}(\lambda\mu)ST + [\varepsilon(m\tilde{[f]}(\lambda\mu)) - \varepsilon(m\tilde{[f]}(\lambda\mu)ST)]^2\} \tag{4.31}$$

where the sum is over all S,T contained in the U(4) irrep $[\tilde{f}]$. $\varepsilon(m[\tilde{f}](\lambda\mu))$ and $\sigma^2(m[\tilde{f}](\lambda\mu))$ label the SU(3) centroid and variance respectively. $d(m[\tilde{f}](\lambda\mu)ST)$ is the dimensionality of the SU(3)/SU(4)ST space and is given by Eq. (4.27). $d(m[\tilde{f}](\lambda\mu))$ is the dimensionality of the SU(3) and U(4) irrep subspace

$$d(m[\tilde{f}](\lambda\mu)) = d_{U(4)}([\tilde{f}])xd(\lambda\mu) \tag{4.32}$$

where $d(\lambda\mu)$ is given by Eq. (4.28) and $d_{U(4)}[\tilde{f}]$ is the dimensionality of the U(4) irrep

$$d_{U(4)}[\tilde{f}] = \prod_{1\leq i<j\leq 4} \frac{(f_i-i-f_j+j)}{(j-i)} \tag{4.33}$$

Likewise the SU(4)ST centroids and widths are related to the SU(3)/SU(4)ST centroids and widths by

$$\varepsilon(m[\tilde{f}]ST) = \sum_{(\lambda\mu)\varepsilon[f]} \frac{d(m[\tilde{f}](\lambda\mu)ST)}{d(m[f]ST)} \varepsilon(m[\tilde{f}](\lambda\mu)ST) \tag{4.34}$$

$$\sigma^2(m[\tilde{f}]ST) = \sum_{(\lambda\mu)\varepsilon[f]} \frac{d(m[\tilde{f}](\lambda\mu)ST)}{d(m[\tilde{f}]ST)} \{\sigma^2(m[\tilde{f}](\lambda\mu)ST) + [\varepsilon(m[\tilde{f}]ST) - \varepsilon(m[\tilde{f}](\lambda\mu)ST)]^2\} \tag{4.35}$$

where the sum is over all $(\lambda\mu)$ contained in the U(6)

irrep [f] which is conjugate to the U(4) irrep $[\tilde{f}]$. $\epsilon(m[\tilde{f}]ST)$ and $\sigma(m[\tilde{f}]ST)$ label the SU(4)ST centroid and width respectively. $d(m[\tilde{f}]ST)$ is the dimensionality of the SU(4)ST and U(6) irrep

$$d(m[\tilde{f}]ST) = d_{U(6)}([f]) x d(SU_S(2) x SU_T(2))$$

$$= (2S+1)(2T+1) x d_{U6}([f]) \qquad (4.36)$$

where $d_{U(6)}([f])$ is the dimensionality of the U(6) irrep

$$d_{U(6)}([f]) = \prod_{1 \le i < j \le 6} \frac{(f_i - i - f_j + j)}{(j-i)} \qquad (4.37)$$

The SU(3) and SU(4)ST centroids and widths for H'(SU(3)/SU(4)ST) of Eq. (4.23) evaluated using Eqs. (4.30-4.37) are shown in Tables 10 and 11.

We observe certain general features of the subspaces labelled by the SU(3)/SU(4)ST irreps. The centroids for $(ds)^4$ varies from about -31.6 to -3.1 MeV and for $(ds)^6$ the centroid varies from a low of -48.3 MeV to a high of -0.25 MeV. The subspace centroids are more or less constant, within about 2 MeV, for all values of ST corresponding to a fixed $m[\tilde{f}](\lambda\mu)$. As seen in Table 12, we also observe a near constant, within about 1 MeV, width for all values of $(\lambda\mu)ST$ corresponding to a fixed $m[\tilde{f}]$. This is not surprising since the widths

corresponding to different SU(4) representations $\tilde{[f]}$ for fixed m have almost the same value.[32]

When it becomes impossible to evaluate subspace widths, such as the case with the SU(4)ST group structure, for a (0+1+2) body Hamiltonian H one can make use of a "constant width approximation" to calculate an equivalent width. One assumes that the value of all subspace widths contained in certain irreps are constant. For example, to calculate a SU(3)/SU(4)ST width for H'(SU(3)/SU(4)ST) using the "constant width approximation" one assumes that for a given $(m\tilde{[f]})$ all widths for the various $(\lambda\mu)$ST multiplets are equal. If we assume that the states belonging to a SU(4) symmetry have a Gaussian distribution then the continuous distribution function will be given by the frequency function

$$f(m\tilde{[f]};E) = \frac{d(m\tilde{[f]})}{\sqrt{2\pi}\sigma(m\tilde{[f]})} \exp - \left\{ \frac{[E - \varepsilon(m\tilde{[f]})]^2}{2\sigma^2(m\tilde{[f]})} \right\} \qquad (4.38)$$

where $\varepsilon(m\tilde{[f]})$ and $\sigma(m\tilde{[f]})$ are SU(4) centroid and width, respectively. If we now take for fixed $m\tilde{[f]}$ a sum of K Gaussians, one for each $(\lambda\mu)$ST, fixing the center of each at $\varepsilon(m\tilde{[f]}(\lambda\mu)ST)$ and assuming the same width σ, then we get a new frequency function

$$f'(m[f];E) = \sum_{\substack{(\lambda\mu)ST \\ \varepsilon[\tilde{f}]}} \frac{d(m[\tilde{f}](\lambda\mu)ST)}{\sqrt{2\pi}\ \sigma}$$

$$\exp - \left\{\frac{[E-\varepsilon(m[\tilde{f}](\lambda\mu)ST)]^2}{2\sigma^2}\right\} \qquad (4.39)$$

We then require the two lowest moments of these two distributions to be equal

$$\int_{-\infty}^{\infty} E\ f(m[\tilde{f}];E)dE = \int_{-\infty}^{\infty} E\ f'(m[\tilde{f}];E)dE \qquad (4.40)$$

and

$$\int_{-\infty}^{\infty} (E-\varepsilon(m[\tilde{f}]))^2\ f(m[\tilde{f}];E)dE = \int_{-\infty}^{\infty} (E-\varepsilon(m[\tilde{f}])^2 \qquad (4.41)$$

$$f'(m[\tilde{f}](\lambda\mu)ST;E)dE$$

The first equation yields

$$\varepsilon(m[\tilde{f}]) = \sum_{\substack{(\lambda\mu)ST \\ \varepsilon[\tilde{f}]}} \frac{d(m[\tilde{f}](\lambda\mu)ST)}{d(m[\tilde{f}]} \varepsilon(m[\tilde{f}](\lambda\mu)ST \qquad (4.42)$$

and is automatically satisfied. The second equation yields

$$d(m[\tilde{f}])\sigma^2(m[\tilde{f}]) = \sum_{\substack{(\lambda\mu)ST \\ \varepsilon[\tilde{f}]}} d(m[\tilde{f}](\lambda\mu)ST) \{\sigma^2 + [\varepsilon(m[\tilde{f}]) - \varepsilon(m[\tilde{f}](\lambda\mu)ST)]^2\} \quad (4.43)$$

The only unknown quantity is σ the "constant width" of each of the K Gaussians, one for each $(\lambda\mu)ST$ contained in $m[\tilde{f}]$. The σ can, therefore, be determined numerically. Results of calculations using the constant width approximation are shown in parenthesis in Table 11. This constant width is more or less the average width of the various $(\lambda\mu)ST$ multiplets.

C.3 Normality of Distribution

We will now examine the nature of the distribution in energy of states belonging to a definite SU(3)/SU(4)ST symmetry. Parikh[32] has shown from detailed shell model calculations for four particles in the ds shell that the exact distributions of states which have different SU(4) symmetries are approximately Gaussians. In view of this and discussions in previous works,[6,32,39-40] we will assume that states belonging to a definite SU(3)/SU(4)ST symmetry have a Gaussian distribution. Whereas the normality of the distribution over all states belonging to a fixed particle number is well understood, this is not the case when one considers distributions over fixed-symmetry subspaces.

If we assume a Gaussian distribution then the continuous distribution function will be given by the frequency function

$$f(g;E) = \frac{d(g)}{\sqrt{2\pi}\ \sigma(g)} \exp - \left\{\frac{[E-\varepsilon(g)]^2}{2\sigma^2(g)}\right\} \tag{4.44}$$

and

$$\int_{-\infty}^{\infty} f(g;E)dE = d(g) \tag{4.45}$$

where $g \equiv m[\tilde{f}](\lambda\mu)ST$ and $d(g)$ is the $SU(3)/SU(4)ST$ dimensionality defined in Eq. (4.27). The centroid, $\varepsilon(g)$, and width, $\sigma(g)$, are calculated from Eqs. (4.25-4.29) using the statistical approximation to the BK interaction $H''(SU(3)/SU(4)ST)$. If we now take for fixed m, a sum of the frequency functions over all g, we get a new frequency function

$$f(m;E) = \sum_{g} f(g;E) \tag{4.46}$$

We want to compare $f(m;E)$ with the frequency function $f'(m;E)$ obtained from the scalar centroid and width for the m particle space.

$$f'(m;E) = \frac{d(m)}{\sqrt{2\pi}\ \sigma^2(m)} \exp - \left\{\frac{[E-\varepsilon(m)]^2}{2\sigma^2(m)}\right\} \tag{4.47}$$

Here $d(m) = \binom{N}{m}$ is the dimensionality of the m particle space. The scalar centroid, $\varepsilon(m)$, and scalar width, $\sigma(m)$, are calculated by averaging over all m-particle states using the statistical approximation to the BK interaction H"(SU(3)/SU(4)ST). We also want to compare f(m;E) with f'(m;E) using the scalar centroid, $\varepsilon(m)$, and scalar width, $\sigma(m)$, of the full BK interaction.[44] In Fig. 6 we show the frequency f(m;E), labeled X, and the frequency functions f'(m;E) obtained from the statistical approximation to the BK interaction, labeled Z, and the full BK interaction,[44] labeled Y, for six particles in the ds shell. We observe that the width of the distribution for the BK interaction is broader than the width of the distribution for the statistical approximation to the BK interaction. For six particles in the ds shell, the width of H"(SU(3)/SU(4)ST) is about 90% of the width of the full BK interaction.[44] The frequency function f(m;E) which results from the sum of several (430) Gaussians, each having the form of Eq. (4.42), and centered about the corresponding centroid energy is itself nearly a Gaussian function. In fact, f(m;E) is very close to being the Gaussian function defined by the frequency function f'(m;E) obtained from the statistical approximation to the BK interaction.

We now want to compare f'(m;E) with a frequency function defined by a sum of the frequency functions

over all SU(4)ST irreps for the m-particle space. That is

$$f''(m;E) = \sum_{m\alpha} f(m\alpha;E) \tag{4.48}$$

where

$$f(m\alpha;E) = \frac{d(m\alpha)}{\sqrt{2\pi}\ \sigma(m\alpha)} \exp - \left\{ \frac{[E- \ (m\alpha)\ ]^2}{2\sigma^2(m\alpha)} \right\} \tag{4.49}$$

and

$$m\alpha \equiv m[\tilde{f}]ST$$

Here $d(m\alpha)$, $\varepsilon(m\alpha)$, and $\sigma(m\alpha)$ are the dimensionality, centroid and width for each SU(4)ST irrep. The centroid, $\varepsilon(m\alpha)$, and the width, $\sigma(m\alpha)$, are from the statistical approximation to the BK interaction H"(SU(3)/SU(4)ST). In Fig. 7 we show the frequency function f"(m;E), labeled X, along with the frequency functions f'(m;E) for the BK interaction, labeled Y, and for the statistical approximation to the BK interaction, labeled Z, for six particles in the ds shell. Here again we see that the frequency function f"(m;E) is close to being the Gaussian function defined by the frequency function f'(m;E) obtained from the statistical approximation to the BK interaction. It appears therefore that in a system with many particles

and where interactions can be restricted to low particle rank the summed distributions are nearly normal.

Figure Captions

2. Scalar widths plotted as a continuous function of particle number for the SU(3) trace-equivalent approximation, $H^{TE}(SU(3)$ [Eq. (4.17)], and the extended SU(3) trace-equivalent approximation, $H'(SU(3))$ [Eq. (4.19)], are compared with the total width of the Brown-Kuo interaction.[44]

3. Excitation spectra for low-lying states of ^{20}Ne $[(ds)^4$ T=0]. Experimental results are on the left with calculated results using a Brown-Kuo interaction[44] and its SU(3) trace equivalent approximations [Eq. (4.19)] on the right. The SU(3) yrast band is from $(\lambda\mu) = (80)$. The 2^+ doublet at 13 MeV is from $(\lambda\mu) = (42)$ and the 0^+, 2^+, doublet at 14.5 MeV from (61) L = 1, S = 1.

4. Excitation spectra for low-lying states of ^{22}Ne $[(ds)^6$ T = 1]. Experimental results are on the left with calculated results using a Brown-Kuo interaction[44] and its SU(3) trace-equivalent approximations [Eq. (4.19)] on the right. The SU(3) yrast band is from $(\lambda\mu) = 82$ for which there is a K-band degeneracy for $J^\pi = 2^+, 4^+,$ .... The o, 2 doublet at 9.3 MeV is from the (90) L=1, S=1 configuration.

5. Scalar widths plotted as a continuous function of particle number for the SU(3)/SU(4)ST trace-equivalent approximation, H^{TE} (SU(3)/SU(4)ST) [eq. (4.21)], and the extended SU(3)/SU(4)ST trace equivalent approximations. H'(SU(3)/SU(4)ST) Eq. (4.23) and H"(SU(3)/SU(4)ST of Eq. (4.24) are compared with the total width of the Brown-Kuo interaction.[44]

6. The normal distribution in $(ds)^6$ derived from scalar moments of the Brown-Kuo interaction, labelled Y, is compared with the normal distribution derived from scalar moments of our statistical approximation to the BK interaction H"(SU(3)/SU(4)ST), labelled Z, and the sum of 430 normal distributions derived from the SU(3)/SU(4)ST moments of our statistical approsimation to the BK interaction, labelled X.

7. The normal distribution in $(ds)^6$ derived from scalar moments of the BK interaction, labelled Y, is compared with the normal distribution derived from scalar moments of our statistical approximation to the BK interaction H"(SU(3)/SU(4)ST), labelled Z, and the sum of 48 normal distributions derived from the SU(4)ST moments of our statistical approximation to the BK interaction, labelled X.

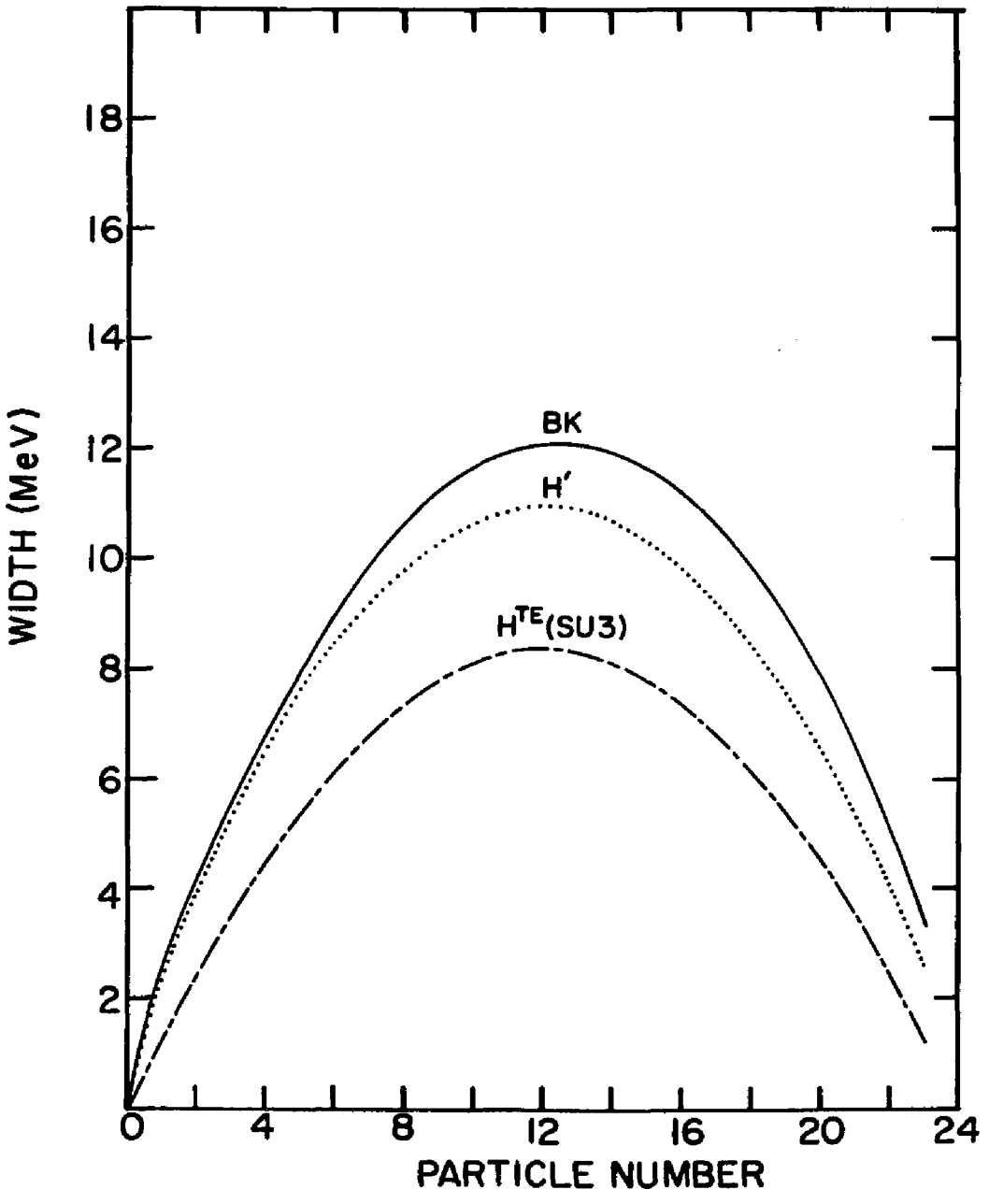
WIDTH (MeV)
18
16
14
12
10
8
6
4
2
0
4
8
12
16
20
24
PARTICLE NUMBER
BK
H'
H^TE(SU3)

Figure 2

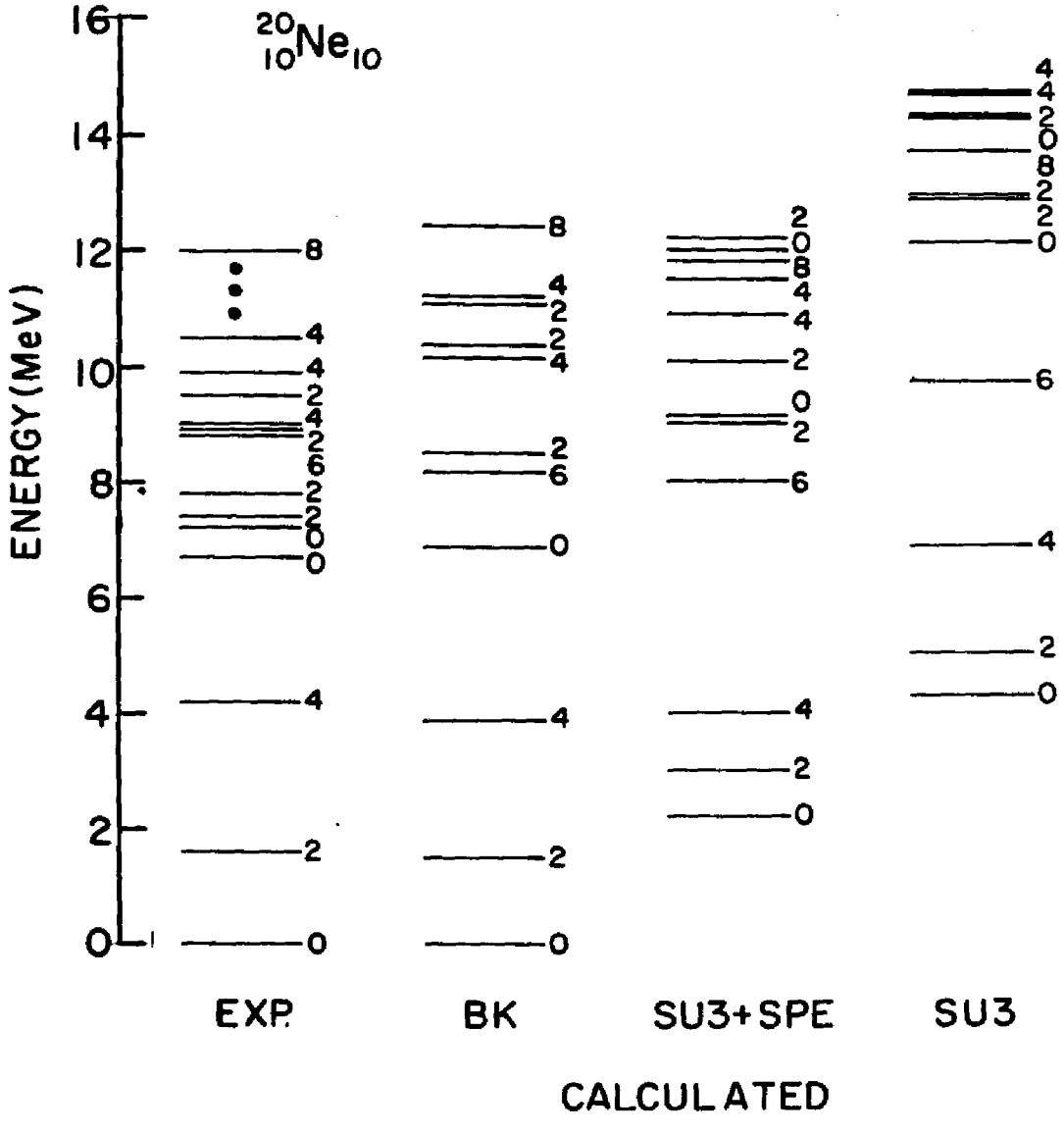
$^{20}_{10}Ne_{10}$
ENERGY (MeV)
16
14
12
10
8
6
4
2
0
EXP
BK
SU3+SPE
SU3
CALCULATED

Figure 3

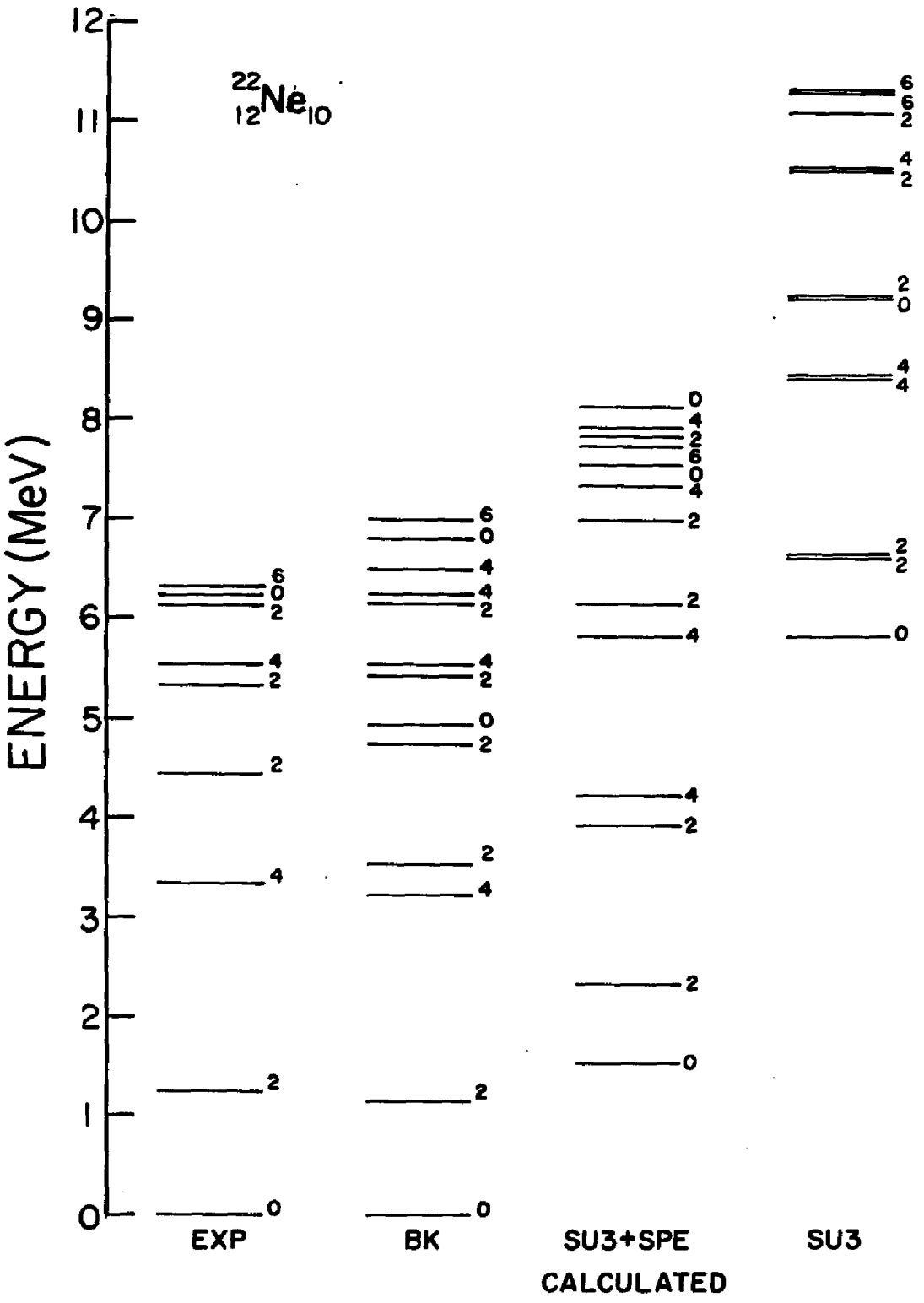
$^{22}_{12}Ne_{10}$
ENERGY (MeV)
12
11
10
9
8
7
6
5
4
3
2
1
0
EXP
BK
SU3+SPE
CALCULATED
SU3

Figure 4

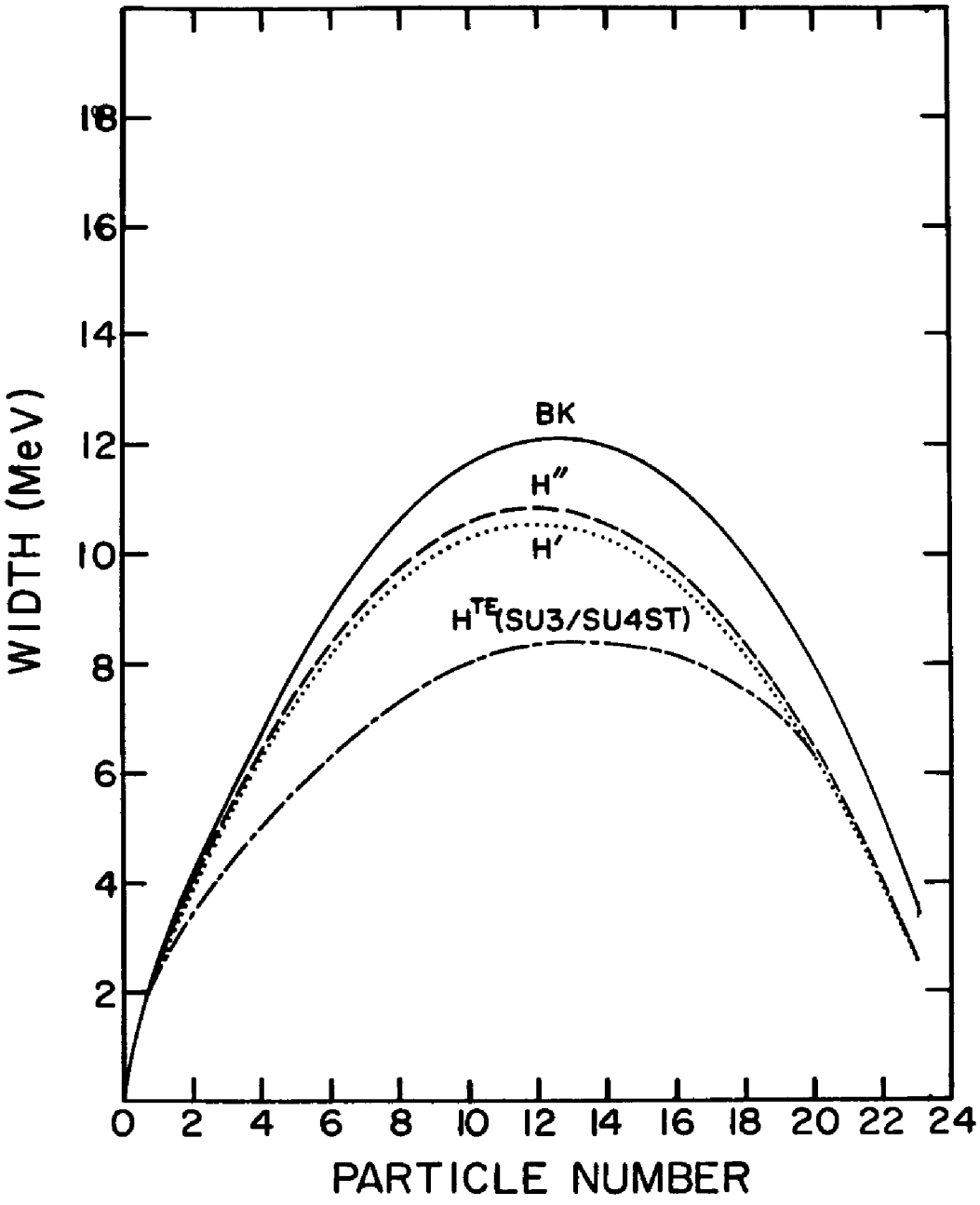
WIDTH (MeV)
18
16
14
12
10
8
6
4
2
0
2
4
6
8
10
12
14
16
18
20
22
24
PARTICLE NUMBER
BK
H''
H'
H^TE(SU3/SU4ST)

Figure 5

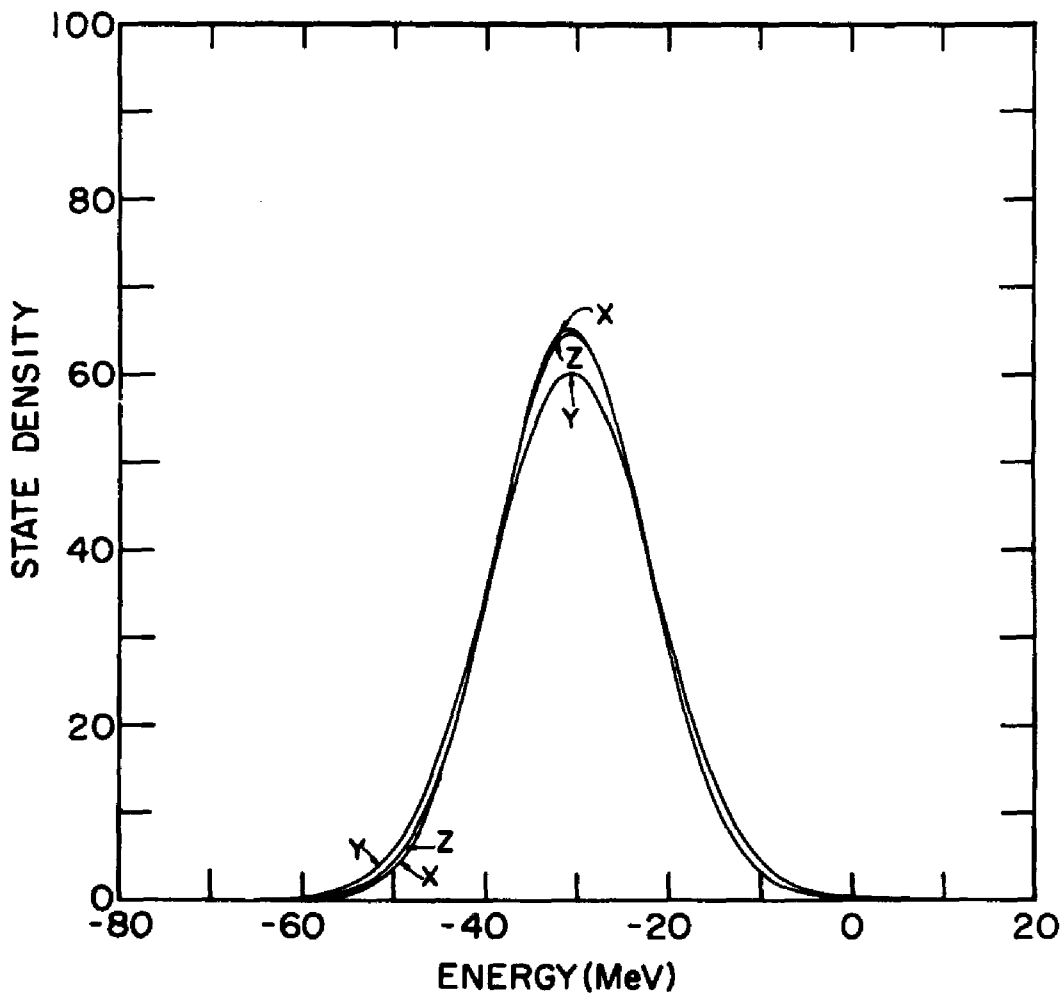
100
80
60
40
20
0
STATE DENSITY
X
Z
Y
Y
Z
X
-80
-60
-40
-20
0
20
ENERGY(MeV)

Figure 6

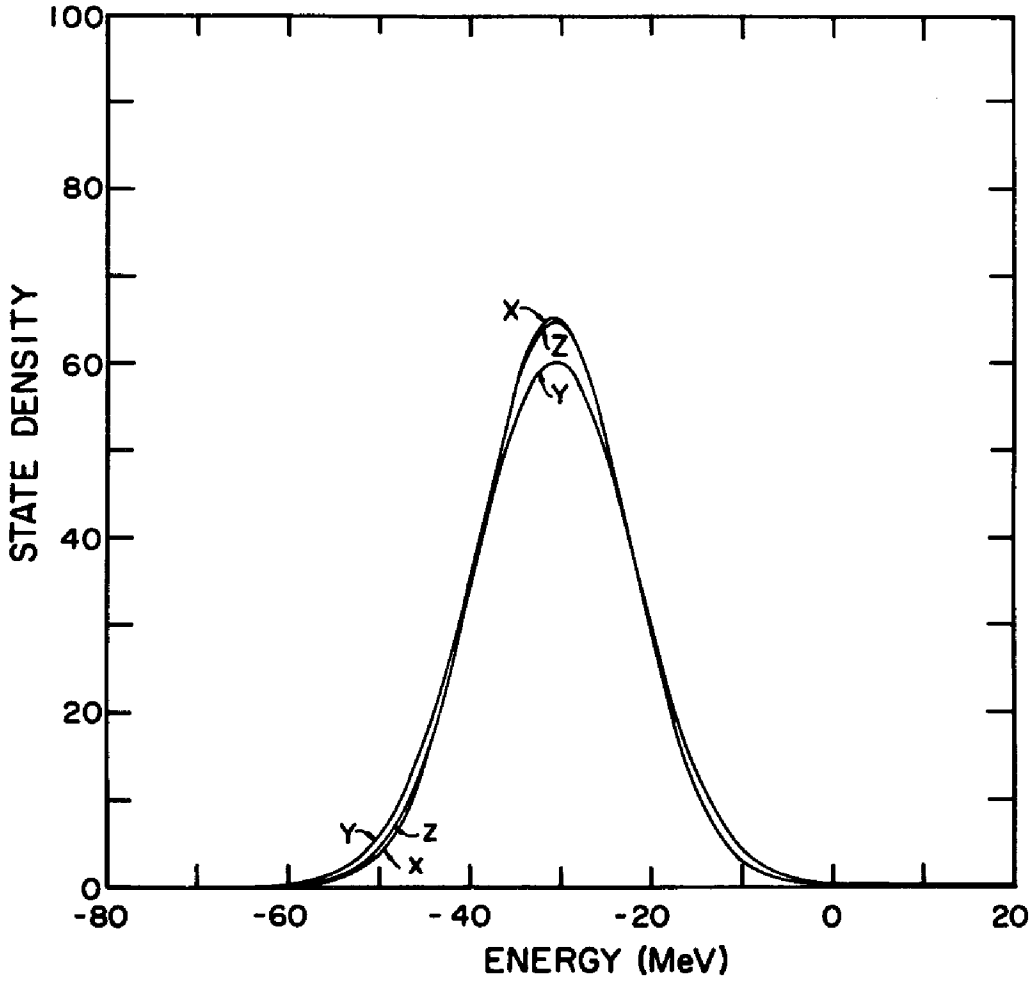
100
80
60
40
20
0
STATE DENSITY
X
Z
Y
Y
Z
X
-80
-60
-40
-20
0
20
ENERGY (MeV)

Figure 7

Table Captions

5. Overlap percentages between eigenstates for $^{20}Ne[(ds)^4\ T = 0]$ generated with the BK interaction and its SU(3) trace-equivalent approximations. Each set of two numbers if for $^{a)}$SU(3) + SPE and $^{b)}$SU(3) [eq. (4.19)]. The sum measures the projection of the BK state into the subspace spanned by the first five eigenstates of the trace-equivalent interaction.

6. Calculated B(E2) values for $^{20}Ne[(ds)^4\ T = 0]$. Each set of three numbers is for $^{a)}$BK interaction $^{b)}$SU(3) + SPE and $^{c)}$SU(3) [eq. (4.19)]. The sum measures the average B(E2) strength to the first five final states.

7. Overlap percentages between eigenstates for $^{22}Ne\ [(ds)^6\ T = 1]$ generated with the BK interaction and its SU(3) trace-equivalent approximations. Each set of two numbers is for $^{a)}$SU(3) + SPE and $^{b)}$SU(3) [Eq. (4.19)]. The sum measures the projection of the BK state into the subspace spanned by the first five eigenstates of the trace-equivalent interaction.

8. Calculated B(E2) values for $^{22}Ne[(ds)^6\ T = 1]$. Each set of three numbers is for $^{a)}$BK interaction

[b] SU(3) + SPE and [c] SU(3) [Eq. (4.19)]. The sum measures the average B(E2) strength to the first five final states.

9. The SU(3)/SU(4)ST polynomial invariants and (0 + 1 + 2 + 3 + 4) -particle defining space irreps. This table demonstrates that it is possible to propagate averages of a (0 + 1 + 2) -body operator simultaneously in the irreps of the SU(4)ST and SU(3) symmetry groups because the number of polynomial invariants equals the number of independent irrep averages in the (0 + 1 + 2) -particle defining space. The table also demonstrates that it is not possible to propagate averages of a (0 + 1 + 2 + 3 + 4) -body operator because the number of polynomial invariants is less than the number of independent irrep averages in the (0 + 1 + 2 + 3 + 4) -particle defining space. See text for details.

10. Dimensionalities and centroids for $1 < m \leq 2$ particles in the ds shell using H'(SU(3)/SU(4)ST).

11. Dimensionalities and widths for $1 < m \leq 2$ particles in the ds shell using H'(SU(3)/SU(4)ST). The numbers in parenthesis were obtained using the constant width approximation.

12. The dimensionalities, centroids, and widths for four particles in the ds shell belonging to the [3100] symmetry using H'(SU(3)/SU(4)ST).

TABLE 5

BK	0_1^+	0_2^+	0_2^+	Σ_1^5
0_1	88[a] 77[b]	5 10	0 2	99 92
0_2	9 14	73 45	5 0	95 93
0_3	0 2	13 29	71 7	96 86

BK	2_1^+	2_2^+	2_3^+	Σ_1^5
2_1^+	93[a] 82[b]	0 3	3 7	95 96
2_2^+	2 3	70 51	9 0	90 58
2_3^+	3 5	15 0	70 68	95 89

BK	4_1^+	4_2^+	4_3^+	Σ_1^5
4_1^+	89[a] 76[b]	0 3	5 11	96 100
4_2^+	9 9	9 1	71 79	95 95
4_3^+	0 4	51 12	16 0	95 67

TABLE 6

J_i \ J_f	0_1^+	0_2^+	0_3^+	$\Sigma_1^5/5$
2_1^+	49.3[a]	2.02	0.03	10.3
	52.9[b]	0.13	<0.01	10.6
	55.9[c]	0	0	11.2
2_2^+	0.09	16.5	0.08	3.4
	<0.01	7.2	0.06	1.5
	0	16.7	0	3.3
2_3^+	0.28	8.8	2.7	2.5
	0.13	18.1	0.8	3.8
	0	11.8	0	2.4

J_i \ J_f	2_1^+	2_2^+	2_3^+	$\Sigma_1^5/5$
4_1^+	61.1[a]	0.38	0.37	12.4
	66.6[b]	0.02	0.15	13.4
	70.9[c]	0	0	14.2
4_2^+	2.9	0.14	13.4	3.5
	0.2	17.1	4.6	4.5
	0	22.8	5.6	5.8
4_3^+	0.22	6.8	0.5	6.1
	0.13	0.13	13.9	3.1
	0	0.02	12.7	2.5

TABLE 7

BK	0_1^+	0_2^+	0_3^+	Σ_1^5
0_1^+	90[a]	0	1	92
	59[b]	8	2	76
0_2^+	2	29	24	80
	3	6	4	56
0_3^+	2	17	52	79
	6	0	19	40

BK	2_1^+	2_2^+	2_3^+	Σ_1^5
2_1^+	94[a]	0	0	94
	71[b]	0	5	76
2_2^+	0	91	0	92
	0	62	0	62
2_3^+	0	0	0	66
	0	0	0	61

BK	4_1^+	4_2^+	4_3^+	Σ_1^5
4_1^+	93[a]	1	0	94
	69[b]	0	8	77
4_2^+	1	85	6	93
	0	62	0	64
4_3^+	0	4	31	71
	0	4	0	35

TABLE 8

J_i \ J_f	0_1^+	0_2^+	0_3^+	$\Sigma_1^5/5$
2_1^+	51.2[a]	1.04	2.28	10.9
	53.6[b]	0.07	1.41	11.1
	71.0[c]	0	0	14.2
2_2^+	3.45	1.8	0.14	1.21
	2.99	1.37	0.03	0.88
	3.78	0	0	0.76
2_3^+	0.95	1.16	0.19	0.51
	0.11	1.77	0.29	0.39
	0	29.35	0	5.87

J_i \ J_f	2_1^+	2_2^+	2_3^+	$\Sigma_1^5/5$
4_1^+	65.9[a]	0.01	2.28	13.8
	69.1[b]	0.43	1.09	14.3
	89.9[c]	0.01	0	18.0
4_2^+	2.75	33.6	0.01	7.29
	0.87	35.5	0.03	7.32
	3.98	39.0	0	8.60
4_3^+	0.03	0.69	7.69	2.08
	0.01	0.22	0.01	0.23
	0	0	89.5	18.0

TABLE 9

Particle Rank	Irreps	Number of Independent irrep	Polynomial Invariants
0	$[0]$	1	1
1	$[1](20), [1]\frac{1}{2}\frac{1}{2}$	1	n
2	$[2](40), [2](02), [1^2]10, [1^2]01$	5	n^2, G_2
	$[1^2](21), [2]00, [2]11$		C_2, S^2, T^2
3	$[3](60), [3](22), [3](00), [1^3]\frac{1}{2}\frac{1}{2}$	12	$n^3, nG_2,$
	$[21](41), [21](22), [21](11), [21]\frac{1}{2}\frac{1}{2}$		nC_2, nS^2
	$[21]\frac{3}{2}\frac{1}{2}, [21]\frac{1}{2}\frac{3}{2}, [1^3](30), [1^3](03)$		C_3
	$[3]\frac{1}{2}\frac{1}{2}, [3]\frac{3}{2}\frac{1}{2}$		
4	$[4](80), [4](42), [4](04), [4](20), [\tilde{1}^4]00$	31	$n^4, n^2G_2,$
	$[31](61), [31](42), [31](23), [31](31), [31](12)$		$n^2C_2, n^2S^2,$
	$[31](20), [\tilde{21}^2]10, [21^2]01, [\tilde{21}^2]11, [22](42)$		$n^2T^2, nG_3,$
	$[22](31), [22](04), [22](20), [\tilde{22}]00,$		$nC_3, (G_1)^2$
	$[\tilde{22}]20, [\tilde{22}]11, [\tilde{22}]02, [21^2](50), [21^2](23)$		$(C_1)^2, (S^2)^2$
	$[21^2](31), [21^2](12), [21^2](01), [\tilde{31}]10, [\tilde{31}]01$		$(T^2)^2, G_2C_2$
	$[\tilde{31}]11, [\tilde{31}]21, [\tilde{31}]12, [1^4](12), [\tilde{4}]00,$		G_2S^2, G_2T^2
	$[\tilde{4}]11, [\tilde{4}]22$		C_2S^2, C_2T^2
			S^2T^2, G_4

TABLE 10

		Dim	Centroid Energies (MeV)
SU(3)/ SU(4)ST	$\varepsilon(1[\tilde{1}](20)11)$	24	-2.312
	$\varepsilon(2[\tilde{1}^2](40)20)$	45	-9.008
	$\varepsilon(2[\tilde{1}^2](40)02)$	45	-7.696
	$\varepsilon(2[\tilde{1}^2](02)02)$	18	-5.494
	$\varepsilon(2[\tilde{1}^2](02)20)$	18	-6.806
	$\varepsilon(2[\tilde{2}](21)00)$	15	-2.994
	$\varepsilon(2[\tilde{2}](21)22)$	135	-4.196
SU(4)ST	$\varepsilon(1[\tilde{1}]11)$	24	-2.312
	$\varepsilon(2[\tilde{1}^2]20)$	63	-8.379
	$\varepsilon(2[\tilde{1}^2]02)$	63	-7.067
	$\varepsilon(2[\tilde{2}]00)$	15	-2.994
	$\varepsilon(2[\tilde{2}]22)$	135	-4.196
SU(3)	$\varepsilon(1[\tilde{1}](20))$	24	-2.312
	$\varepsilon(2[\tilde{1}^2](40))$	90	-8.352
	$\varepsilon(2[\tilde{1}^2](02))$	36	-6.149
	$\varepsilon(2[\tilde{2}](21))$	150	-4.076

TABLE 11

		Dim	Width
SU(3)/ SU(4)ST	$\sigma(1[\tilde{1}]\ (20)11)$	24	2.359 (2.359)
	$\sigma(2[\tilde{1}^2]\ (40)20)$	45	3.278 (4.129)
	$\sigma(2[\tilde{1}^2]\ (40)02)$	45	2.947 (4.129)
	$\sigma(2[\tilde{1}^2]\ (02)02)$	18	3.466 (4.129)
	$\sigma(2[\tilde{1}^2]\ (02)20)$	18	3.752 (4.129)
	$\sigma(2[\tilde{2}]\ (21)00)$	15	3.638 (3.262)
	$\sigma(2[\tilde{2}]\ (21)22)$	135	3.217 (3.262)
SU(4)ST	$\sigma(1[\tilde{1}]11)$	24	2.359
	$\sigma(2[\tilde{1}^2]20)$	63	4.403
	$\sigma(2[\tilde{1}^2]02)$	63	4.085
	$\sigma(2[\tilde{2}]00)$	15	3.638
	$\sigma(2[\tilde{2}]22)$	135	3.217
SU(3)	$\sigma(1[\tilde{1}]\ (20))$	24	2.359
	$\sigma(2[\tilde{1}^2]\ (40))$	90	3.540
	$\sigma(2[\tilde{1}^2]\ (02))$	36	4.039
	$\sigma(2[\tilde{2}]\ (21))$	150	3.389

TABLE 12

$\tilde{[f]}$	$(\lambda\mu)ST$	Dim	$\epsilon(m\tilde{[f]}(\lambda\mu)ST)$	$\sigma(m\tilde{[f]}(\lambda\mu)ST)$
[3100]	(50)20	63	-13.847	3.154
	(50)02	63	-12.536	3.028
	(50)22	189	-13.792	3.002
	(50)42	315	-16.306	2.950
	(50)24	315	-13.682	2.673
	(23)20	126	-13.114	3.238
	(23)02	126	-11.802	3.116
	(23)22	378	-13.058	3.090
	(23)42	630	-15.572	3.039
	(23)24	630	-12.948	2.771
	(31)20	72	-12.012	3.360
	(31)02	72	-10.701	3.242
	(31)22	216	-11.957	3.218
	(31)42	360	-14.471	3.169
	(31)24	360	-11.847	2.913
	(12)20	45	-10.911	3.478
	(12)02	45	-9.599	3.364
	(12)22	135	-10.856	3.341
	(12)42	225	-13.369	3.294
	(12)24	225	-10.745	3.048
	(01)20	9	-9.443	3.629
	(01)02	9	-8.131	3.520
	(01)22	27	-9.387	3.498
	(01)42	45	-11.901	3.453
	(01)24	45	-9.277	3.219

CHAPTER V

ALPHA PARTICLE TRANSFER STRENGTH BY SPECTRAL DISTRIBUTION METHODS

A. Introduction

In this chapter, we apply spectral distribution methods to a study of alpha particle transfer strengths. We make specific predictions for the reactions $^{18}O+\alpha \rightleftarrows {}^{22}Ne$ and $^{20}Ne+\alpha \rightleftarrows {}^{24}Mg$. The method involves partitioning the fixed J, T initial (target nucleus) and final (residual nucleus) state model space according to the supermultiplet symmetry.[47] We then calculate the two lowest moments of our effective interaction H"(SU(3)/SU(4)ST) in each configuration and use the moments to estimate the eigenenergies and configuration densities for the initial and final state subspaces. We also calculate traces of the operator products $0^{+}H^{q}0H^{p}$, $q\leq 1$ and $p\leq 1$, which together with the initial and final state densities allows us to evaluate a CLT approximation for the alpha particle transfer strengths.

B. Fixed Symmetry Moments

We partition the fixed J initial and final state model spaces according to the SU(4)ST symmetry. In the ds shell, this is achieved by partitioning the model

space into its spatial and spin-isospin parts, $U(24) \supset U(6) \otimes U(4)$ with the further decomposition $U(4) \supset SU(4)$ $SU_S(2) \otimes SU_T(2)$ where the U(4) decomposition involves the direct product of the spin and isospin SU(2) groups. For totally antisymmetric states the irreps of $U(4) \supset SU_S(2) \otimes SU_T(2)$ define the partitioning uniquely and are labelled in the standard way by $\{m[\tilde{f}]ST\}$. Here $[\tilde{f}] = [\tilde{f}_1, \tilde{f}_2, \tilde{f}_3, \tilde{f}_4]$ labels the U(4) irreps and ST labels the $SU_S(2) \otimes SU_T(2)$ irreps contained in $[\tilde{f}]$. We are interested in those $m[\tilde{f}]ST$ irreps that lead to states of fixed J. The fixed J $\{m[\tilde{f}]ST\}$ dimensionality is the number of times the fixed J value occurs. For example, the model space of J=0, T=0 states of ^{20}Ne, $(ds)^4$, is 21 dimensional. The supermultiplet symmetry partitions the space into five subspaces: $4[1^4]00$, $4[21^2]20$, $4[2^2]00$, $4[2^2]40$, and $4[31]20$ with dimensionalities 4, 4, 3, 5 and 5 respectively.

The Hamiltonian of our system is given by H"(SU(3)/SU(4)ST), our statistical approximation[31,36] to the BK interaction,

$$\begin{aligned} H"(SU(3)/SU(4)ST) = {} & H^{TE}(SU(3)/SU(4)ST) \\ & - 1.7051(n_1 - n_1^{TE}(SU(3)/SU(4)ST)) \\ & + 3.4933(n_2 - n_2^{TE}(SU(3)/SU(4)ST)) \\ & + 0.1285(L^2 - L^{2TE}(SU(3)/SU(4)ST)) \end{aligned} \qquad (5.1)$$

Here $H^{TE}(SU(3)/SU(4)ST)$ is given by Eq. (4.21). If we assume a normal distribution for states belonging to a definite $\{m[\tilde{f}]ST,J\}$ then the following two moments characterize the distribution

$$\varepsilon(m[\tilde{f}]ST,J) = \langle H''\rangle^{m[\tilde{f}]ST,J}$$

$$= d^{-1}(m[\tilde{f}]ST,J) \sum_{i\varepsilon[f]ST,J} \langle i|H''|i\rangle \qquad (5.2)$$

$$\sigma^2(m[\tilde{f}]ST,J) = \langle (H''-\langle H''\rangle^{m[\tilde{f}]ST,J})^2\rangle^{m[\tilde{f}]ST,J}$$

$$= \langle H''^2\rangle^{m[\tilde{f}]ST,J} - \varepsilon^2(m[\tilde{f}]ST,J) \qquad (5.3)$$

where

$$\langle H''^2\rangle = d^{-1}(m[\tilde{f}]ST,J) \sum_{i\varepsilon m[f]ST,J} \langle i|H''^2|i\rangle$$

$$= d^{-1}(m[\tilde{f}]ST,J) \sum_{\substack{i\varepsilon m[f]ST,J \\ j\varepsilon m[\tilde{f}]ST,J}} \langle i|H''|j\rangle\langle j|H''|i\rangle$$

$$+ \sum_{\substack{i\varepsilon m[f]ST,J \\ j\notin m[\tilde{f}]ST,J}} \langle i|H''|j\rangle\langle j|H''|i\rangle \qquad (5.4)$$

and

$$d(m\tilde{[f]}ST,J) = \sum_{i\varepsilon m\tilde{[f]}ST,J} \langle i|i\rangle \qquad (5.5)$$

In Eqs. (5.2-5.5) the sum is over all basis states that belong to the irrep $\{m\tilde{[f]}ST,J\}$ and $d(m\tilde{[f]}ST,J)$ is the total number of states over which the sum is taken. Here $\varepsilon(m\tilde{[f]}ST,J)$ and $\sigma(m\tilde{[f]}ST,J)$ are, respectively, the centroid and width of the fixed$\{m\tilde{[f]}ST,J\}$ configuration. Due to technical difficulties in obtaining all of the necessary matrix elements of the orbital number operator we had to use H"(SU(3)/SU(4)ST) without the n_r dependence to calculate the moments. The effects of this restriction will be discussed in the next section. Centroids, widths, and dimensionalities for the $\{m\tilde{[f]}ST,J\}$ needed for our study of alpha particle transfer strengths are shown in Tables 13-16. Observe that for $(ds)^4$ the centroid span is ~28 MeV; however, for m=2 the span is only ~3 MeV. Also note that those SU(4)ST irreps for which the centroids lie lowest have the largest widths. This can be seen even more clearly from calculating the intensity of the various irreps.

C. Ground State and Low-Lying Energies And Relative Intensities

The spectral moments can be used to estimate the ground state and low-lying energies using a procedure suggested by Ratcliff.[8] The method is based on making a continuous approximation to the exact discrete distribution. The cummulative distribution function, F(E,J), is defined as the integral of the sum of all the SU(4)ST frequency functions for a fixed J, i.e.,

$$F(E,J) = \sum_{m[\tilde{f}]ST,J} \frac{d(m[\tilde{f}]ST,J)}{\sqrt{2\pi}\sigma(m[\tilde{f}]ST,J)} \int_{-\infty}^{E} \exp - \frac{(E'-\varepsilon(m[\tilde{f}]ST,J))^2}{2\sigma^2(m[\tilde{f}]ST,J)} \, dE' \qquad (5.6)$$

The continuous distribution function F(E,J) can be regarded as a best fit to the exact discrete function if at the eigenenergy E_i (i=1,2,3,...) it takes on the value (i - 1/2). Ratcliff uses this relationship to define the approximate eigenenergy E_i as that value of E for which F(E,J) = i - 1/2. More precisely

$$F(E_i,J) = \sum_{m[\tilde{f}]ST,J} \frac{d(m[\tilde{f}]St,J)}{\sqrt{2\pi}\sigma(m[\tilde{f}]ST,J)}$$

$$\int_{-\infty}^{E_i} \exp - \frac{(E'-\varepsilon(m[\tilde{f}]St,J))^2}{2\sigma^2(m[\tilde{f}]ST,J)} \, dE' = i - 1/2$$

(5.7)

The 2J+1 rotational degeneracy factor has not been included in the definition of F(E,J). For example, to estimate the $J = 0_1^+$ state of ^{20}Ne one must sum and integrate, using an iterative procedure with convergence checks, the five J=0, T=0 distributions whose dimensionality, centroids, and widths are given in Table 14 to determine that value of E such that $F(E_1, J=0_1^+) = 1/2$. To estimate the $J = 4_2^+$ state of ^{22}Ne$((ds)^6_{T=1})$ we would have to integrate and sum seventeen J=4, T=1 distributions to find E such that $F(E_2, J=4_2^+) = 1.5$. Using such a procedure we were able to estimate the ground state and some low-lying states of the ds shell nuclei needed for our study. Results of these calculations are shown in Tables 17 and 18 together with results obtained from detailed shell model calculations[45] using our effective interaction H"(SU(3)/SU(4)ST). There is reasonably good agreement between the spectral distribution energy predictions and the shell model eigenenergies.

There are at most a 2-3 MeV differences. In the case of ^{20}Ne the $J=0_2^+$ state is reproduced exactly. Note that the spectral distribution method predicts the $J=2_1^+$ and 4_1^+ states of ^{22}Ne$\{(ds)^6_{T=1}\}$ and ^{24}Mg$\{(ds)^8_{T=0}\}$ to be lower than the ground state. This discrepancy is probably due to the exclusion of the orbital number operator in calculating the spectral distribution moments for these nuclei.

Having determined approximate eigenenergies using spectral distribution methods, we take a more detailed look at the distributions to find out the contribution made by each SU(4)ST irrep to the total area under the F(E,J) curve. We interpret these contributions as the relative intensities of the various SU(4)ST representations in the eigenstate region. Specifically, if $\vec{m}$ labels an SU(4)ST symmetry $\{m[\tilde{f}]ST,J\}$ and W is an eigenenergy then the relative intensity of the configuration $\vec{m}$ at W is defined as

$$\frac{I_{\vec{m}}(W)}{I_m(W)} = \frac{\int_{-\infty}^{W} f(\vec{m},E')\,dE'}{F(m,W)} \qquad (5.8)$$

with the normalization condition

$$\sum_{\vec{m}} \frac{I_{\vec{m}}(W)}{I_m(W)} = 1 \ . \tag{5.9}$$

The frequency function $f(\vec{m},E)$ is given by

$$f(\vec{m},E) = \frac{d(\vec{m})}{\sqrt{2\pi}\sigma(\vec{m})} \exp - \frac{(E-\varepsilon(\vec{m}))^2}{2\sigma^2(\vec{m})} \tag{5.10}$$

and

$$F(m,W) = \sum_{\vec{m}} \int_{-\infty}^{W} f(\vec{m},E')\,dE' \tag{5.11}$$

The relative intensities of the different configurations, evaluated at the predicted eigenenergies, can be interpreted as the intensities of the various components in the eigenfunction. Relative intensities of low-lying states in ^{18}O, ^{20}Ne, ^{22}Ne and ^{24}Mg for the SU(4)ST irreps are shown in Tables 19 and 20. These intensities were calculated directly using Eqs. (5.8-5.11). The numbers in parentheses are the intensities obtained by Arima and Strottman[46] using the Brown-Kuo interaction.[44] In their study they calculated the low-lying wavefunction in the SU(3) scheme and then determined what percentage of the state has a given SU(4) symmetry. There is very good agreement between the analysis done using low moment distributions and the more complete SU(3) analysis. Relative intensities of various configurations indicate

that for the lower half of the ds shell the SU(4)ST is a reasonably good symmetry.

The relative intensity of a configuration, properly weighted by configuration averages of an excitation operator and the Hamiltonian H gives the contribution that configuration makes to the total excitation strength. If $\chi^{+}{}^{[4]00,J_o}$ is the four nucleon transfer operator then the zeroth approximation to the alpha particle transfer strength is given by[9]

$$R(W,W') \sim \sum_{\vec{m}\vec{m}'} \frac{I_{\vec{m}}(W)\, I_{\vec{m}'}(W')}{I_{m}(W)\, I_{m'}(W')} \langle\langle \chi(\vec{m}'-\vec{m})\, \chi^{+} \rangle\rangle^{\vec{m}} \qquad (5.12)$$

where the sum is over initial and final state configurations. The product of the two intensity functions, one for the target and one for the final nucleus, is weighted by the average strength, $\langle\langle \chi(\vec{m}'-\vec{m})\, \chi^{+} \rangle\rangle^{\vec{m}}$ with which the transfer operator couples the two configurations $\vec{m}$ and $\vec{m}'$. The histograms in Figs. 8 and 9 display cases of interest in $^{18}O+\alpha \rightarrow {}^{22}Ne$ and $^{20}Ne+\alpha \rightarrow {}^{24}Mg$. For example the $\{2[1^2]02,\ J=0\}$ configuration in the ^{18}O ground state (85% intensity) coupled to the $\chi^{+}{}^{[4]00,J_o}$ four nucleon transfer operator carries one to the $\{6[2^2 1^2]02,J\}$ configuration of ^{22}Ne (53% intensity for J=0, 54% for J=2, 55% for J=4, 53% for J=6 and 50% for J=8). Likewise the $\{2[22]2,\ J=0\}$ configuration in the ^{18}O ground state (15% intensity) coupled to the transfer operator carries

one to the $\{6[31^2]22,J)\}$ configuration in ^{22}Ne (32% for J=0, 29% for J=2, 27% for J=4, 29% for J=6 and 32% for J=8). In this case the sum is only over two configurations and the averages $<<\chi(\vec{m}'-\vec{m})\chi^+>>^{\vec{m}}$ are very easy to evaluate. The alpha particle transfer operator χ^+ and the averages $<<\chi(\vec{m}'-\vec{m})\chi^+>>^{\vec{m}}$ will be discussed in greater detail in the next section.

D. The Alpha Particle Transfer Strength Function

For the ds shell the alpha particle transfer operator is built from four nucleon creation operators, a^+, properly coupled to quantum numbers $[4](80)L_oS_oJ_oT_o$.[2]

$$\chi^{+[4](80)L_oS_oJ_oT_o} = [a^+xa^+xa^+xa^+]^{[4](80)L_oS_oJ_oT_o} \tag{5.13}$$

For states labelled by $[f]\alpha(\lambda\mu)\beta STM_T\kappa_L LJ$, the reduced (double-barred) matrix element of the four nucleon creation operator of Eq. (5.13) is given by[2,3] (see Chapter 2 for details)

$$<[f']\alpha'(\lambda'\mu')\beta'S'T'M_T'\kappa_L'L'J'||\chi^{[4](80)L_oS_oJ_oT_o}$$

$$||[f]\alpha(\lambda\mu)\beta STM_T\kappa_L LJ>$$

$$= X\begin{pmatrix} L & S & J \\ L_o & S_o & J_o \\ L' & S' & J' \end{pmatrix} <(\lambda\mu)\kappa_L L;(80)L||(\lambda'\mu')\kappa_L'L'>$$

$$x <[f]\alpha(\lambda\mu)\beta ST;[4](80)L_oS_oT_o|\}[f']\alpha'(\lambda'\mu')\beta'S'T'>$$

$$x <TM_TT_oM_{T_o}|T'M_T'> \qquad (5.14)$$

Here X( ) is an angular momentum 9-j coefficient in unitary form and the double-barred coefficient is an SU(3)/R(3) Wigner coefficient. The factor $<[f]\alpha(\lambda\mu)\beta ST;[4](80)L_oS_oT_o|\}[f']\alpha'(\lambda'\mu')\beta'S'T'>$ is the SU(6)/SU(3) and SU(4)ST factors of a four particle coefficient of fractional parentage. The representation $[\tilde{f}] = [1^4]$ (contragredient to [f] = [4]) corresponds to the scalar representation of SU(4) with $S_o=T_o=0$ so that $L_o=J_o=0$, 2, 4, 6, and 8. Therefore the operator $\chi^{+[4](80)L_oS_oJ_oT_o}$ will only couple states with the same SU(4)ST symmetry, i.e., $[\tilde{f}]ST = [\tilde{f}']S'T'$. The reduced matrix elements of the operator $\chi^{+[4](80)L_oS_oJ_oT_o}$ are related to the reduced matrix elements of the operator

$$(\chi^{+[4](80)L_oS_oJ_oT_o})^{+} \equiv \chi^{[4^5](08)L_oS_oJ_oT_o}$$

by

$$\langle \Gamma J||\chi^{\Gamma'_o}||\Gamma'J'\rangle = (-)^{J+J_o-J'}[(2J'+1)/(2J+1)]^{1/2}\langle \Gamma'J'||\chi^{+\Gamma_o}||\Gamma J\rangle \qquad (5.15)$$

where Γ and Γ' are the additional quantum numbers needed to specify the initial and final state. Γ'_o and Γ_o are the quantum numbers needed to describe the transfer operators. The full matrix element of the operator $\chi^{+\Gamma_o}$ is given by

$$\langle \Gamma'J'M'_J|\chi^{+\Gamma_o}|\Gamma JM_J\rangle = \langle J'M'_JJ_oM_o|J'M'_J\rangle\langle \Gamma'J'||\chi^{+\Gamma_o}||\Gamma J\rangle \qquad (5.16)$$

The reduced SU(3)/R(3) Wigner coefficients and the four particle SU(6){SU(4)} cfp needed to calculate the reduced matrix element of $\chi^{+\Gamma_o}$ was obtained from the SU(3) code of Draayer[10] and Akiyama and the SU(3)-SU(4) CFP code of Braunschweig.[11]

If $\chi^{+\Gamma_o}$ is the alpha particle transfer operator then the polynomial expansion of the alpha particle

transfer strength function in the CLT limit is given by[9] (see Chapter 3 for details)

$$R(mW;m'W') = \sum_{\vec{m}\vec{m}'} \frac{I_{\vec{m}}(W)\, I_{\vec{m}'}(W')}{I_m(W)\, I_{m'}(W')} \left[d(\vec{m})\, d(\vec{m}')\right]^{-1} \sum_{\mu=0}^{1} \sum_{\nu=0}^{1}$$

$$\langle\langle \chi^{\Gamma'_o}(\vec{m}'-\vec{m})\, P_\mu^{\vec{m}'}(H'')\, \chi^{+\,\Gamma_o} P_\nu^{\vec{m}}(H'')\rangle\rangle^{\vec{m}} P_\mu^{\vec{m}'}(W')\, P_\nu^{\vec{m}}(W) \qquad (5.17)$$

The polynomial expansion of the non-energy weighted sum rule associated with $\chi^{+\,\Gamma_o}$ for the CLT limit is given by[9]

$$M_o(W) = \sum_{\vec{m}} \frac{I_{\vec{m}}(W)}{I_m(W)} \sum_{\nu=0}^{1} \langle \chi^{\Gamma'_o}(\vec{m}'-\vec{m})\, \chi^{+\,\Gamma_o} P_\nu^{\vec{m}}(H'')\rangle^{\vec{m}} P_\nu^{\vec{m}}(W) \qquad (5.18)$$

where

$$P_o^{\vec{m}}(x) = 1 \quad \text{and} \quad P_1^{\vec{m}}(x) = \frac{(x-\varepsilon(\vec{m}))}{\sigma(\vec{m})} \; ; \quad P_o^{\vec{m}'}(x) = 1$$

$$\text{and } P_1^{\vec{m}'}(x) = \frac{(x-\varepsilon(\vec{m}'))}{\sigma(\vec{m}')}$$

Here W and W' are eigenenergies of the initial and final state model spaces. In the strength function we are summing over all initial, $\vec{m} \equiv m[\tilde{f}]ST$, and final, $\vec{m}' \equiv m'[\tilde{f}']S'T'$, state configurations. $\varepsilon(\vec{m})$ and $\varepsilon(\vec{m}')$, $\sigma(\vec{m})$ and $\sigma(\vec{m}')$, and $d(\vec{m})$ and $d(\vec{m}')$ are the centroid, width and

dimensionality of the initial and final state configurations, respectively. The double bracket denotes a trace and the single bracket an average. The Hamiltonian H" is given by Eq. (5.1). The relative intensities $I^{\rightarrow}_{\vec{m}}(W)/I_m(W)$, dimensionalities, centroids, widths of all configurations are given in Tables 13-16 and Figs. 8-9. So the task comes down to evaluating the trace of the operators

$$\chi^{\Gamma'_o}\left(\frac{H''-\varepsilon(m')}{\sigma(\vec{m}')}\right)^q \chi^{+\Gamma_o}\left(\frac{H''-\varepsilon(\vec{m})}{\sigma(\vec{m})}\right)^p \quad \text{(with } p,q = 0,1)$$

in each $\{m[\tilde{f}]ST,J\}$ space. Evaluation of the necessary traces is discussed in Appendix A. The traces needed to study the reaction $^{18}O((ds)^2_{T=1})+\alpha \overset{\rightarrow}{\leftarrow} {}^{22}Ne((ds)^6_{T=1})$ are given in Table 21 and the required traces for the reaction $^{20}Ne((ds)^4_{T=0})+\alpha \overset{\rightarrow}{\leftarrow} {}^{24}Mg((ds)^8_{T=0})$ are given in Table 23. Due to technical difficulties in evaluating all the matrix elements of the orbital number operators, $\sum_r n_r$, in the $(ds)^8$ system the traces for $^{20}Ne+\alpha \overset{\rightarrow}{\leftarrow} {}^{24}Mg$ were evaluated using H" without the orbital number operator. To study the effect of this approximation we also evaluated the traces for $^{18}O+\alpha \overset{\rightarrow}{\leftarrow} {}^{22}Ne$ using H" without the orbital number operator. The results are shown in Table 22. There is little difference between the traces evaluated using H" and those evaluated using H" without the orbital number operator. The magnitude of the traces increase

as more correlations are included. All traces are of the same order of magnitude except for configurations connecting the $J=0^+$ state of ^{18}O to the $J=8$ state of ^{22}Ne. The cause and effect of this will be discussed in the next section. We are now in a position to predict alpha particle transfer strengths for the reaction $^{18}O+\alpha \rightleftarrows {}^{22}Ne$ and $^{20}Ne+\alpha \rightleftarrows {}^{24}Mg$.

E. Predicted Strengths

Our objective is to tabulate results which will help determine whether spectral distribution methods can be an alternative to the conventional approach of calculating alpha particle transfer strengths. With this in mind we will compare our predictions with predictions from detailed shell model calculations[23,26] and the SU(3) pure symmetry model[3] as well as experiment.[16,20,25] We have defined and used the alpha particle transfer strength function (Eq. 5.17) to calculate strengths for the alpha particle stripping and pickup reactions $^{18}O+\alpha \rightleftarrows {}^{22}Ne$ and $^{20}Ne+\alpha \rightleftarrows {}^{24}Mg$.

The predicted strengths for $^{18}O+\alpha \rightleftarrows {}^{22}Ne$ and $^{20}Ne+\alpha \rightleftarrows {}^{24}Mg$ are given in Tables 24 and 25, respectively. We have calculated the CLT approximation to the strength, labelled CLT limit. In the case of $^{18}O+\alpha \rightleftarrows {}^{22}Ne$, the first set of CLT predictions was obtained using our statistical approximation to the Brown Kuo interaction H" and the

second set of CLT predictions was obtained using H" without the orbital number operators. This was done to determine the effects of the single particle energies. For $^{20}NE+\alpha \rightleftarrows {}^{24}Mg$ the CLT predictions were obtained using H" without the orbital number operators because of technical difficulties in obtaining all the matrix elements of the number operators in the $(ds)^8$ system. We compare our CLT predictions with predictions based on the SU(3) pure symmetry model,[3] detailed shell model calculations using the Brown-Kuo interaction[23,26] and, where possible, experimental findings.[16,20,25] The numbers in parenthesis are the absolute value of the ground state to ground state strengths. All other numbers are relative to the predicted ground state strength and are therefore to be compared to unity. The absolute value of any other strength can be determined by simply multiplying the tabulated result by the number given in parenthesis. There is reasonable agreement between the CLT predictions and the other theoretical predictions. There is also good agreement with experimental results. Comparing the two CLT predictions for $^{18}O+\alpha \rightleftarrows {}^{22}Ne$, we observe that the single particle shell structure has negligible effect on the strength. For the reaction $^{18}O+\alpha \rightleftarrows {}^{22}Ne$ the CLT limit predicts the strength for the $J=8^+_1$ to be very strong whereas the SU(3) symmetry model predicts the strength to be very weak. This discrepancy is due in part because

the pure symmetry model assumes the $J=8^+_1$ state of ^{22}Ne to have quantum numbers $[\tilde{f}](\lambda\mu)\kappa \equiv [42](82)0$. In the statistical theory the sum is over all basis states with quantum number $(\lambda\mu)\kappa$ contained in $[\tilde{f}]ST$ and for $J=8^+_1$ there are large contributions from other $(\lambda\mu)\kappa$ in the $[\tilde{f}] = [42]$ symmetry, such as the (82)1, (63)1, (63)2 and (71)1. Since the partitioning is by $[\tilde{f}]ST$ these non dominant SU(3) representations $(\lambda\mu)\kappa$ are weighted by the same intensity factor as the dominant SU(3) representation (80)1. This problem could be corrected by partitioning the model space according to $\{m[\tilde{f}](\lambda\mu)ST,J\}$. Then for the $J=8^+_1$ state we would only get large contributions from the dominant representations $(\lambda\mu)\kappa \equiv (82)0$ and (82)1. The contributions from the other non-dominant representations will be small because they will be weighted by smaller intensity factors. For the reaction $^{22}Ne+\alpha \rightarrow {}^{18}O$ the CLT predicts the strength for the $J=4^+_1$ to be weak whereas the pure symmetry model predicts the strength to be very strong. This is because the pure symmetry model assumes the $J=4^+_1$ state of ^{18}O to be pure $(\lambda\mu)=(40)$ when in fact it is only about 52% $(\lambda\mu)=(40)$ and the rest $(\lambda\mu)=(21)$ L=3, S=1. In this case representation mixing is important. When representation mixing is taken into account there is a reduction from 2.28 to 0.87 in the SU(3) predictions. Likewise for the reaction $^{24}Mg+\alpha \rightarrow {}^{20}Ne$ the pure symmetry model predicts

the $J'=6_1^+$ and $J'=8_1^+$ states to have relative strength of 1.84 and 1.02, respectively whereas we predict the strengths to be 0.38 and 0.14. When representation mixing is taken into account there is a reduction from 1.84 to 1.02 and from 1.02 to 0.57.

The strength, R(W',W), multiplied by the initial and final states densities give us the density-weighted strength which is the strength per unit energy,

$$S(W',W) = I(W')R(W',W)I(W) \tag{5.19}$$

In Fig. 10 we display three dimensional plots for the strength, R(W',W), two perspectives of the strength per unit energy, S(W',W), and the product of the initial and final state densities, I(W') I(W), for the reaction $^{18}O(J=0^+)+\alpha \rightarrow {}^{22}Ne(J=2^+)$. Similar results are given in Fig. 11 for the reaction $^{20}Ne(J=0^+)+\alpha \rightarrow {}^{24}Mg(J=2^+)$. For the reaction $^{18}O(J=0^+)+\alpha \rightarrow {}^{22}Ne(J=2^+)$, the plot for the strength, R(W',W), shows the strength is strongest for energies near the ground state (W ~ -12 MeV) of ^{18}O and low-lying 2^+ states (W' ~ -60 MeV) of ^{22}Ne. The strength falls to a minimum past the ground state region. There is a small increase in the strength at energies near the $J = 0_3^+$ state of ^{18}O (W ~ -3 MeV) and higher lying 2^+ states (W' ~ -30 MeV) of ^{22}Ne. The strength per unit

energy, S(W',W), similarly shows a peak for W near the ground state of ^{18}O and for W' at the low end of the 2^+ spectrum of ^{22}Ne. There is a second peak in S(W',W) near the $J=0^+_3$ state of ^{18}O and at intermediate 2^+ energies of ^{22}Ne. The second peak is enhanced primarily by the 2^+ intensity factor which is large because W' ~ -30 MeV is close to the centroid of the 2^+ spectrum. The three dimensional plot of I(W)I(W'), which is essentially the product of two Gaussians, demonstrates the normality of the product distribution. As expected the intensity product has a maximum at W = -6.6 MeV, W' = -32.0 MeV the centroids of the $(ds)^2$ J=0 T=1 subspace and the centroid of the $(ds)^6$ J=0 T=1 subspace, respectively. Note that the strength is not a maximum at these energies. This is a unique feature, not found in studies of other excitation processes. Figure 11 shows similar features for $^{20}Ne(J=0^+)+\alpha \rightarrow {}^{24}Mg(J=2^+)$. The intensity product has a maximum value at W = -19.8 MeV, W' = -52.8 MeV the centroids of the $(ds)^4$ J=0 T=0 subspace and the centroid of the $(ds)^8$ J=2 T=0 subspace, respectively. The strength is again not a maximum at these energies. The strength is strongest for energies near the ground state of ^{20}Ne (W ~ -40 MeV) and low-lying 2^+ states of ^{24}Mg (W' ~ -90 MeV) and falls rapidly for higher energies. The strength per unit energy, S(W',W), show peaks at energies near the ground state of ^{20}Ne (W ~ -35 MeV) and

at low-lying 2^+ states of ^{24}Mg (W' ~ 75 MeV) as well as at energies W ~ -20 MeV and W' ~ -55 MeV. From these results we conclude that the alpha transfer strength is strongly concentrated in the ground state region.

We have calculated the non-energy weighted sums (Eq. 5.18) in the CLT limit.[9] Each sum is a prediction for the total strength originating from the ground state of the target nuclei to all states of fixed J^π in the residual nuclei. Table 26 shows the percentage of this summed strength which resides in the transition from the ground state to the J' state of the residual nucleus. Note that a large fraction of the summed strength is concentrated in the ground state to ground state band transitions. The stripping strength from the ground state of ^{18}O to the $J^\pi = 0_1^+$ state in ^{22}Ne, for example, accounts for 40% of the sum rule strength. The remaining 60% resides in transitions to excited 0^+ states of ^{22}Ne. The strengths from the ground state of ^{20}Ne to the $J = 2_1^+$ and 2_2^+ states of ^{24}Mg are 25% and 16% of the summed strength, respectively. We note that the $J = 8_1^+$ state of ^{22}Ne accounts for 89% of the summed strength. This prediction is a direct result of the problem discussed earlier. Our results are consistent with conclusions drawn from studies with the SU(3) pure symmetry model. Draayer[3] and others[1,2] concluded in their studies that most of the α transfer strength is concentrated in the ground state rotational band

whenever the SU(3) symmetry is good as it is for nuclei in the first half of the ds shell.

Figure Captions

8. Relative configuration intensities for calculating alpha particle transfer strengths for the reaction $^{18}O + \alpha \rightleftarrows {}^{22}Ne$. The lowest order approximation to the strength is a sum over the product of the two configuration intensity functions weighted by the average strength, $\langle\langle \chi^{\Gamma'_o}_{o}(\vec{m}'-\vec{m})\ \chi^{+\Gamma_o}_{o}\rangle\rangle^{\vec{m}}$, with which the excitation operator couples the two configurations.

9. Relative configuration intensities for calculating alpha particle transfer strengths for the reaction $^{20}Ne + \alpha \rightleftarrows {}^{24}Mg$. The lowest order approximation to the strength is a sum over the product of the two configuration intensity functions weighted by the average strength, $\langle\langle \chi^{\Gamma'_o}_{o}(\vec{m}'-\vec{m})\ \chi^{+\Gamma_o}_{o}\rangle\rangle^{\vec{m}}$, with which the excitation operator couples the two configurations.

10. Three dimensional plots for a) the strength R(W',W) [Eq. (3.15)], b) and c) two perspectives of the density-weighted strength S(W',W) [Eq. (5.19)], and d) the product of the initial and final state densities, I(W') I(W), for the reaction $^{18}O(J = 0^+) + \alpha \rightarrow {}^{22}Ne\ (J = 2^+)$.

11. Three dimensional plots for a) the strength $R(W',W)$ [Eq. (5.17)], b) and c) two perspectives of the density-weighted strength $S(W',W)$ [Eq. (5.19)], and d) the product of the initial and final state densities, $I(W')\ I(W)$, for the reaction $^{20}Ne\ (J = 0^+) + \alpha \rightarrow {}^{24}Mg\ (J = 2^+)$.

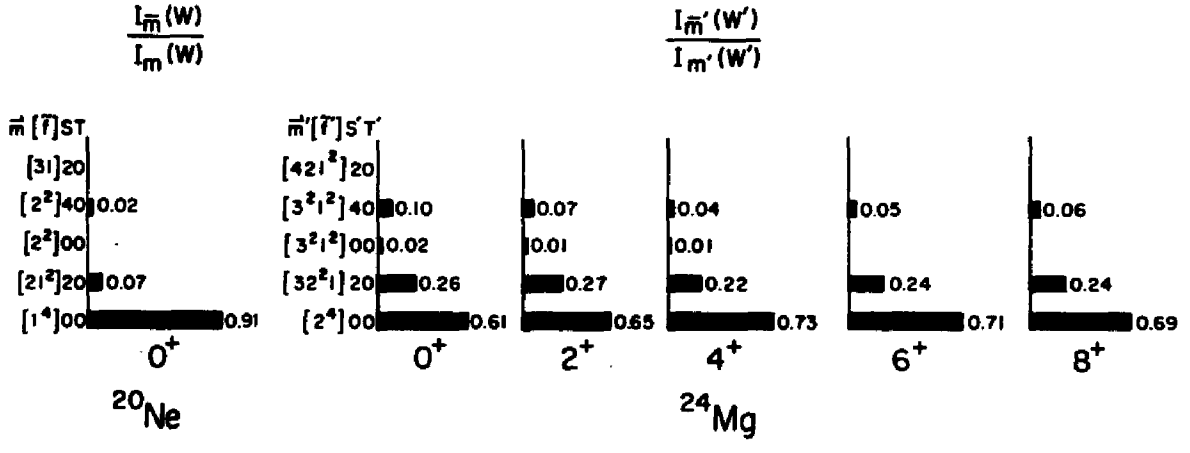

Figure 9

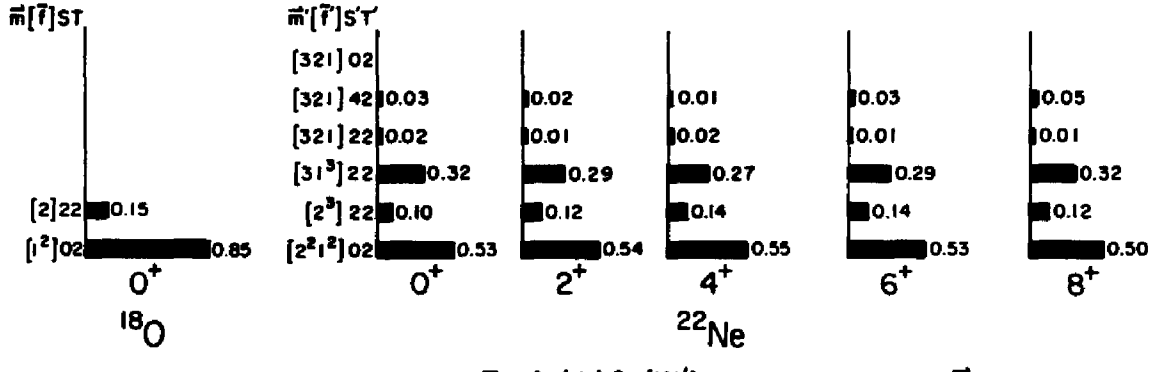

$$R(W,W') \sim \sum_{\vec{m}\vec{m}'} \frac{I_{\vec{m}}(W)\, I_{\vec{m}'}(W')}{I_m(W)\, I_{m'}(W')} \; \langle\langle \chi(\vec{m}'-\vec{m})\, \chi^+ \rangle\rangle^{\vec{m}}$$

Figure 8

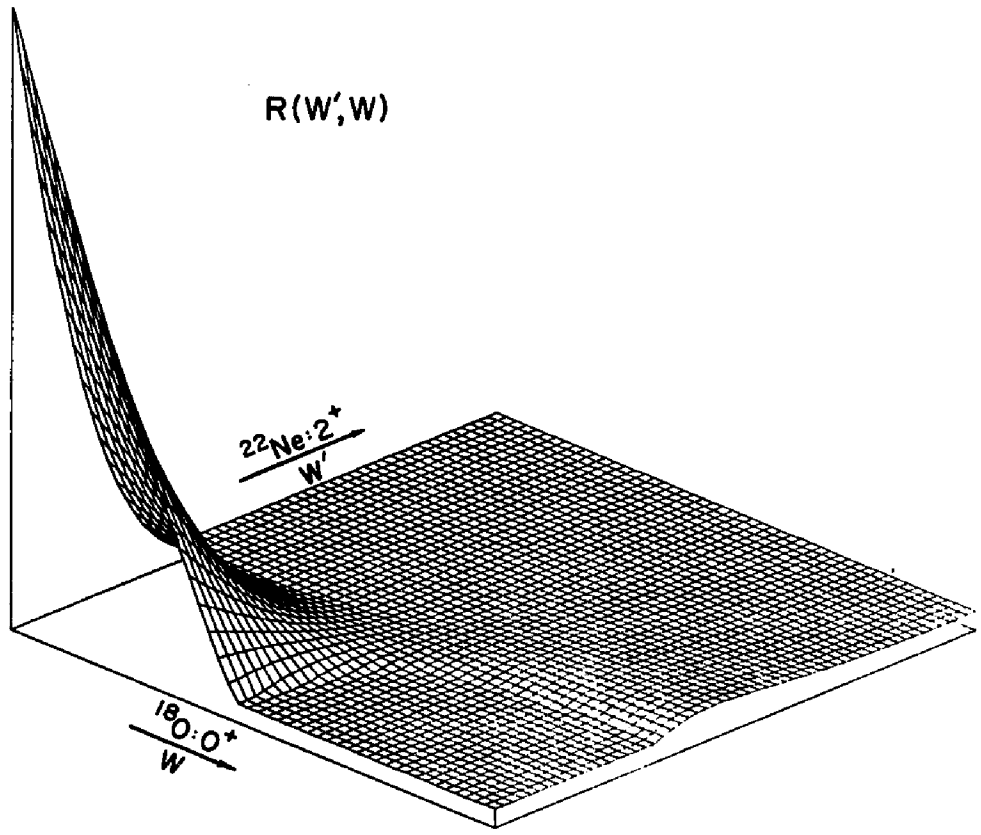

Figure 10a

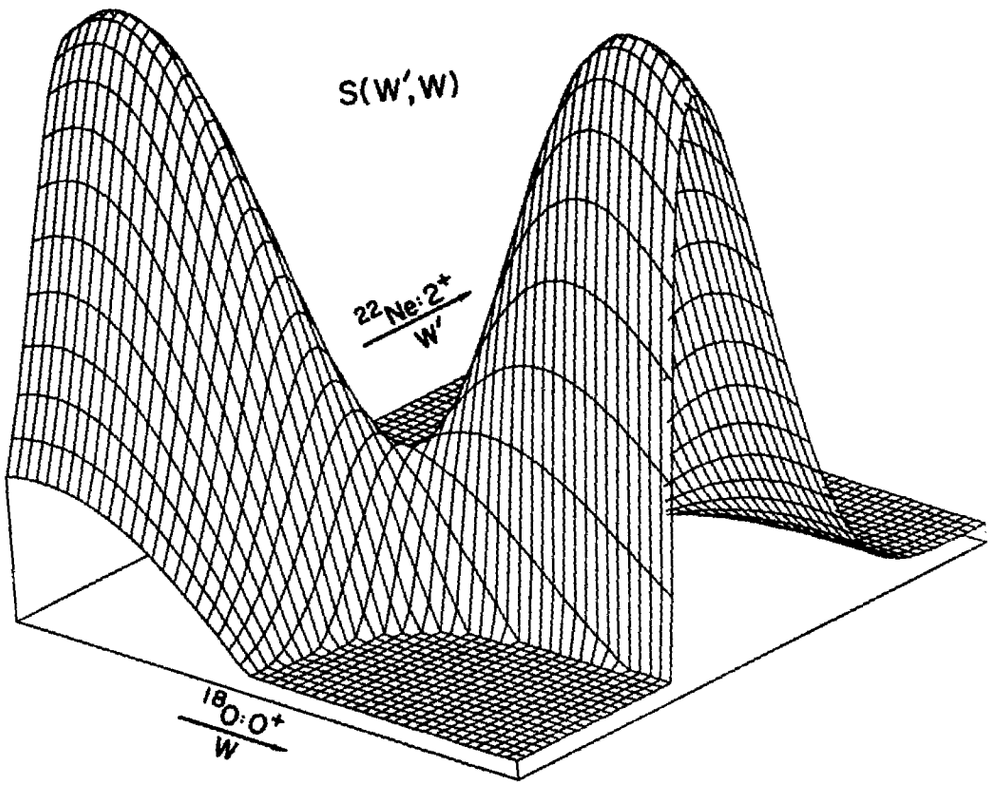

Figure 10b

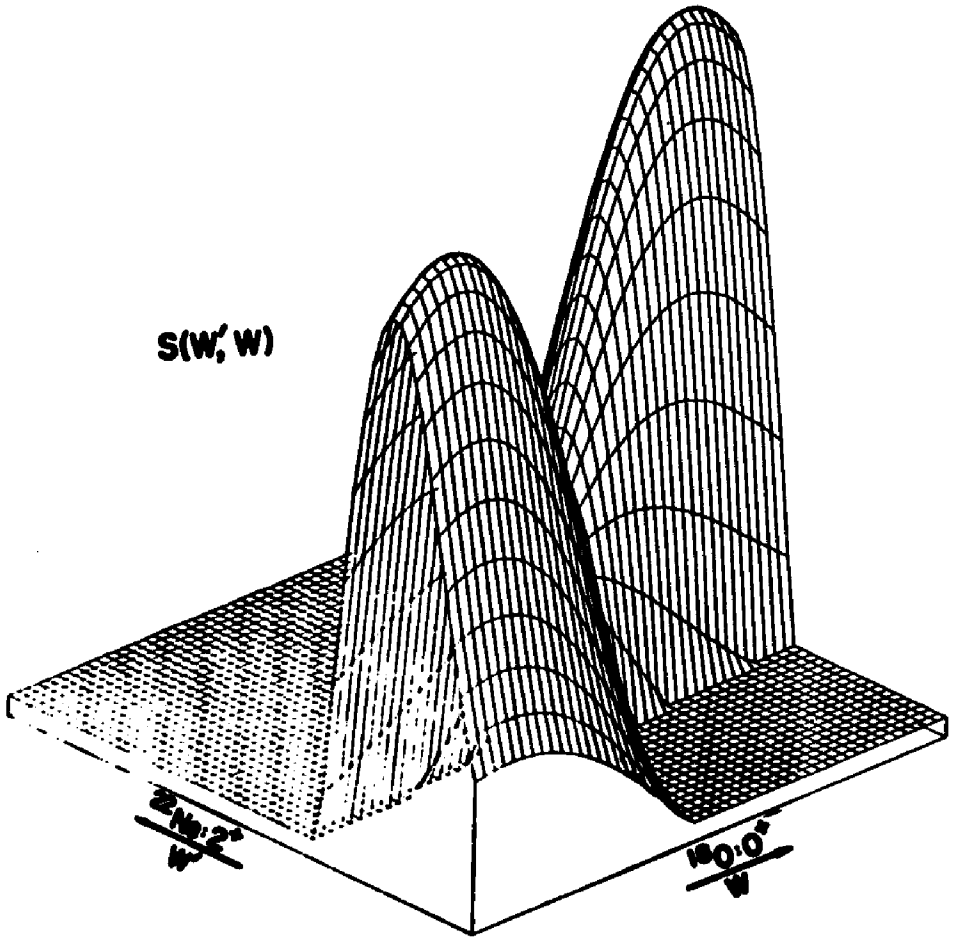

Figure 10c

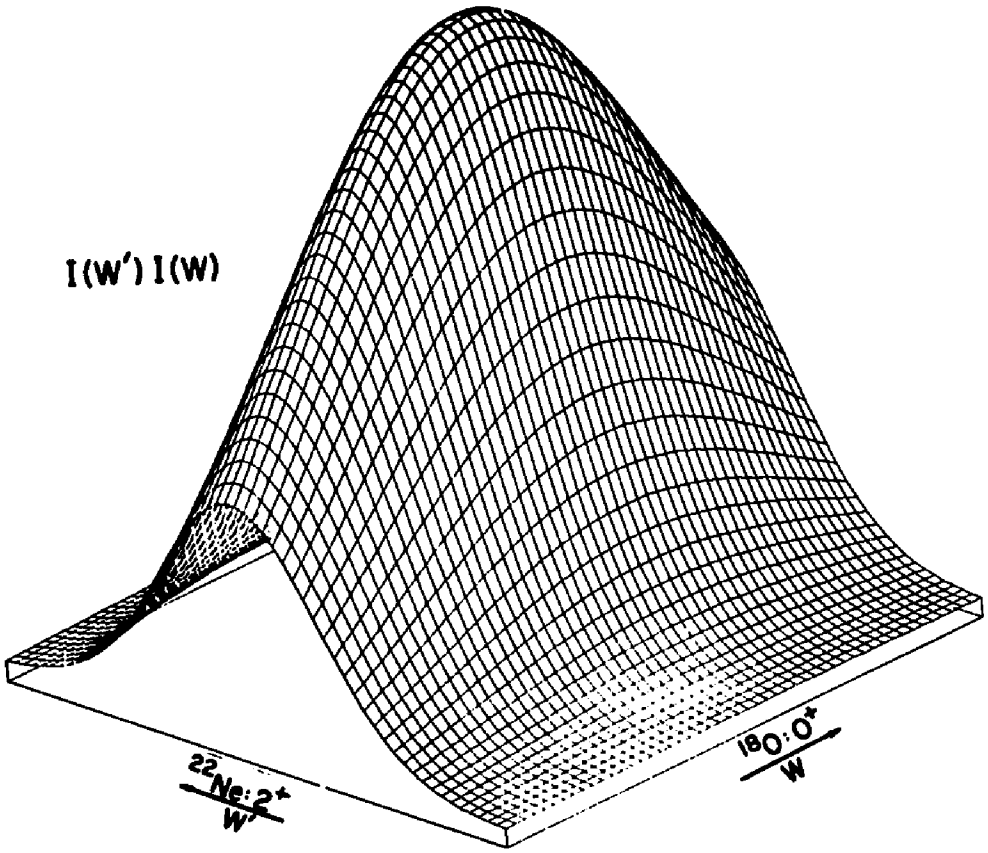

Figure 10d

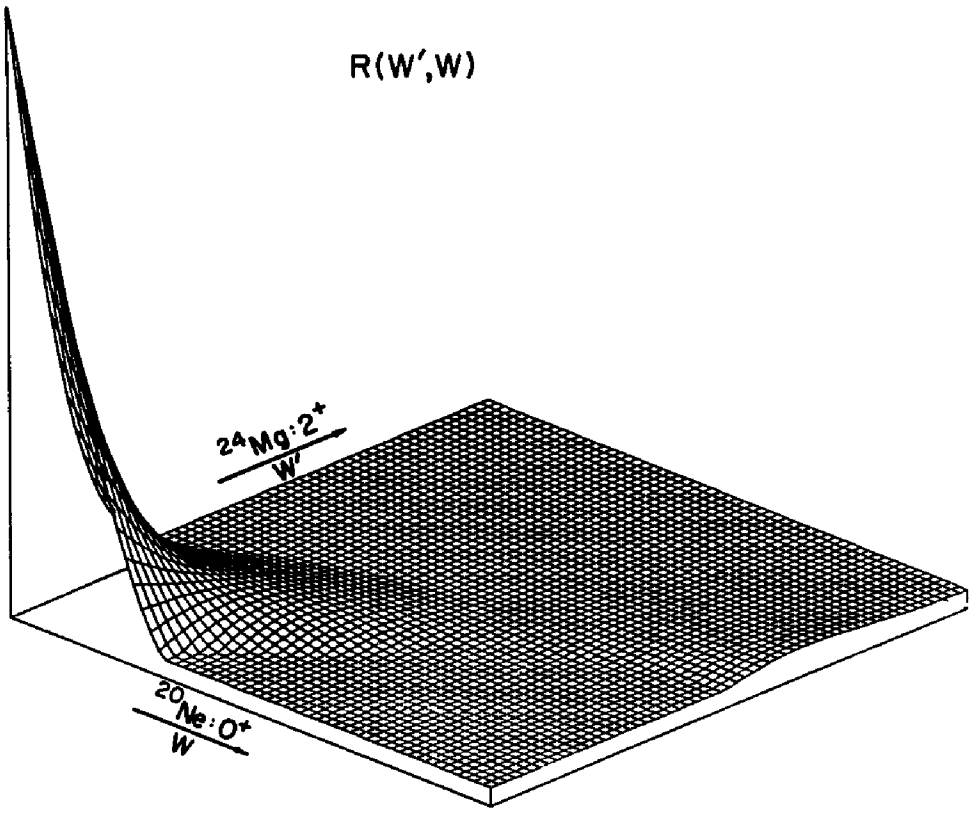

Figure 11a

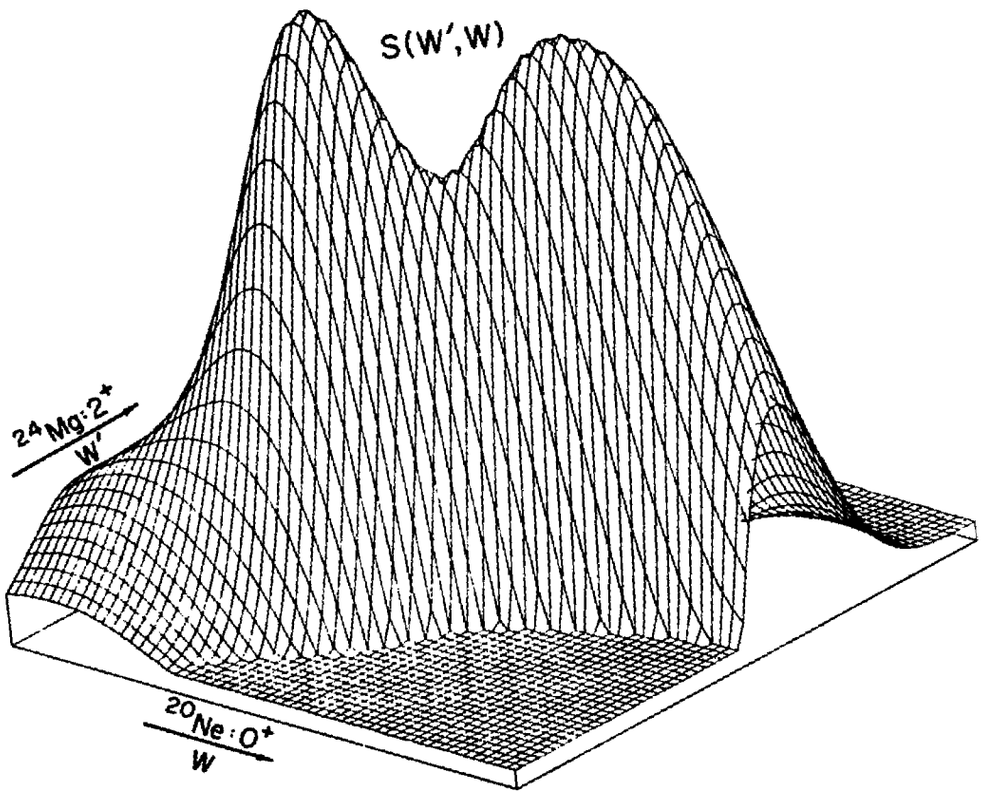

Figure 11b

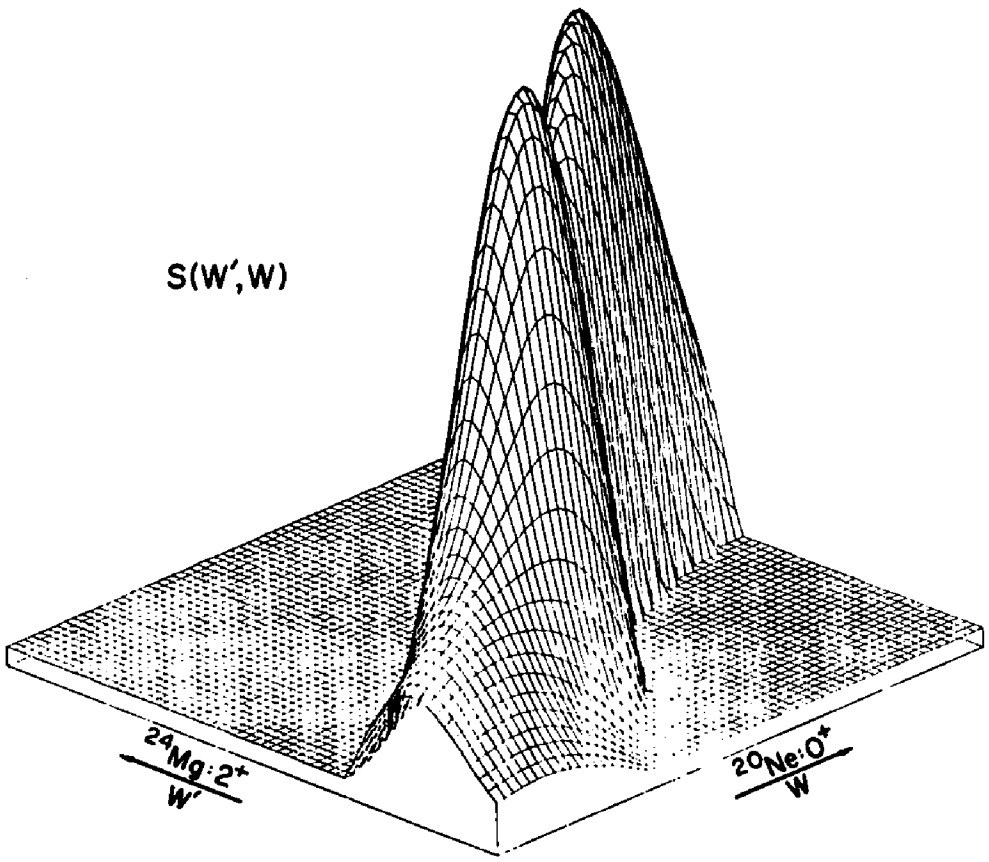

Figure 11c

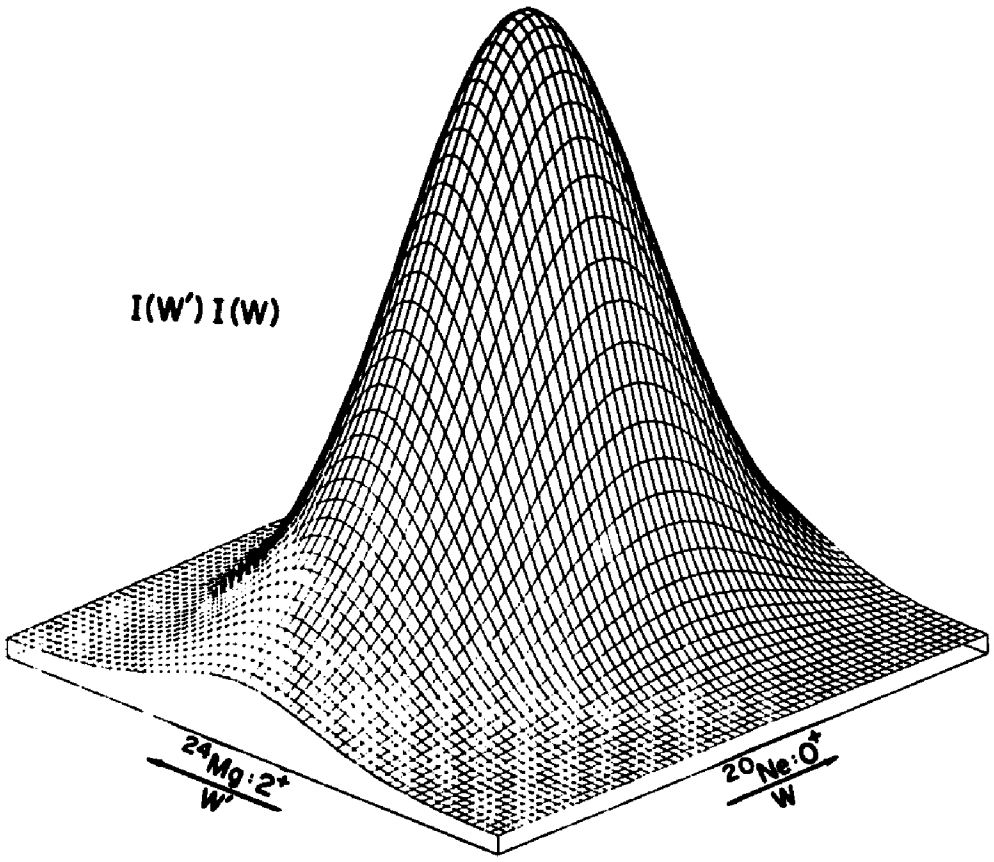

Figure 11d

Table Captions

13. The dimension, centroid and width for $\{m[\tilde{f}]2S,2T,2J\}$ configurations of the $(ds)^2$ 2J,2T = 2 model spaces. The Hamiltonian is our statistical approximation to the Brown-Kuo interaction H"(SU(3)/SU(4)ST) [Eq. (5.1)].

14. The dimension, centroid and width for $\{m[\tilde{f}]2S,2T,2J\}$ configurations of the $(ds)^4$ 2J,2T = 0 model spaces. The Hamiltonian is our statistical approximation to the Brown-Kuo interaction H"(SU(3)/SU(4)ST) [Eq. (5.1)] without the orbital number operator.

15. The dimension, centroid and width for $\{m[\tilde{f}]2S,2T,2J\}$ configurations of the $(ds)^6$ 2J,2T = 2 model spaces. The Hamiltonian is our statistical approximation to the Brown-Kuo interaction H"(SU(3)/SU(4)ST) [Eq. (5.1)] without the orbital number operator.

16. The dimension, centroid and width for $\{m[\tilde{f}]2S,2T,2J\}$ configurations of the $(ds)^8$ 2J,2T = 0 model spaces. The Hamiltonian is our statistical approximation to the Brown-Kuo interaction H"(SU(3)/SU(4)ST) [Eq. (5.1)] without the orbital number operator.

17. Ground state and low-lying energies for ^{18}O and ^{20}Ne using SU(4)ST distributions and our statistical approximation to the Brown-Kuo interaction H"(SU(3)/SU(4)ST) [Eq. (5.1)]. The moments of the SU(4)ST distributions were calculated using H"(SU(3)/SU(4)ST) without the orbital number operators $\sum_r n_r$. The last column gives the energies obtained from shell model calculations using the same interaction.

18. Ground state and low-lying energies for ^{22}Ne and ^{24}Mg using SU(4)ST distributions and our statistical approximation to the Brown-Kuo interaction H"(SU(3)/SU(4)ST) [Eq. (5.1)]. The moments of the SU(4)ST distributions were calculated using H"(SU(3)/SU(4)ST) without the orbital number operators $\sum_r n_r$. The last column gives the energies obtained from shell model calculations using the same interaction.

19. Relative intensities of SU(4)ST irreps in the wave function of low-lying states in $^{18}O[(ds)^2\ T = 1]$ and $^{20}Ne[(ds)^4\ T = 0]$ as determined using spectral distribution methods and our statistical approximation to the Brown-Kuo interaction H"(SU(3)/SU(4)ST) [Eq. (5.1)]. The numbers in parenthesis are those

obtained by Arima and Strottman (ref. 46) using the Brown-Kuo interaction.

20. Relative intensities of SU(4)ST irreps in the wave function of low lying states in ^{22}Ne[$(ds)^6$ T = 1] and ^{24}Mg[$(ds)^8$ T = 1] using spectral distribution methods and our statistical approximation to the Brown-Kuo interaction H"(SU(3)/SU(4)ST) [Eq. (5.1)].

21. Configuration traces for the operator

$$\chi^{\Gamma_o'}\left(\frac{H'' - \varepsilon(m')}{\sigma(\vec{m}')}\right)^q \quad \chi^{+\Gamma_o}\left(\frac{H'' - \varepsilon(m)}{\sigma(\vec{m})}\right) \quad \text{in each}$$

$\{m[\tilde{f}]2S,2T,2J\}$ space. Here $\vec{m} \equiv m[\tilde{f}]2S2T,2J\}$ and $\vec{m}' \equiv \{m'[f']2S'2T',2J'\}$ are the initial and final state configurations, respectively. The Hamiltonian of the system is our statistical approximation to the BK interaction H"(SU(3)/SU(4)ST) [Eq. (5.1)]. TRACE1 is for p = q = 0, TRACE2 for p = 0, q = 1, TRACE3 for p = 1, q = 0 and TRACE4 for p = q = 1. The traces are needed to study the reaction $^{18}O + \alpha \rightleftarrows {}^{22}Ne$.

23. Configuration traces for the operator

$$\chi^{\Gamma_o'}\left(\frac{H'' - \varepsilon(\vec{m}')}{\varepsilon(\vec{m}')}\right)^q \quad \chi^{+\Gamma_o}\left(\frac{H'' - \varepsilon(\vec{m})}{\varepsilon(\vec{m})}\right)^p \quad \text{in each}$$

$\{m[\tilde{f}]2S2T,2J\}$ space. Here $\vec{m} \equiv \{m[\tilde{f}]2S2T,2J\}$ and

$\vec{m}' \equiv \{m'[\tilde{f}']2S'2T',2J'\}$ are the initial and final state configurations, respectively. The Hamiltonian of the system is our statistical approximation to the BK interaction H"(SU(3)/SU(4)ST) [Eq. (5.1)] without the orbital number operators $\sum_r \eta_r$. TRACE1 is for p = q = 0, TRACE2 for p = 0, q = 1, TRACE3 for p = 1, q = 0 and TRACE4 for p=q=1. The traces are needed to study the reaction $^{20}Ne+\alpha \rightleftarrows {}^{24}Mg$.

22. Configuration traces for the operator $\chi^{\Gamma_o'}\left(\frac{H" - \varepsilon(\vec{m}')}{\varepsilon(\vec{m}')}\right)^q \chi^{+\Gamma_o}\left(\frac{H" - \varepsilon(\vec{m})}{\varepsilon(\vec{m})}\right)^p$ in each $\{m[\tilde{f}]2S2T,2J\}$ space. Here $\vec{m} \equiv \{m[\tilde{f}]2S2T,2J\}$ and $\vec{m}' \equiv \{m'[\tilde{f}']2S'2T',2J'\}$ are the initial and final state configurations, respectively. The Hamiltonian of the system is our statistical approximation to the BK interaction H"(SU(3)/SU(4)ST) [Eq. (5.1)] without the orbital number operators $\sum_r \eta_r$. TRACE1 is for p = q = 0, TRACE2 for p = 0, q = 1, TRACE3 for p = 1, q = 0 and TRACE4 for p = q = 1. The traces are needed to study the reaction $^{18}O + \alpha \rightleftarrows {}^{22}Ne$.

24. Relative alpha particle transfer strengths for the stripping and pickup reaction $^{18}O + \alpha \rightleftarrows {}^{22}Ne$ as predicted using spectral distribution methods. The spectral distribution predictions are compared with predictions from the SU(3) model (ref. 3) and were

possible shell model (ref. 22) and experimental findings (ref. 16). The first set of CLT predictions was obtained using our statistical approximations to the BK interaction H"(SU(3)/SU(4)ST) [Eq. (5.1)] and the second set of CLT predictions was obtained using H"(SU(3)/SU(4)ST) without the orbital number operators, $\sum_r n_r$.

25. Relative alpha particle transfer strengths for the stripping and pickup reaction $^{20}Ne + \alpha \rightleftarrows {}^{24}Mg$ as predicted using spectral distribution methods. The spectral distribution predictions are compared with predictions from the SU(3) model (ref. 3) and were possible the shell model (ref. 26) and experimental findings (ref. 20,25). The CLT prediction was obtained using our statistical approximation to the BK interaction H"(SU(3)/SU(4)ST) [Eq. (5.1)] without the orbital number operator, $\sum_r n_r$.

26. Percent of total transfer strength originating from the ground state of the target nuclei to the J' state of the residual nuclei.

TABLE 13

$\tilde{m}[f]2S2T,2J$	DIM	CENTROID	WIDTH
$2[1^2]02,0$	2	-7.81633	3.65147
2[2]22,0	1	-4.96698	3.22256
$2[1^2]02,4$	2	-7.04503	3.65147
2[2]22,4	3	-4.19568	3.22256
$2[1^2]02,8$	1	-6.92508	3.05077
2[2]22,8	1	-3.68148	3.22256

TABLE 14

$\tilde{m}$[f]2S2T,2J	DIM	CENTROID	WIDTH
4[1^4]00,0	4	-28.87811	7.33604
4[21^2]20,0	4	-21.75989	5.95890
4[2^2]00,0	3	-16.21152	5.71002
4[2^2]40,0	5	-19.77014	5.47824
4[31]20,0	5	-13.13822	5.54799
4[1^4]00,4	5	-28.21880	6.91142
4[21^2]20,4	17	-21.04510	5.82618
4[2^2]40,4	15	-19.13405	5.25763
4[2^2]00,4	5	-16.0012	5.58987
4[31]20,4	13	-12.83852	5.27656
4[4]00,4	1	-3.33355	5.12226
4[1^4]00,8	4	-27.98685	6.37255
4[21^2]20,8	14	-20.69550	5.42818
4[2^2]40,8	13	-19.01251	5.02908
4[2^2]00,8	4	-15.18028	5.24021
4[31]20,8	9	-12.36224	5.00068
4[1^4]00,12	2	-27.95833	6.21655
4[21^2]20,12	6	-20.38829	4.99802
4[2^2]40,12	6	-18.74883	4.89165
4[2^2]00,12	1	-14.17192	4.82349
4[31]20,12	2	-12.00245	4.87950
4[1^4]00,16	1	-28.02124	4.82176
4[21^2]20,16	1	-20.27739	4.71669
4[2^2]40,16	1	-17.94191	4.69367

TABLE 15

$m[\tilde{f}]2S2T,2J$	DIM	CENTROID	WIDTH
$6[2^2 1^2]02,0$	10	-42.26401	8.10378
$6[2^3]22,0$	7	-39.51067	7.15194
$6[31^3]22,0$	16	-39.40068	7.65438
$6[321]22,0$	30	-33.13736	6.72317
$6[321]42,0$	22	-35.41644	6.66223
$6[321]02,0$	5	-32.24980	6.76378
$6[41^2]22,0$	8	-26.52414	6.41527
$6[41^2]42,0$	7	-29.16318	6.24850
$6[41^2]02,0$	1	-24.40474	5.73313
$6[3^2]02,0$	5	-25.74854	6.88520
$6[3^2]42,0$	7	-29.56311	6.09692
$6[42]22,0$	12	-22.67520	6.16100
$6[42]42,0$	6	-25.04762	5.99185
$6[42]62,0$	7	-28.55292	5.81430
$6[51]02,0$	1	-14.53774	5.72859
$6[51]42,0$	3	-16.60323	5.83322
$6[51]22,0$	1	-12.73773	5.87501
$6[2^2 1^2]02,4$	24	-42.10861	7.70685
$6[2^3]22,4$	27	-39.07350	6.99482
$6[31^3]22,4$	51	-38.92415	7.28793
$6[321]22,4$	118	-32.81795	6.59494
$6[321]42,4$	84	-35.08009	6.44974
$6[321]02,4$	22	-31.64645	6.75432
$6[41^2]22,4$	25	-26.32545	6.33153

TABLE 15 (Continued)

$6[41^2]42,4$	32	-28.64993	6.14114
$6[41^2]02,4$	7	-25.39317	6.34660
$6[3^2]42,4$	23	-28.85007	6.08704
$6[3^2]02,4$	7	-25.79311	6.19742
6[42]22,4	38	-22.32224	6.04442
6[42]42,4	25	-24.65079	5.86579
6[42]62,4	27	-28.23529	5.67738
6[51]42,4	7	-16.24072	5.73340
6[51]02,4	3	-12.83324	5.93818
6[51]22,4	5	-13.78985	5.87425
$6[2^21^2]02,8$	25	-41.73111	7.27576
$6[2^3]22,8$	29	-38.76297	6.74315
$6[31^3]22,8$	51	-38.60216	6.88613
6[321]42,8	89	-34.75751	6.14140
6[321]22,8	116	-32.43602	6.27378
6[321]02,8	20	-31.27452	6.42204
$6[41^2]22,8$	21	-26.14752	6.03343
$6[41^2]42,8$	30	-28.52765	5.89965
$6[41^2]02,8$	6	-25.00659	5.97021
$6[3^2]42,8$	21	-28.43497	5.71324
$6[3^2]02,8$	6	-25.00659	6.07841
6[42]62,8	28	-28.12724	5.62111
6[42]42,8	22	-24.37851	5.69531
6[42]22,8	30	-21.95067	5.79002

TABLE 15 (Continued)

6[51]42,8	5	-16.31200	5.71171
6[51]22,8	2	-13.67332	5.69253
6[51]02,8	1	-11.96674	5.72859
$6[2^2 1^2]02,12$	15	-41.23227	6.84347
$6[2^3]22,12$	18	-38.23280	6.24226
$6[31^3]22,12$	30	-38.33730	6.45392
6[321]42,12	52	-34.44690	5.81604
6[321]22,12	60	-31.92241	5.88136
6[321]02,12	9	-30.84477	5.93211
$6[41^2]42,12$	14	-28.40083	5.63977
$6[41^2]22,12$	8	-25.79340	5.67875
$6[41^2]02,12$	2	-24.32484	5.70985
$6[3^2]42,12$	10	-28.25787	5.65524
$6[3^2]02,12$	3	-24.04489	5.59309
6[42]62,12	16	-28.09830	5.54458
6[42]42,12	9	-24.19919	5.56449
6[42]22,12	8	-21.17764	5.57138
6[51]42,12	1	-15.73674	5.61972
$6\ 2^2 1^2]02,16$	6	-40.71661	6.51051
$6[2^3]22,16$	6	-37.58937	5.79716
$6[31^3]22,16$	11	-38.13316	5.96312
6[321]42,16	16	-34.15685	5.59608
6[321]22,16	14	-31.25044	5.59894

TABLE 15 (Continued)

$6[321]02,16$	2	-29.88118	5.57855
$6[41^2]42,16$	3	-27.91870	5.48198
$6[41^2]22,16$	1	-25.18161	5.46985
$6[3^2]42,16$	3	-27.81490	5.48153
$6[42]62,16$	4	-27.46098	5.38334
$6[42]42,16$	1	-23.40605	5.44994

TABLE 16

m[$\tilde{f}$[2S2T,2J	DIM	CENTROID	WIDTH
8[2^4]00,0	10	-69.79131	9.86751
8[32^21]20,0	46	-62.74734	8.58657
8[3^21^2]00,0	19	-57.57855	8.89545
8[3^21^2]40,0	49	-60.95071	8.24405
8[421^2]20,0	35	-54.09937	8.05029
8[51^3]00,0	4	-45.35402	7.90617
8[3^22]20,0	21	-54.61127	7.99286
8[42^2]40,0	23	-52.54240	7.40446
8[42^2]00,0	5	-48.86699	7.63822
8[431]40,0	27	-48.35269	7.28120
8[431]60,0	26	-51.93283	7.03004
8[431]20,0	16	-46.07359	7.20460
8[521]20,0	9	-39.36699	7.12464
8[521]40,0	12	-41.97272	6.91915
8[4^2]00,0	3	-36.53635	7.06367
8[4^2]40,0	5	-40.09496	6.87767
8[4^2]80,0	4	-48.07178	6.37437
8[53]20,0	5	-33.46301	6.93335
8[53]60,0	5	-39.58069	6.47678
8[62]40,0	1	-27.42836	6.50332
8[2^4]00,4	25	-69.80386	9.27627
8[32^21]20,4	184	-62.41309	8.43514
8[3^21^2]40,4	180	-60.70200	8.04375

TABLE 16 (Continued)

$8[3^2 1^2]00,4$	49	-57.18073	8.31863
$8[421^2]20,4$	130	-53.84482	7.84853
$8[51^3]00,4$	10	-44.69463	7.59548
$8[3^2 2]20,4$	77	-54.29057	7.75674
$8[42^2]40,4$	98	-52.14145	7.30990
$8[42^2]00,4$	23	-48.77240	7.48743
8[431]40,4	102	-47.94106	7.10214
8[431]20,4	69	-45.68019	7.23203
8[431]60,4	111	-51.56126	6.87890
8[521]20,4	33	-39.24835	6.97586
8[521]40,4	46	-41.54910	6.83268
$8[61^2]20,4$	2	-28.76395	6.75673
$8[4^2]40,4$	15	-39.45885	6.70327
$8[4^2]00,4$	5	-36.32495	6.96691
$8[4^2]80,4$	13	-48.13399	6.30079
8[53]20,4	13	-33.16330	6.71812
8[53]60,4	17	-38.98763	6.41972
8[62]40,4	3	-27.17126	6.50332
8[62]00,4	1	-23.65836	6.59763
$8[2^4]00,8$	30	-69.40396	9.152051
$8[32^2 1]20,8$	217	-62.08615	8.14807
$8[3^2 1^2]40,8$	209	-60.10684	7.66540
$8[3^2 1^2]00,8$	52	-56.80630	8.00932
$8[421^2]20,8$	140	-53.63060	7.58078
$8[51^3]00,8$	8	-44.18277	7.26133

TABLE 16 (Continued)

$8[3^2 2]20,8$	85	-53.72752	7.43545
$8[42^2]40,8$	109	-51.82268	7.04460
8[42]00,8	24	-48.45161	7.27551
8[431]40,8	107	-47.63142	6.83943
8[431]60,8	128	-51.22968	6.65666
8[431]20,8	68	-45.33412	6.96976
8[521]40,8	43	-41.41187	6.61950
8[521]20,8	28	-39.07585	6.73756
$8[61^2]20,8$	1	-28.64400	6.45192
$8[4^2]80,8$	17	-47.99429	6.32557
$8[4^2]40,8$	13	-39.33730	6.52555
$8[4^2]00,8$	4	-35.50510	6.68962
8[53]60,8	17	-38.98763	6.41972
8[53]20,8	9	-32.68701	6.50368
8[62]40,8	2	-26.97844	6.50332

TABLE 17

Nuclei	J^{π}	Moment Method	Shell Model
^{18}O	0_1^+	-10.53 MeV	-11.46 MeV
	2_1^+	-10.11	-10.45
	4_1^+	-7.73	-8.82
^{20}Ne	0_1^+	-37.50	-39.31
	0_2^+	-32.30	-32.31
	2_1^+	-37.45	-38.46
	2_2^+	-33.34	-32.24
	4_1^+	-35.69	-36.51
	4_2^+	-31.69	-30.47
	6_1^+	-32.70	-33.49
	8_1^+	-28.62	-29.55

TABLE 18

Nuclei	J^{π}	Moment Method	Shell Model
^{22}Ne	0_1^+	-57.51 Mev	-58.21 MeV
	2_1^+	-59.32	-57.43
	2_2^+	-56.25	-56.02
	4_1^+	-58.07	-55.54
	4_2^+	-55.16	-54.11
	6_1^+	-55.27	-52.10
	8_1^+	-51.49	-48.48
^{24}Mg	0_1^+	-87.45	-87.40
	2_1^+	-89.94	--
	2_2^+	-86.30	--
	4_1^+	-89.62	--
	4_2^+	-85.99	--
	6_1^+	-86.98	--
	8_1^+	-83.41	--

TABLE 19

$\tilde{m}$[f]2S2T	0_1^+	2_1^+	4_1^+
2[1^2]02	0.86(0.87)	0.69(0.75)	0.69(0.51)
2[2]22	0.14(0.13)	0.31(0.25)	0.31(0.49)

$\tilde{m}$[f]2S2T	0_1^+	2_1^+	4_1^+	6_1^+
4[1^4]00	0.91(0.91)	0.83(0.90)	0.82(0.87)	0.75(0.82)
4[21^2]20	0.07(0.08)	0.15(0.09)	0.15(0.12)	0.18(0.17)
4[2^2]40	0.00	0.00	0.00	0.00(0.01)
4[2^2]40	0.02	0.02	0.03	0.07(0.02)
4[31]20	0.00	0.00	0.00	0.00

TABLE 20

$\tilde{m}$[f]2S2T	0_1^+	2_1^+	4_1^+	6_1^+	8_1^+
6[$2^2 1^2$]02	0.53	0.54	0.55	0.53	0.50
6[2^3]22	0.10	0.12	0.14	0.14	0.12
6[31^3]22	0.32	0.29	0.27	0.29	0.32
6[321]22	0.02	0.01	0.01	0.01	0.01
6[321]42	0.03	0.02	0.02	0.03	0.05

$\tilde{m}$[f]2S2T	0_1^+	2_1^+	4_1^+	6_1^+	8_1^+
8[2^4]00	0.61	0.65	0.75	0.71	0.69
8[$32^2 1$]20	0.26	0.27	0.22	0.24	0.24
8[$3^2 1^2$]40	0.10	0.07	0.04	0.05	0.06
8[$3^2 1^2$]00	0.02	0.01	0.00	0.00	0.00

TABLE 21

Initial Configuration $m[\tilde{f}]2S2T,2J$	Final Configuration $m'[\tilde{f}']2S'2T',2J'$	TRACE1	TRACE2	TRACE3	TRACE4
$2[1^2]02,0$	$6[2211]02,0$	0.06237	-0.05812	0.00092	1.53971
$2[2]22,0$	$6[31^3]22,0$	0.04822	-0.03544	0.06728	0.58418
$2[1^2]02,0$	$6[2^21^2]02,4$	0.05728	-0.02682	0.00221	1.41958
$2[2]22,0$	$6[31^3]22,4$	0.03320	-0.01656	0.04633	0.41830
$2[1^2]02,0$	$6[2^21^2]02,8$	0.07329	0.14639	0.00629	1.56701
$2[2]22,0$	$6[31^3]22,8$	0.04258	0.09316	0.05942	0.57276
$2[1^2]02,0$	$6[2^21^2]02,12$	0.15661	1.39250	0.01979	1.68726
$2[2]22,0$	$6[31^3]22,12$	0.08070	0.76598	0.11261	1.20926
$2[1^2]02,0$	$6[2^21^2]02,16$	0.54974	12.40829	0.06411	-6.27298
$2[2]22,0$	$6[31^3]22,16$	0.22490	5.45763	0.31384	4.03866
$6[2^21^2]02,0$	$2[1^2]02,4$	0.02399	-0.00843	0.02230	0.44916
$6[31^3]22,0$	$2[2]22,4$	0.02752	-0.02378	0.08777	0.02544
$6[2^21^2]02,0$	$2[1^2]02,8$	0.03643	-0.04779	0.24307	-0.21323
$6[31^3]22,0$	$2[22]22,8$	0.02432	-0.02204	0.13156	-0.27834

TABLE 22

Initial Configuration $m[\tilde{f}]2S2T,2J$	Final Configuration $m'[\tilde{f}']2S'2T',2J'$	TRACE1	TRACE2	TRACE3	TRACE4
$2[1^2]02,0$	$6[2^21^2]02,0$	0.06237	-0.05588	0.00537	1.47451
$2[2]22,0$	$6[31^3]22,0$	0.04822	-0.04127	0.01154	0.76953
$2[1^2]02,0$	$6[2^21^2]02,4$	0.05728	-0.02506	0.00626	1.35987
$2[2]22,0$	$6[31^3]22,4$	0.03320	-0.00705	0.00795	0.52498
$2[1^2]02,0$	$6[2^21^2]02,8$	0.07329	0.14784	0.01138	1.50283
$2[2]22,0$	$6[31^3]22,8$	0.04258	0.10757	0.01019	0.58039
$2[1^2]02,0$	$6[2^21^2]02,12$	0.15661	1.39404	0.03051	1.63158
$2[2]22,0$	$6[31^3]22,12$	0.08070	0.78500	0.01931	0.56397
$2[1^2]02,0$	$6[2^21^2]02,16$	0.54974	12.40669	0.10189	-5.87041
$2[2]22,0$	$6[31^3]22,16$	0.22490	5.43198	0.05383	-1.47226
$6[2^21^2]02,0$	$2[1^2]02,4$	0.02399	-0.00739	0.02251	0.40423
$6[31^3]22,0$	$2[2]22,4$	0.02752	-0.02572	0.03369	0.24382
$6[2^21^2]02,0$	$2[1^2]02,8$	0.03643	-0.04676	0.24159	-0.20131
$6[31^3]22,0$	$2[2]22,8$	0.02432	-0.02277	0.06404	0.02133

TABLE 23

Initial Configuration $m[\tilde{f}[2S2T,2J$	Final Configuration $m'[\tilde{f}']2S'2T',2J'$	TRACE1	TRACE2	TRACE3	TRACE4
$4[1^4]00,0$	$8[2^4]00,0$	0.04341	-0.04187	-0.02750	2.76002
$4[21^2]20,0$	$8[32^21]20,0$	0.00804	-0.00694	-0.00042	0.45436
$4[2^2]00,0$	$8[3^21^2]00,0$	0.02756	-0.02039	0.00254	1.05179
$4[2^2]40,0$	$8[3^21^2]40,0$	0.00831	-0.00338	0.00295	0.43545
$4[31]20,0$	$8[421^2]20,0$	0.01227	-0.00670	0.00154	0.39510
$4[1^4]00,0$	$8[2^4]00,4$	0.02220	-0.01383	-0.00483	1.39991
$4[21^2]20,0$	$8[32^21]20,4$	0.00436	-0.00121	-0.00015	0.24067
$4[2^2]00,0$	$8[3^21^2]00,4$	0.02227	-0.00900	0.00217	0.88018
$4[2^2]40,0$	$8[3^21^2]40,4$	0.00507	0.00232	0.00182	0.25725
$4[31]20,0$	$8[421^2]20,4$	0.00735	0.00001	0.00090	0.23382
$4[1^4]00,0$	$8[2^4]00,8$	0.03426	0.04942	-0.00968	1.92470
$4[21^2]20,0$	$8[32^21]20,8$	0.00486	0.01104	-0.00011	0.23624
$4[2^2]00,0$	$8[3^21^2]00,8$	0.02415	0.04584	0.00268	0.84945
$4[2^2]40,0$	$8[3^21^2]40,8$	0.00581	0.01992	0.00219	0.26362

TABLE 23 (Continued)

$4[31]20,0$	$8[421^2]20,8$	0.00904	0.02212	0.00107	0.25357
$4[1^4]00,0$	$8[2^4]00,12$	0.06314	0.43447	-0.00940	2.47448
$4[21^2]20,0$	$8[32^21]20,12$	0.00835	0.07146	-0.00034	0.25818
$4[2^2]00,0$	$8[3^21^2]00,12$	0.03805	0.30927	0.00454	0.84923
$4[2^2]40,0$	$8[3^21^2]40,12$	0.00988	0.09442	0.00395	0.30325
$4[31]20,0$	$8[421^2]20,12$	0.01715	0.14832	0.00196	0.30433
$4[1^4]00,0$	$8[2^4]00,16$	0.16554	2.94681	0.00432	0.76264
$4[21^2]20,0$	$8[32^21]20,16$	0.01973	0.40229	0.00057	-0.04534
$4[2^2]00,0$	$8[3^21^2]00,16$	0.11967	2.45111	0.00592	-0.64773
$4[2^2]40,0$	$8[3^21^2]40,16$	0.02395	0.47872	0.01079	0.14525
$4[31]20,0$	$8[421^2]20,16$	0.05117	1.05229	0.00591	-0.15921
$8[2^4]00,0$	$4[1^4]00,4$	0.01087	-0.00692	-0.00231	0.66875
$8[32^21]20,0$	$4[21^2]20,4$	0.00452	-0.00360	0.00288	0.23049
$8[3^21^2]40,0$	$4[2^2]40,4$	0.00438	-0.00174	0.00611	0.20225
$8[3^21^2]00,0$	$4[2^2]00,4$	0.01341	-0.01119	0.00489	0.49605
$8[421^2]20,0$	$4[31]20,4$	0.00640	-0.00333	0.00528	0.18492
$8[51^3]00,0$	$4[4]00,4$	0.17569	-0.12964	0.07742	0.97098

TABLE 23 (Continued)

$8[2^4]00,0$	$4[1^4]00,8$	0.01410	-0.01653	0.03903	0.66103
$8[32^21]20,0$	$4[21^2]20,8$	0.00371	-0.00282	0.01332	0.12609
$8[3^21^2]40,0$	$4[2^2]40,8$	0.00442	-0.00187	0.01767	0.14049
$8[3^21^2]00,0$	$4[2^2]00,8$	0.01400	-0.01321	0.05416	0.22626
$8[421^2]20,0$	$4[31]20,8$	0.00647	-0.00389	0.02377	0.08063
$8[2^4]00,0$	$4[1^4]00,12$	0.02602	-0.02262	0.26169	-0.02722
$8[32^21]20,0$	$4[21^2]20,12$	0.00480	-0.00449	0.05802	-0.09162
$8[3^21^2]40,0$	$4[2^2]40,12$	0.00383	-0.00166	0.02560	0.06217
$8[3^21^2]00,0$	$4[2^2]00,12$	0.01588	-0.01254	0.21249	-0.62157
$8[421^2]20,0$	$4[31]20,12$	0.00646	-0.00336	0.05045	-0.07482
$8[2^4]00,0$	$4[1^4]00,16$	0.04841	-0.04034	1.47990	-5.33905
$8[32^21]20,0$	$4[21^2]20,16$	0.00496	-0.00265	0.10499	-0.33923
$8[3^21^2]40,0$	$4[2^2]40,16$	0.00367	-0.00028	0.05041	-0.08910

TABLE 24

$^{18}O(J=0_1^+) + \alpha \rightarrow {}^{22}Ne$	$J'=0_1^+$	$J'=2_1^+$	$J'=4_1^+$	$J'=6_1^+$	$J'=8_1^+$	$J'=2_2^+$	$J'=4_2^+$
CLT Limit	1.00(1.16)	0.47	0.35	0.01	2.45	0.34	0.25
CLT Limit	1.00(1.15)	0.47	0.34	0.02	2.62	0.34	0.24
SU(3) Model	1.00(0.41)	0.77	0.36	0.04	0.07	0.24	0.65
Shell Model	1.00	0.76	0.40	0.06	----	0.00	0.06
Exp	1.00	0.32	0.10	----	----	0.08	0.04

$^{22}Ne(J=0_1^+) + \alpha \rightarrow {}^{18}O$	$J'=0_1^+$	$J'=2_1^+$	$J'=4_1^+$
CLT Limit	1.00(1.16)	0.10	0.30
CLT Limit	1.00(1.15)	0.13	0.20
SU(3) Model	1.00(0.41)	0.00	2.28

TABLE 25

$^{20}Ne(J=0_1^+) + \alpha \rightarrow {}^{24}Mg$	$J'=0_1^+$	$J'=2_1^+$	$J'=4_1^+$	$J'=6_1^+$	$J'=8_1^+$	$J'=2_2^+$	$J'=4_2^+$
CLT Limit	1.00(3.41)	0.29	0.12	0.28	0.16	0.19	0.22
SU(3) Model	1.00(0.49)	0.37	0.00	0.15	0.00	0.05	0.46
Shell Model	1.00(0.44)	0.44	0.04	0.00	----	0.02	0.29
Exp	1.00(0.71)	0.42	0.03	0.10	----	0.13	0.28

$^{24}Mg(J=0_1^+) + \alpha \rightarrow {}^{20}Ne$	$J'0_1^+$	$J'=2_1^+$	$J'=4_1^+$	$J'=6_1^+$	$J'=8_1^+$
CLT Limit	1.00(3.41)	0.12	0.27	0.38	0.14
SU(3) Model	1.00(0.49)	0.13	0.80	1.84	1.02
Shell Model	1.00(0.44)	0.13	0.60	0.88	0.34
Exp	1.00(0.45)	0.35	0.96	0.82	0.64

TABLE 26

$^{A}X(J=0_1^+) + \alpha \rightarrow {}^{A+4}Y$	J^{π}	Percent
$^{18}O(J=0_1^+) + \alpha \rightarrow {}^{22}Ne$	0_1^+	40
	2_1^+	38
	2_2	24
	4_1	39
	4_2	28
	6_1	21
	8_1	89
$^{20}Ne(J=0_1^+) + \alpha \rightarrow {}^{24}Mg$	0_1^+	43
	2_1^+	25
	2_2^+	16
	4_1^+	16
	4_2^+	30
	6_1^+	27
	8_1^+	29

CHAPTER VI

CONCLUSION

In this thesis, we have developed and tested statistical spectroscopy methods for calculating alpha particle transfer strengths in large model spaces. We take this opportunity to review briefly what we have accomplished and examine how the procedures can be extended, for example, to calculate alpha particle transfer strengths in other mass regions.

We have tested an algorithm for expanding any interaction in terms of a given set of operators.[31,36] The algorithm has special significance when the space is first partitioned by symmetries and the approximation is required to reproduce subspace centroids. The norm in the full space of the approximation compared to the norm of the interaction itself is a measure for completeness of the expansion and the goodness of the corresponding symmetry. We constructed an SU(3) symmetry preserving approximation to the Brown-Kuo (BK) interaction. The width of the approximation was about 74% of the total width of the BK interaction. To study the importance of single particle shell structure, we extended the SU(3) approximation to include projections of H (BK) along the symmetry breaking orbital number operators. The width of the approximation increased to 96% of the total

width of the BK interaction.

We made detailed shell model comparisons of spectra, overlaps and B(E2) values for ^{20}Ne [$(ds)^4_{T=0}$] and ^{22}Ne[$(ds)^6_{T=1}$] using the BK interaction[44] and SU(3) trace-equivalent approximations.[36] The comparisons show that the microscopic details, for the lowest members of each spin as generated using a realistic effective interaction, can be reasonably well reproduced with the SU(3) trace-equivalent approximations. For other states level-by-level comparisons of eigenenergies, overlaps and B(E2) strengths show some significant differences. Over a range of energy that includes several states, averaged results are nonetheless in good agreement.

Using a deeper understanding of the interplay between group theory and the notion of propagating operator averages,[37] we constructed a trace equivalent operator to the BK interaction in the ds-shell that reproduces centroids of H in irreps of the SU(3)/SU(4)ST symmetry. We extended the trace-equivalent operator, H^{TE}(SU(3)/SU(4)ST), to include projections of H along the symmetry preserving operator L^2 and the symmetry breaking number operators. We calculated the centroid and width of the extended SU(3)/SU(4)ST statistical approximation to the BK interaction in irreps $\{m[\tilde{f}](\lambda\mu)ST\}$ of the SU(3)/SU(4)ST symmetry. We used the moments of this statistical approximation to examine

the nature of the distribution of states belonging to definite $\{m[\tilde{f}](\lambda\mu)ST\}$ and $\{m[\tilde{f}]ST\}$ symmetries. The summed distribution was found to be very close to Gaussian. The normality of a distribution for fixed symmetry is not understood, although it is clear that some extended version of the central limit theorem in statistics must be operable. More work needs to be done in this area.

We used the $\{m[\tilde{f}]ST,J\}$ moments of our statistical approximation to estimate the ground state and low-lying energies of ^{18}O, ^{20}Ne, ^{22}Ne and ^{24}Mg. There was good agreement between the spectral distribution results and the results obtained from detailed shell model calculations[45] using our statistical approximation to the BK interaction. The 2_1^+ and 4_1^+ states of ^{22}Ne and ^{24}Mg are overbound compared to the corresponding 0_1^+ state; nevertheless, the discrepancies are not large, they are understood, and on the average there is generally good agreement with shell model results.

We calculated the relative intensities of the various SU(4)ST configurations in the predicted eigenstate regions for the same nuclei. The relative configuration intensities of the low-lying states agree remarkably well with the relative intensities from the SU(3) model.[46] Relative configuration intensities are of prime importance in deciding which configurations are significant in the low-lying spectra of complex nuclei.

The relative intensities of each SU(4)ST configuration together with the traces of the operator $\chi H^q \chi^+ H^p$ (with p,q = 0,1) enabled us to calculate the alpha particle transfer strengths for the stripping and pickup reactions $^{18}O+\alpha \rightleftarrows {}^{22}Ne$ and $^{20}Ne+\alpha \rightleftarrows {}^{24}Mg$. We found good agreement between our predictions and those of the SU(3) pure symmetry model[3] and detailed shell model calculations[5] as well as experimental findings.[16,20,24,25] Results for non-energy weighted sums showed that a large fraction of the total strength is concentrated in ground-state to ground-state band transitions.

For the reaction $^{20}Ne+\alpha \rightleftarrows {}^{24}Mg$ the strengths were calculated using our statistical approximation to the BK interaction H" without the orbital number operator. For the $(ds)^8$ system we were unable to calculate all of the necessary one-body reduced SU(3) matrix elements using Braunschweig's computer code.[11] In particular we had trouble calculating the reduced SU(3) matrix elements for basis states with low spatial symmetries and low $(\lambda\mu)$ values; we had no trouble with states of high spatial symmetries. However, based on the results for $^{18}O+\alpha \rightleftarrows {}^{20}Ne$ we can say the orbital number operator has negligible effect on the strength.

The statistical procedures we used to calculate alpha particle transfer strengths are valid in large model spaces. Spectral distribution methods[6-9] are

complementary in spirit to the conventional approach of calculating alpha particle transfer strengths. There are no matrices to construct and diagonalize. The theory is not limited by dimensionality considerations. It can in principle be applied to nuclei in other mass regions where the SU(3) symmetry is not good. For example, to study the reaction $^{42}Ca+\alpha \rightarrow {}^{46}Ti$ one would partition the initial and final state model spaces by standard configurations, $\bar{m}$, as well as J and T. An appropriate Hamiltonian for the system would be the extended French trace-equivalent (FTE) statistical approximation to the BK interaction in the fp shell.[6,31,36] One would calculate the two lowest moments of the extended FTE statistical approximation to the BK interaction in each configuration and use the moments to estimate the eigenenergies and relative intensities for the initial and final state configurations. The alpha particle transfer operator would have to be expressed as a coupling between the two coupled protons and the two coupled neutrons. Specifically, if $\theta^{\Gamma} = (a^{+}xa^{+})^{\Gamma}$ is a coupled two-nucleon creation operator, then the alpha particle transfer operator would be given by[4]

$$(\chi^{\Gamma_\alpha})^{+} = [\theta^{\Gamma_n^{+}} \times \theta^{\Gamma_p^{+}}]^{\Gamma_\alpha} \qquad (6.1)$$

Traces of the type $<<\chi^{\Gamma_\alpha}\chi^{\Gamma_\alpha}>>^{\vec{m},J,T}$, required for strengths, would involve the reduced matrix elements of a pair of two-particle transfer operators. One would therefore have to be able to calculate matrix elements of the θ^+ operators between standard configurations, a non trivial task.

REFERENCES

1. M. Ichimura, A. Arima, E. C. Halbert and T. Terasawa, Nucl. Phys. A204 (1973) 225.

2. K. T. Hecht and D. Braunschweig, Nucl. Phys. A244 (1975) 365.

3. J. P. Draayer, Nucl. Phys. A237 (1975) 157.

4. D. Kurath and I. S. Towner, Nucl. Phys. A22 (1974) 1.

5. W. Chung, J. van Hienen, B. H. Wildenthal, and C. L. Bennett, Phys. Lett. 79B (1978) 381.

6. J. B. French, in "Nuclear Structure", edited by A. Hossain (North-Holland Publishing Co., Amsterdam, The Netherlands, 1967); F. S. Chang, J. B. French, T. H. Thio, Ann. of Phys. 66 (1971) 137.

7. J. B. French, in "Dynamic Structure of Nuclear States", ed. D. J. Rowe, L. E. H. Trainor, S. S. M. Wong and T. W. Donnelly (University of Toronto, Ontario, Canada, 1972).

8. J. B. French and K. F. Ratcliff, Phys. Rev. C3 (1971) 117.

9. J. P. Draayer, J. B. French and S. S. M. Wong, Ann. of Phys. 106 (1977) 472; 503.

10. Y. Akiyama and J. P. Draayer, Computer Phys. Commun. 5 (1973) 405.

11. D. Braunschweig, Computer Phys. Commun. 14 (1978) 109.

12. P. D. Kunz, University of Colorado report.

13. J. L. Perrenoud, R. M. DeVries, Phys. Lett. B36 (1971) 18.

14. R. M. DeVries, Computer Phys. Commun. 11 (1976) 249.

15. H. W. Fulbright "Annual Review of Nuclear and Particle Science", Vol. 29 (1979) 161.

16. N. Anantaraman, H. E. Gove, J. Toke, and J. P. Draayer, Nucl. Phys. A279 (1977) 474.

17. N. Austern, "Direct Nuclear Reaction Theories", London: Wiley (1970) 390.

18. N. Austern, R. M. Drisko, E. C. Halbert, G. R. Satchler, Phys. Rev. B133 (1964) 3.

19. G. R. Satchler, Nucl. Phys. 55 (1964) 1.

20. N. Anantaraman, H. E. Gove, J. P. Trentelman, J. P. Draayer, and F. C. Jundt, Nucl. Phys. A276 (1977) 119.

21. U. Strohbusch et al., Phys. Rev. C9 (1974) 965.

22. B. M. Preedom and B. H. Wildenthal, Phys. Rev. C6 (1972) 1633.

23. M. Conze, Ph.D. Dissertation, Darmstadt (1976).

24. N. Anantaraman, H. E. Gove, R. A. Lindgren, J. Toke, J. P. Trentelman, J. P. Draayer, F. C. Jundt and G. Guillaume, Nucl. Phys. A313 (1979) 445.

25. W. Oelert, W. Chune, A. Djabeis, C. Mayer-Boricke and P. Turek, Phys. Rev. C22 (1980) 408.

26. W. Chung, J. van Hienen, B. H. Wildenthal, and C. L. Bennett, Phys. Lett. 79B (1978) 381.

27. K. Mon and J. B. French, Ann. Phys. 95 (1975) 90.

28. A. Gervois, Nucl. Phys. A184 (1972), 507.

29. J. B. French and S. S. M. Wong, Phys. Lett. 33B (1970) 449; J. B. French and S. S. M. Wong, Phys. Lett. 35B (1971) 5.

30. J. B. French, Phys. Lett. 26B (1967) 75.

31. T. R. Halemane, K. Kar and J. P. Draayer, Nucl. Phys. A311 (1978) 301.

32. J. C. Parikh, Ann. of Phys. 76 (1973) 202.

33. H. Cramer, "Mathematical Methods of Statistics", Princeton, 1946; G. Szero, "Orthogonal Polynomials", American Mathematical Society Colloquium Publications, Vol. XXIII, 1939.

34. F. S. Chang and J. B. French, Phys. Lett. B44 (1973) 131; 135.

35. K. Kar, Ph.D. Thesis, University of Rochester.

36. C. R. Countee, J. P. Draayer, T. R. Halemane and K. Kar, Nucl. Phys. A356 (1981) 1.

37. T. R. Halemane, Ph.D. Thesis, University of Rochester.

38. J. C. Parikh, Phys. Lett. 41B (1972) 468.

39. J. C. Parikh, Nucl. Phys. A220 (1974) 349.

40. J. C. Parikh, Nucl. Phys. A273 (1976) 410.

41. J. P. Draayer, in "Theory and Applications of Moment Methods in Many-Fermion Systems", edited by B. J. Dalton, S. M. Grimes, J. P. Vary, and S. A. Williams, (Plenum Press, New York, 1980).

42. T. H. Thio, Ph.D. Thesis, University of Rochester.

43. J. P. Elliott, Proc. Roy. Soc. A245 (1958) 128, 562. M. Harvey, "Advances in Nuclear Physics", Vol. 1, eds. M. Barranger and E. Vogt, (Plenum, New York, 1968).

44. T. T. S. Kuo, Nucl. Phys. A103 (1967) 71.

45. J. B. French, E. C. Halbert, J. B. McGrory, S. S. M. Wong, "Advances in Nuclear Physics", Vol. 3, eds. M. Barranger and E. Vogt, (Plenum, New York, 1969).

46. D. Strottman and A. Arima, Nuclear Physics Theoretical Group Report No. 46, Nuclear Physics Laboratory, Oxford University, 1973.

47. E. P. Wigner, Phys. Rev. 51 (1937), 106.

APPENDIX A

EVALUATION OF TRACES OF $\chi^{\Gamma'_o} \frac{(H''-\varepsilon(m'))^q}{\sigma(\vec{m}')} \chi^{+\Gamma_o} \frac{(H''-\varepsilon(m))^p}{\sigma(\vec{m})}$

The Hamiltonian H" of our system is given by

$$
\begin{aligned}
H''(SU(3)/SU(4)ST) &= H^{TE}(SU(3)/SU(4)ST) \\
&\quad - 1.7051(n_1 - n_1^{TE}(SU(3)/SU(4)ST) \\
&\quad + 3.4933(n_2 - n_2^{TE}(SU(3)/SU(4)ST) \\
&\quad + 0.12855(L^2 - L^{2TE}(SU(3)/SU(4)ST)
\end{aligned}
\tag{A.1}
$$

For the purpose of evaluating traces, we combined the orbital number operator $(n_1 - n_1^{TE}(SU(3)/SU(4)ST)$ and $(n_2 - n_2^{TE}(SU(3)/SU(4)ST)$ to form one operator we call n_r. For convenience in writing we will omit the label SU(3)/SU(4) ST in the trace equivalent operators. We will also omit the labels $(\vec{m}'-\vec{m})$ that gives the connecting configurations.

Case 1: $p = q = 0$

$$\text{TRACE1} \equiv \langle\langle \chi^{\Gamma'_o} \chi^{+\Gamma_o} \rangle\rangle m[\tilde{f}]ST,J$$

$$= \sum_{\Gamma} \langle [\tilde{f}]STJM_J\Gamma | \chi^{\Gamma'_o} \chi^{+\Gamma_o} | [\tilde{f}]STJM_J\Gamma \rangle$$

$$= \sum_{\Gamma\Gamma'} \langle [\tilde{f}]STJM_J\Gamma | \chi^{\Gamma'_o} | [\tilde{f}']S'T'J'M'_J\Gamma' \rangle \langle [\tilde{f}']S'T'J'M'_J\Gamma'$$

$$| \chi^{+\Gamma_o} | [\tilde{f}]STJM_J$$

$$= \sum_{\Gamma\Gamma'} \langle [\tilde{f}]STJM_J\Gamma | \chi^{\Gamma'_o} | [\tilde{f}]STJ'M'_J\Gamma' \rangle \langle [\tilde{f}]STJ'M'_J\Gamma'$$

$$| \chi^{+\Gamma_o} | [\tilde{f}]STJM_J\Gamma \rangle \quad . \tag{A.2}$$

We have used the selection rule that the operator $\chi^{+\Gamma_o}$ only couples states of the same $[\tilde{f}]ST$ symmetry. Γ and Γ' are additional quantum numbers needed to specify the initial and final state.

Case 2: $p = 0, q = 1$

$$\text{TRACE2} \equiv \langle\langle \chi^{\Gamma'_o} \frac{(H''-\epsilon(m'[\tilde{f}']S'T',J'))}{\sigma(m'[\tilde{f}']S'T',J')} \chi^{+\Gamma_o} \rangle\rangle m[\tilde{f}]ST,J$$

(A.3)

$$\text{TRACE2} \times \sigma(m'[\tilde{f}']S'T',J') = \langle\langle \chi^{\Gamma'} o_{H''} \chi^{+\Gamma} o_{>>} m[\tilde{f}]ST,J$$

$$- \varepsilon(m'[\tilde{f}']S'T',J')\langle\langle \chi^{\Gamma'} o_{\chi}{}^{+\Gamma} o_{>>}$$

$$= \langle\langle \chi^{\Gamma'} o_{H}{}^{TE} \chi^{+\Gamma} o_{>>} m[\tilde{f}]ST,J + \langle\langle \chi^{\Gamma'} o_{(L^2-L^{2TE})} \chi^{+\Gamma} o_{>>} m[\tilde{f}]ST,J$$

$$+ \langle\langle \chi^{\Gamma'} o_{n_r} \chi^{+\Gamma} o_{>>} - \varepsilon(m'[f']S'T',J')\langle\langle \chi^{\Gamma'} o_{\chi}{}^{+\Gamma} o_{>>} m[\tilde{f}]ST,J$$

(A.4)

Now we consider the first term

$$\text{TR21} \equiv \langle\langle \chi^{\Gamma'} o_{H}{}^{TE} \chi^{+\Gamma} o_{>>} m[\tilde{f}]ST,J$$

$$= \Sigma \langle [\tilde{f}]STJM_J\Gamma | \chi^{\Gamma'} o_{H}{}^{TE} \chi^{+\Gamma} o | [\tilde{f}]STJM_J\Gamma \rangle$$

$$= \sum_{\Gamma\Gamma'} \langle [\tilde{f}]STJM_J\Gamma | \chi^{\Gamma'} o_{H}{}^{TE} | [\tilde{f}']S'T'J'M_J'\Gamma' \rangle$$

$$\langle [\tilde{f}']S'T'J'M_J'\Gamma' | \chi^{+\Gamma} o | [\tilde{f}]STJM_J\Gamma \rangle$$

$$= \sum_{\Gamma\Gamma'} \langle [\tilde{f}]STJM_J\Gamma | \chi^{\Gamma'} o_{H}{}^{TE} | [\tilde{f}]STJ'M_J'\Gamma' \rangle$$

$$\langle [\tilde{f}]STJ'M_J'\Gamma' | \chi^{+\Gamma} o | [f]STJM_J\Gamma \rangle$$

$$= \sum_{\Gamma\Gamma'} \varepsilon(m'[\tilde{f}]ST(\lambda'\mu')) \langle [\tilde{f}]STJM_J\Gamma | \chi^{\Gamma'}_{o} | [\tilde{f}]STJ'M'_J\Gamma' \rangle$$

$$\langle [\tilde{f}]STJ'M'_J\Gamma' | \chi^{+\Gamma}{}_{o} | [\tilde{f}]STJM_J\Gamma \rangle \qquad \text{(A.5)}$$

Here $\varepsilon(m'[\tilde{f}]ST(\lambda'\mu'))$ is the expectation value of H^{TE} which is diagonal in this scheme. The expectation value of H^{TE}, $\varepsilon(m'[\tilde{f}]ST(\lambda'\mu'))$, was evaluated in Chapter 4. Since the operator (L^2-L^{2TE}) is also diagonal in this scheme we have for the second term

$$\text{TR22} \equiv \langle\langle \chi^{\Gamma'}_{o} (L^2-L^{2TE}) \chi^{+\Gamma}{}_{o} \rangle\rangle^{m[\tilde{f}]ST,J}$$

$$= \sum_{\Gamma\Gamma'} \langle [\tilde{f}]STJM_J\Gamma | \chi^{\Gamma'}_{o} (L^2-L^{2TE}) | [\tilde{f}']S'T'J'M'_J\Gamma' \rangle$$

$$\langle [\tilde{f}']S'T'J'M'_J\Gamma' | \chi^{+\Gamma}{}_{o} | [\tilde{f}]STJM_J\Gamma \rangle$$

$$= \sum_{\Gamma\Gamma'} \langle [\tilde{f}]STJM_J\Gamma | \chi^{\Gamma'}_{o} (L^2-L^{2TE}) | [\tilde{f}]STJ'M'_J\Gamma' \rangle$$

$$\langle [\tilde{f}]STJ'M'_J\Gamma' | \chi^{+\Gamma}{}_{o} | [\tilde{f}]STJM_J\Gamma \rangle$$

$$= \sum_{\Gamma\Gamma'} \{L'(L'+1) - \langle L'^{2TE} \rangle\} \langle [\tilde{f}]STJM_J\Gamma | \chi^{\Gamma'}_{p} | [\tilde{f}]STJ'M'_J\Gamma' \rangle$$

$$\langle [\tilde{f}]STJ'M'_J\Gamma' | \chi^{+\Gamma}{}_{o} | [\tilde{f}]STJM_J\Gamma \rangle \qquad \text{(A.6)}$$

Here $\{L'(L'+1)-\langle L'^{2TE}\rangle\}$ is the expectation value of L^2-L^{2TE}. The eigenvalue of L^{2TE} is given by $\langle L'^{2TE}\rangle = 0.5\langle C_2'\rangle = 0.5(\lambda'+\mu'+3)(\lambda'+\mu')-\lambda'\mu'$ where C_2' is the SU(3) Casmir operator. For the third term we have

$$\text{TR23} \equiv \langle\langle \chi^{\Gamma'_o} n_r \chi^{+\Gamma_o} \rangle\rangle^{m[\tilde{f}]ST,J}$$

$$= \sum_{\Gamma} \langle [\tilde{f}]STJM_J\Gamma | \chi^{\Gamma'_o} n_r \chi^{+\Gamma_o} | [\tilde{f}]STJM_J\Gamma \rangle$$

$$= \sum_{\Gamma\Gamma'} \langle [\tilde{f}]STJM_J\Gamma | \chi^{\Gamma'_o} n_r | [\tilde{f}']S'T'J'M'_J\Gamma' \rangle$$

$$\langle [\tilde{f}']S'T'J'M'_J\Gamma' | \chi^{+\Gamma_o} | [\tilde{f}]STJM_J\Gamma \rangle \qquad \text{(A.7)}$$

In the last step we used the coupling rules $[f]ST = [f]S'T' = [f]S"T"$ and $J" = J'$. Combining Eqs. (A.3-A.7) together with Eq. (A.2) we have

$$\text{TRACE2} = \langle\langle \chi^{\Gamma'_o} \frac{(H" - \varepsilon(m'[\tilde{f}']S'T',J'))}{\sigma(m'[f']S'T',J')} \chi^{+\Gamma_o} \rangle\rangle^{m[\tilde{f}]ST,J}$$

$$= \frac{\text{TR21} + \text{TR22} + \text{TR23} - \varepsilon(m'[\tilde{f}']S'T',J')\ \text{TRACE1}}{\sigma(m'[\tilde{f}']S'T',J')} \qquad \text{(A.8)}$$

Case 3: $p = 1,\ q = 0$

$$\text{TRACE3} \equiv \langle\langle \chi^{\Gamma'_o}\ \chi^{+\Gamma_o}\ \frac{(H" = \varepsilon(m[\tilde{f}]ST,J))}{\sigma(m[\tilde{f}]ST,J)} \rangle\rangle^{m[\tilde{f}]ST,J} \qquad \text{(A.9)}$$

$$\text{TRACE3} \times \sigma(m[\tilde{f}]ST,J) = \langle\langle \chi^{\Gamma'_o} \chi^{+}_{H''} \rangle\rangle^{m[\tilde{f}]ST,3}$$

$$- \varepsilon(m[\tilde{f}]ST,J) \langle\langle \chi^{\Gamma'_o} \chi^{+\Gamma_o} \rangle\rangle^{m[\tilde{f}]ST}$$

$$= \langle\langle \chi^{\Gamma'_o} \chi^{+\Gamma_o}{}_{H^{TE}} \rangle\rangle^{m[\tilde{f}]ST,J}$$

$$+ \langle\langle \chi^{\Gamma'_o} \chi^{+\Gamma_o}{}_{(L^2-L^{2TE}} \rangle\rangle^{m[\tilde{f}]ST,J}$$

$$+ \langle\langle \chi^{\Gamma'_o} \chi^{+\Gamma_o}{}_{\eta_r} \rangle\rangle^{m[\tilde{f}]ST,J}$$

$$- \varepsilon(m[\tilde{f}]ST,J) \langle\langle \chi^{\Gamma'_o} \chi^{+\Gamma_o} \rangle\rangle^{m[\tilde{f}]ST,J}$$

The first, second, and third term of TRACE3 are very similar to the first, second, and third term of TRACE2. Thus following the same procedure we get

$$\text{TR31} \equiv \langle\langle \chi^{\Gamma'_o} \chi^{+\Gamma_o}{}_{H^{TE}} \rangle\rangle^{m[\tilde{f}]ST,J}$$

$$= \sum_{\Gamma\Gamma} \langle [\tilde{f}]STJM_J\Gamma | \chi^{\Gamma'_o} | [f']S'T'J'M'_J\Gamma' \rangle \langle [\tilde{f}']S'T'J'\Gamma' |$$

$$\chi^{+\Gamma_o} H^{TE} | [\tilde{f}]STJM_J\Gamma \rangle$$

$$= \sum_{\Gamma\Gamma'} \varepsilon(m[\tilde{f}]ST(\lambda\mu) \langle [\tilde{f}]STJM_J\Gamma | \chi^{\Gamma'_o} | [\tilde{f}]STJ'M'_J\Gamma' \rangle$$

$$\langle [\tilde{f}]STJ'M'_J\Gamma' | \chi^{+\Gamma_o} | [\tilde{f}]STJM_J\Gamma \rangle \qquad \text{(A.11)}$$

$$\text{TR32} \equiv \langle\langle \chi^{\Gamma'_o} \chi^{+\Gamma_o} (L^2 - L^{2TE}) \rangle\rangle^{m[\tilde{f}]ST,J}$$

$$= \sum_{\Gamma\Gamma'} \langle [\tilde{f}]STJM_J\Gamma | \chi^{\Gamma'_o} | [\tilde{f}']S'T'M'_J\Gamma' \rangle$$

$$\langle [\tilde{f}']S'T'J'M'_J\Gamma' | \chi^{+\Gamma_o} (L^2 - L^{2TE}) | [\tilde{f}]STJM_J\Gamma \rangle$$

$$= \sum \{L(L+1) - \langle L^{2TE} \rangle\} \langle [\tilde{f}]STJM_J\Gamma | \chi^{\Gamma'_o} | [\tilde{f}]STJ'M'_J\Gamma' \rangle$$

$$\langle [\tilde{f}]STJ'M'_J\Gamma' | \chi^{+\Gamma_o} | [\tilde{f}]STJM_J\Gamma \rangle \qquad \text{(A.12)}$$

For the third term we get

$$\text{TR33} \equiv \langle\langle \chi^{\Gamma'_o} \chi^{+\Gamma}{}_o \eta_r \rangle\rangle^{m[\tilde{f}]ST,J}$$

$$= \sum_{\Gamma\Gamma'} \langle [\tilde{f}]STJM_J\Gamma | \chi^{\Gamma'_o} | [\tilde{f}']S'T'J'M'_J\Gamma' \rangle$$

$$\langle m[\tilde{f}']S'T'J'\Gamma' | \chi^{+\Gamma_o} \eta_r | [\tilde{f}]STJM_J\Gamma \rangle$$

$$= \sum \langle [\tilde{f}]STJM_J\Gamma | \chi^{\Gamma'_o} | [\tilde{f}]STJ'M'_J\Gamma' \rangle \langle [\tilde{f}]STJ'M'_J\Gamma' | \chi^{+\Gamma_o} |$$

$$[\tilde{f}]STJM_J\Gamma'' \rangle \langle [\tilde{f}]STJM_J\Gamma'' | \eta_r | [\tilde{f}]STJM_J\Gamma \rangle \qquad \text{(A.13)}$$

Combining Eqs. (A.9-A.13) together with Eq. (A.2) we have

$$\text{TRACE3} = \frac{\text{TR31} + \text{TR32} + \text{TR33} - \epsilon(m[f]ST,J)\ \text{TRACE1}}{\sigma(m[\tilde{f}]ST,J)} \qquad \text{(A.14)}$$

<u>Case 4:</u> p = 1, q = 1

$$\text{TRACE 4} \equiv \langle\langle \chi^{\Gamma'_o} \frac{(H'' - \varepsilon(m'[\tilde{f}]S'T',J'))}{\sigma(m'[\tilde{f}']S'T',J')} \chi^{+\Gamma_o}$$

$$\chi^{+\Gamma_o} \frac{(H'' - \varepsilon(m[\tilde{f}]ST,J))}{\sigma(m'[\tilde{f}']S'T',J')} \rangle\rangle^{m[\tilde{f}]ST,J} \qquad \text{(A.15)}$$

$$\text{TRACE4} \times \sigma(m'[\tilde{f}']S'T' \times \sigma(m[\tilde{f}]ST,J) = \langle\langle \chi^{\Gamma'_o} H'' \chi^{+\Gamma_o} H'' \rangle\rangle^{m[\tilde{f}]ST,J}$$

$$- \varepsilon(m[\tilde{f}]ST,J) \langle\langle \chi^{\Gamma'_o} H'' \chi^{+\Gamma_o} \rangle\rangle^{m[\tilde{f}]ST,J}$$

$$- \varepsilon(m'[\tilde{f}']S'T',J') \langle\langle \chi^{\Gamma_o} \chi^{+\Gamma_o} H'' \rangle\rangle^{m[\tilde{f}]ST,J}$$

$$+ \varepsilon(m[\tilde{f}]ST,J)\ \varepsilon(m'[\tilde{f}']S'T',J')$$

$$\langle\langle \chi^{\Gamma'_o} \chi^{+\Gamma_o} \rangle\rangle^{m[\tilde{f}]ST,J}$$

$$= \langle\langle \chi^{\Gamma'_o} H'' \chi^{+\Gamma_o} H'' \rangle\rangle^{m[\tilde{f}]ST,J} - \varepsilon(m[\tilde{f}]ST,J)\ \text{TRACE2}$$

$$- \varepsilon(m'[\tilde{f}']S'T',J')\ \text{TRACE3} + \varepsilon(m[\tilde{f}]ST,J)$$

$$\varepsilon(m'[\tilde{f}']S'T',J')\ \text{TRACE1} \qquad \text{(A.16)}$$

From Eq. (A.16) we observe that only the first term needs to be evaluated. Thus consider

$$
\begin{aligned}
TR4 &= \langle\langle \chi^{\Gamma_o'}\, H^{TE}\, \chi^{+\Gamma_o}\, H'' \rangle\rangle^{m[\tilde{f}]ST,J} \\
&= \langle\langle \chi^{\Gamma_o'}\, H^{TE}\, \chi^{+\Gamma_o}\, H^{TE} \rangle\rangle^{m[\tilde{f}]ST,J} \\
&+ \langle\langle \chi^{\Gamma_o'}\, (L^2-L^{2TE})\, \chi^{+\Gamma_o}\, (L^2-L^{2TE}) \rangle\rangle^{m[\tilde{f}]ST,J} \\
&+ \langle\langle \chi^{\Gamma_o'}\, H^{TE}\, \chi^{+\Gamma_o}\, (L^2-L^{2TE}) \rangle\rangle^{m[\tilde{f}]ST,J} \\
&+ \langle\langle \chi^{\Gamma_o'}\, (L^2-L^{2TE})\, \chi^{+}\, H^{TE} \rangle\rangle^{[\tilde{f}]ST,J} \\
&+ \langle\langle \chi^{\Gamma_o'}\, H^{TE}\, \chi^{+\Gamma_o}\, \eta_r \rangle\rangle^{m[\tilde{f}]ST,J} \\
&+ \langle\langle \chi^{\Gamma_o'}\, (L^2-L^{2TE})\, \chi^{+\Gamma_o}\, \eta_r \rangle\rangle^{m[\tilde{f}]ST,J} \\
&+ \langle\langle \chi^{\Gamma_o'}\, \eta_r\, \chi^{+\Gamma_o}\, H^{TE} \rangle\rangle^{m[\tilde{f}]ST,J} \\
&+ \langle\langle \chi^{\Gamma_o'}\, \eta_r\, \chi^{+\Gamma_o}\, (L^2-L^{2TE}) \rangle\rangle^{m[\tilde{f}]ST,J} \\
&\quad \langle\langle \chi^{\Gamma_o'}\, \eta_r\, \chi^{+\Gamma_o}\, \eta_r \rangle\rangle^{m[\tilde{f}]ST,J}
\end{aligned}
\tag{A.17}
$$

The first eight terms of Eq. (5.34) are combinations of the terms in TRACE2 and TRACE3 and can be written immediately. The last term (9^{th} term) is not obvious and thus will be considered in detail. Upon inspection of the terms in TRACE2 and TRACE3 we get for the first eight terms:

$$
\begin{aligned}
TR41 &= \langle\langle \chi^{\Gamma_o'}\, H^{TE}\, \chi^{+\Gamma_o}\, H^{TE} \rangle\rangle^{m[\tilde{f}]ST,J} \\
&= \sum_{\Gamma\Gamma'} \varepsilon(m'[\tilde{f}]ST(\lambda'\mu'))\ \varepsilon(m[\tilde{f}]ST(\lambda\mu))\ \langle [\tilde{f}]STJM_J\Gamma | \chi^{\Gamma_o'} | \\
&\quad [\tilde{f}]STJ'M_J'\Gamma' \rangle\ \langle [\tilde{f}]STJ'M_J'\Gamma' | \chi^{+\Gamma_o} | [\tilde{f}]STJM_J\Gamma \rangle
\end{aligned}
\tag{A.18}
$$

$$TR42 = \langle\langle \chi^{\Gamma_o'} (L^2 - L^{2TE}) \chi^{+\Gamma_o} (L^2 - L^{2TE}) \rangle\rangle^{m[\tilde{f}]ST,J}$$

$$= \sum_{\Gamma\Gamma'} \{L'(L'+1) - \langle L'^{2TE}\rangle\} \{L(L+1) - \langle L^{2TE}\rangle\}$$
$$\langle [\tilde{f}]STJM_J\Gamma | \chi^{\Gamma_o} | [f]STJ'\Gamma'\rangle \langle [\tilde{f}]STJ'M_J'\Gamma' | \chi^{+\Gamma_o} |$$
$$[\tilde{f}]STJM_J\Gamma\rangle \qquad (A.19)$$

where $\langle L'^{2TE}\rangle = 0.5\langle C_2'\rangle = 0.5\ (\lambda'+\mu'+3)(\lambda'+\mu') - \lambda'\mu'$
and $\langle L^{2TE}\rangle = 0.5\ \langle C_2\rangle = 0.5(\lambda+\mu+3)\ (\lambda+\mu) - \lambda\mu.$

$$TR43 = \langle\langle \chi^{\Gamma_o'} H^{TE} \chi^{+\Gamma_o} (L_2 - L^{2TE}) \rangle\rangle^{m[\tilde{f}]ST,J}$$

$$= \sum_{\Gamma\Gamma} \varepsilon(m'[\tilde{f}]ST(\lambda'\mu'))\ \{L(L+1) - \langle L^{2TE}\rangle\}$$
$$\langle [\tilde{f}]STJ\Gamma | \chi^{\Gamma_o'} | [\tilde{f}]STJ'M_J'\Gamma'\rangle \langle [\tilde{f}]STJM_J'\Gamma' | \chi^{+\Gamma_o} |$$
$$[\tilde{f}]STJM_J\Gamma\rangle \qquad (A.20)$$

$$TR44 = \langle\langle \chi^{\Gamma_o'} (L^2 - L^{2TE}) \chi^{+\Gamma_o} H^{TE} \rangle\rangle^{m[\tilde{f}]ST,J}$$

$$= \sum_{\Gamma\Gamma'} \{L'(L'+1) - \langle L'^{2TE}\rangle\}\ \varepsilon(m[\tilde{f}]ST\Gamma)\ \langle [\tilde{f}]STJM_J\Gamma | \chi^{\Gamma_o'} |$$
$$[\tilde{f}]STJ'M_J'\Gamma'\rangle \langle [\tilde{f}]STJ'M_J'\Gamma' | \chi^{+\Gamma_o} | [\tilde{f}]STJM_J\Gamma\rangle \qquad (A.21)$$

$$TR45 = \langle\langle \chi^{\Gamma_o'} H^{TE} \chi^{+\Gamma_o} \eta_r \rangle\rangle^{m[\tilde{f}]ST,J}$$

$$= \sum_{\Gamma\Gamma'\ "} \varepsilon(m'[\tilde{f}]ST(\lambda'\mu')\ \langle [\tilde{f}]STJM_J\Gamma | \chi^{\Gamma_o'} | [\tilde{f}]STJ'M_J'\Gamma'\rangle$$
$$\langle [\tilde{f}]STJ'M_J'\Gamma' | \chi^{+\Gamma_o} | [\tilde{f}]STJ'M_J'\Gamma'\rangle \langle [\tilde{f}]STJM_J\Gamma" | \eta_r |$$
$$[\tilde{f}]STJM_J\Gamma\rangle \qquad (A.22)$$

$$TR46 = \langle\langle \chi^{\Gamma_o'} \, (L^2 - L^{2TE}) \, \chi^{+\Gamma_o} \, \eta_r \rangle\rangle^{m[\tilde{f}]ST,J}$$

$$= \sum_{\Gamma\Gamma'\Gamma''} \{L'(L'+1) - \langle L'^{2TE} \rangle\} \langle [\tilde{f}]STJM_J\Gamma | \chi^{\Gamma_o'} | [\tilde{f}]STJ'M_J'\Gamma' \rangle \langle [\tilde{f}]STJ'\Gamma' | \chi^{+\Gamma_o} | [\tilde{f}]STJM_J\Gamma'' \rangle$$

$$\langle [\tilde{f}]STJM_J\Gamma'' | \eta_r | [\tilde{f}]STJM_J\Gamma \rangle \qquad (A.23)$$

$$TR47 = \langle\langle \chi^{\Gamma_o'} \, \eta_r \, \chi^{+\Gamma_o} \, H^{TE} \rangle\rangle^{m[\tilde{f}]ST,J}$$

$$= \sum_{\Gamma\Gamma'\Gamma''} \varepsilon(m[\tilde{f}]ST(\lambda\mu)) \langle [\tilde{f}]STJM_J\Gamma | \chi^{\Gamma_o'} | [\tilde{f}]STJ'M_J'\Gamma'' \rangle$$

$$\langle [\tilde{f}]STJ'M_J'\Gamma'' | \eta_r | [\tilde{f}]STJ'M_J'\Gamma' \rangle \langle [\tilde{f}]STJ'M_J'\Gamma' | \chi^{+\Gamma_o} |$$

$$[\tilde{f}]STJM_J\Gamma \rangle \qquad (A.24)$$

$$TR48 = \langle\langle \chi^{\Gamma_o'} \, \eta_r \, \chi^{+\Gamma_o} \, (L^2 - L^{2TE}) \rangle\rangle^{m[\tilde{f}]ST,J}$$

$$= \sum_{\Gamma\Gamma\Gamma} \{L(L+1) - \langle L^{2TE} \rangle\} \langle [\tilde{f}]STJM_J\Gamma | \chi^{\Gamma_o'} | [\tilde{f}]STJ'M_J'\Gamma'' \rangle$$

$$\langle [\tilde{f}]STJ'M_J'\Gamma'' | \eta_r | [\tilde{f}]STJ'M_J'\Gamma' \rangle \langle [\tilde{f}]STJ'M_J'\Gamma' | \chi^{+\Gamma_o} |$$

$$[\tilde{f}]STJM_J\Gamma \rangle \qquad (A.25)$$

For the last term we get

$$\text{TR49} = \langle\langle \chi^{\Gamma'_o} \eta_r \; \chi^{+\Gamma_o} \eta_r \rangle\rangle^{m[\tilde{f}]ST,J}$$

$$= \sum_{\Gamma} \langle [\tilde{f}]STJM_J\Gamma | \chi^{\Gamma'_o} \eta_r \; \chi^{+\Gamma_o} \eta_r | [\tilde{f}]STJM_J\Gamma \rangle$$

$$= \sum_{\Gamma\Gamma'} \langle [\tilde{f}]STJM_J\Gamma | \chi^{\Gamma'_o} \eta_r | [\tilde{f}']S'T'J'M'_J\Gamma' \rangle$$

$$\langle [\tilde{f}']S'T'J'\Gamma' | \chi^{+\Gamma_o} \eta_r | [\tilde{f}]STJM_J\Gamma \rangle$$

$$= \sum_{\Gamma\Gamma'\Gamma''\Gamma''} \langle [\tilde{f}]STJM_J\Gamma | \chi^{\Gamma'_o} | [\tilde{f}'']S''T''J''M''_J\Gamma'' \rangle$$

$$\langle [\tilde{f}'']S''T''J''M''_J\Gamma'' | \eta_r | [\tilde{f}']S'T'J'M'_J\Gamma' \rangle$$

$$\langle [\tilde{f}']S'T'J'M'_J\Gamma' | \chi^{+\Gamma_o} | [\tilde{f}''']S'''T'''J'''M'''_J\Gamma''' \rangle$$

$$\langle "\tilde{f}'"]S'"T'"J'"M'''_J\Gamma'"' | \eta_r | [\tilde{f}]STJM_J\Gamma \rangle$$

$$= \sum_{\Gamma\Gamma'\Gamma''\Gamma''} \langle "\tilde{f}'STJM_J\Gamma | \chi^{\Gamma'_o} | [\tilde{f}]STJ'M'_J\Gamma'' | \eta_r | [\tilde{f}']S'T'J'M'_J\Gamma' \rangle$$

$$\langle [\tilde{f}']S'T'J'M'_J\Gamma' | \chi^{+\Gamma_o} | [\tilde{f}']S'T'JM_J\Gamma''' \rangle$$

$$\langle [\tilde{f}']S'T'JM_J\Gamma''' | \eta_r | [\tilde{f}]STJM_J\Gamma \rangle \qquad \text{(A.26)}$$

Now combining Eqs. (A.16-A.26) we can write Eqs. (A.15) as

$$\text{TRACE4} = \langle\langle \chi^{\Gamma'_o} \frac{(H'' - \varepsilon(m'[\tilde{f}']S'T'J'))\chi^{+\Gamma_o}(H - \varepsilon(m[\tilde{f}]ST,J))}{\sigma(m'[\tilde{f}']S'T',J' \quad \sigma(m[\tilde{f}]ST,J)} \rangle\rangle$$

$$= [\text{TR41} + \text{TR42} + \text{TR43} + \text{TR44} + \text{TR45} + \text{TR46} + \text{TR47}$$

$$+ \text{TR48} + \text{TR49} - \varepsilon(m[\tilde{f}]ST,J)\ \text{TRACE2}$$

$$- \frac{\varepsilon(m'[\tilde{f}']S'T',J')\ \text{TRACE3}}{\sigma(m'[\tilde{f}']S'T',J')}$$

$$+ \frac{\varepsilon(m[\tilde{f}]ST,J)\ \varepsilon(m'[\tilde{f}']S'T',J')\ \text{TRACE 1}}{\sigma(m[\tilde{f}]ST,J)} \qquad \text{(A.27)}$$

Now for H" without the orbital number operator the traces are given by

$$\text{TRACE2} = \frac{\text{TR21} + \text{TR22} - \varepsilon(m'[\tilde{f}']S'T',J')\ \text{TRACE 1}}{\sigma(m'[\tilde{f}']S'T',J')} \qquad \text{(A.28)}$$

$$\text{TRACE3} = \frac{\text{TR31} + \text{TR32} - \varepsilon(m''\tilde{f}'ST,J)\ \text{TRACE 1}}{\sigma(m[\tilde{f}]ST,J)} \qquad \text{(A.29)}$$

$$\text{TRACE4} = \text{TR41} + \text{TR42} + \text{TR43} + \text{TR44} - \varepsilon(m[\tilde{f}]ST,J)\ \text{TRACE2}$$

$$\frac{-\varepsilon(m'[\tilde{f}']S'T',J')\ \text{TRACE3} + \varepsilon(m[\tilde{f}]ST,J)\ \varepsilon(m'[\tilde{f}']S'T',J'\ \text{TRACE1}}{\sigma(m'[\tilde{f}']S'T',J')\ \sigma(m[\tilde{f}]ST,J)}$$

(A.30)

VITA

Calvin Ray Countee was born on December 22, 1953 in Alexandria, Louisiana. He graduated from Peabody High School in Alexandria. He received an academic scholarship to attend Grambling State University in Grambling, Louisiana, where he majored in Physics and Mathematics. He graduated, magna cum laude, with a Bachelor of Arts degree in 1975. In the same year, he accepted a graduate teaching assistantship in the Department of Physics and Astronomy at Louisiana State University in Baton Rouge, Louisiana. In 1977 he received his Master of Science degree in Physics from Louisiana State University. He is currently a candidate for the degree of Doctor of Philosophy in the Department of Physics and Astronomy at Louisiana State University.

EXAMINATION AND THESIS REPORT

Candidate: Calvin Ray Countee

Major Field: Nuclear Physics

Title of Thesis: "Statistical Spectroscopy Study of Alpha Particle Transfer Strengths"

Approved:

J. P. Draayer
Major Professor and Chairman

Dean P. McGlynn
Dean of the Graduate School

EXAMINING COMMITTEE:

Joseph Callaway

R. W. Huggett

per letter

Edward Zganjar

Date of Examination:

October 9, 1981